ICP design methods for driven piles in sands and clays

Richard Jardine *Imperial College London*
Fiona Chow *WorleyParsons Australia*
Robert Overy *Shell UK Ltd*
Jamie Standing *Imperial College London*

Thomas Telford

Published by Thomas Telford Publishing, Thomas Telford Ltd, 1 Heron Quay, London E14 4JD.
www.thomastelford.com

Distributors for Thomas Telford books are
USA: ASCE Press, 1801 Alexander Bell Drive, Reston, VA 20191–4400, USA
Japan: Maruzen Co. Ltd, Book Department, 3–10 Nihonbashi 2-chome, Chuo-ku, Tokyo 103
Australia: DA Books and Journals, 648 Whitehorse Road, Mitcham 3132, Victoria

First published 2005

A catalogue record for this book is available from the British Library
ISBN: 0 7277 3272 2

Printed and bound in Great Britain by Bell & Bain Ltd, Glasgow

CONTENTS

1 INTRODUCTION

In 1996 the UK Marine Technology Directorate (MTD) published a booklet by Jardine and Chow that summarised a new integrated approach for calculating the axial capacity of tubular piles driven in sands and clays. Axial capacity is often the governing criterion when designing driven piles and a simplified treatment had been developed at Imperial College London through four consecutive PhD studies (Jardine 1985, Bond 1989, Lehane 1992 and Chow 1997). The work had been co-funded by Industry, the UK's Health and Safety Executive and the Engineering and Physical Science Research Council through MTD, with the main focus being on offshore pile behaviour. The recommendations made by Jardine and Chow relied heavily on the earlier contributions made by Bond (1989) and Lehane (1992), testing, extending, updating and applying their work in the light of the research by Chow (1997).

The recommendations have been applied world-wide by the Authors and others in dozens of offshore, marine and onshore projects. Applications have ranged from major new offshore platforms (including 13 such structures commissioned and operated by Shell Exploration and Production) to large bridges and smaller scale foundations for light industrial facilities. Offshore Engineers often refer to the procedures as the 'MTD' or Imperial College Pile (ICP) design method. However, the Marine Technology Directorate no longer operates and we suggest that the acronym 'ICP' is now the most appropriate.

This second edition, published by Thomas Telford Ltd, broadens and updates the original work. New contributions are included and we emphasise the wide range of potential civil engineering applications. Reference is made to relevant research completed since 1996 and to lessons learned through practice. Substantial new sections are included on choosing appropriate factors of safety, the selection of geotechnical parameters, case histories, non-cylindrical pile shapes, ageing processes, a wider range of soil types (including calcareous sands), group action, cyclic loading and seismic action. The prediction of load-displacement behaviour, including the response to lateral loading, is not addressed here. However, reference is made to other publications that describe how improved predictive procedures have been developed from associated research at Imperial College.

Our aim is to provide:

- Descriptions of the axial capacity calculation procedures that are sufficiently detailed and clear to allow their application by suitably qualified geotechnical engineers.
- Demonstrations of the theoretical and practical advantages offered in comparison with conventional design methods.
- Evidence of the greater reliability and accuracy offered by the methods.
- Worked examples with references to case histories.
- Commentaries on how pile shape, age, group action, cyclic loading and seismic action can influence field performance.
- Guidance on applying the methods to a wider range of soil types.

Details of the experimental research, background theory and validation studies cannot be covered in this deliberately short publication. Instead, a substantial list of references is provided and Appendices are included covering (A) the methodology recommended for ring shear testing; (B) worked examples of the ICP method's use in sands and clays; and (C) the notation and symbols employed.

2 BACKGROUND

2.1 Rationale for developing new design approaches

The approaches applied by most practitioners to predict the axial capacity, Q, of displacement piles are relatively unreliable. This may be demonstrated by comparing independent predictions, made by a statistically meaningful group of well qualified practitioners, with data from well conducted field tests in 'predictions competitions', or through database analyses in which a single individual (or team) applies a range of methods to a collection of load tests. The first approach relies on just one site, which might not be generally representative, while the second often has to rely on incomplete information drawn from the literature, and may be biased by the subjective judgments of the single individual or team concerned.

Jardine et al. (2001) report a study of the first type that focused on piles driven in dense sand at the Dunkirk research site in northern France. Full details of the site conditions and loading procedures were published through a dedicated website. Axial capacity predictions were offered in confidence, to an independent body, by a wide range of international consultants, researchers and specialists. Figure 1 shows the compression test capacity measured on site and the wide spread of predictions offered, which ranged from around one third of the measured capacity to about twice this value. The calculated capacities Q_c fell on average around 21% below the measured value Q_m and gave a Coefficient of Variation (COV)[1] for (Q_c /Q_m) of around 0.53. Database studies by Briaud and Tucker (1988) and Jardine and Chow (1996) show that even the best conventional approaches give COVs of a similarly high magnitude and may also be subject to substantial bias. Despite their limitations, predictions competitions and database studies lead to similar conclusions: predictive reliability is generally far poorer than many practitioners recognise.

Pile load tests are specified in many projects to help mitigate the effects of predictive scatter. However, this option is rarely available to offshore engineers and can be difficult to carry forward with large piles in more general applications. Jardine and Chow (1996), and others since, considered how well the procedures most commonly used by Offshore Engineers predict the capacities held in high quality databases. They found little overall bias but report COV values as high as 0.5 to 0.7 that sit uncomfortably with the relatively low safety margins (typically 1.5 to 2.0) that are commonly adopted for offshore pile design. Jardine and Chow showed that the existing offshore methods are subject to strong and systematic skewing of (Q_c/Q_m) with respect to factors such as pile slenderness (L/D), sand relative density (D_r) or clay apparent over-consolidation ratio (YSR). Existing offshore methods may be conservative in some cases, including low L/D piles in dense sands or high YSR clays, and non-conservative in others, such as slender piles driven in loose sands or low YSR clays.

---

[1] The Coefficient of Variation (COV) is defined as the standard deviation, s, divided by the mean value μ. In an ideal method μ should tend to unity and the COV to zero.

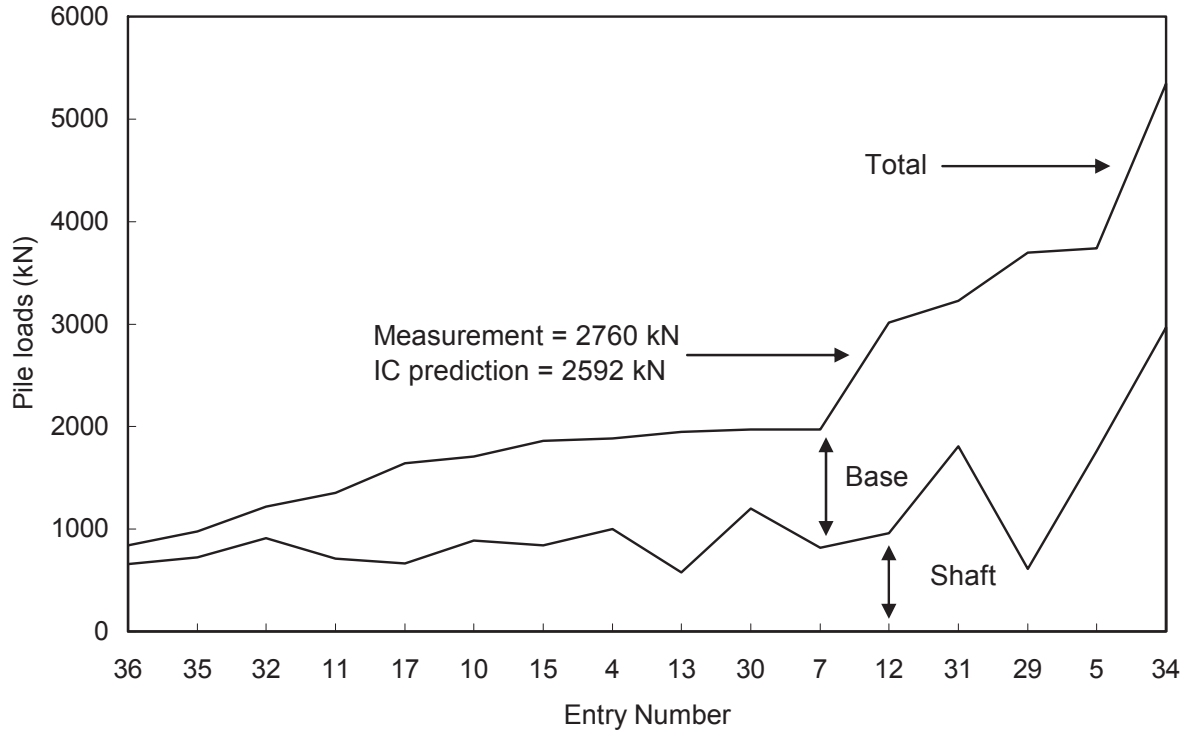

Figure 1. Results from pile predictions competition based on tests in Dunkirk sand; entries stacked in order of ascending total pile capacity estimate

Reports of piled structures experiencing difficulties due to axial capacity failures are rare. However, a clear need exists to improve predictive methods to obtain economies, where possible, and enhance performance, and safety, in other cases. The implementation of improved methods needs to be co-ordinated with any parallel developments in site characterisation techniques and the specification of loading. The latter applies particularly in cases involving high levels of environmental load, and caution is required when working with structural arrangements that impose unusual requirements on their foundations.

2.2 Imperial College research programmes

2.2.1 Research aims

The research carried out at Imperial College has sought to achieve: (i) a more fundamental and thorough understanding of pile behaviour, and (ii) practical design methods that capture the basic mechanics of driven piles as simply as possible. The main tasks were to identify:

- How piles behave in different soils and layering sequences.
- The scaling laws that relate the behaviour of models to that of full-scale piles.
- The effects on capacity of pile properties (dimensions, wall thickness, end conditions, surface roughness, material hardness, etc.) and installation methods.

- Any changes in capacity and stiffness associated with time after pile installation.
- The response to different loading types, including group effects, cyclic loading and seismic action.
- The controlling soil parameters that should be measured in site investigations.

The research reached a sufficiently developed state in 1996 for it to be applied practically. Ample scope remained then, and now, for further discussion and research; several issues remain open to academic discussion and potential improvement. However, as set out below, the ICP methods offer substantially increased overall accuracy and hence tangible engineering benefits in improved reliability and cost-effectiveness. They have also been widely applied and tested in practice since the mid 1990s.

2.2.2 Research phases

The research at Imperial College has taken place in five main phases, principally involving the sites and profiles identified in Table 1 and Figure 2, but also supplemented by data gathered at other locations ranging from Belfast to Mexico City.

The first phase of work involved developing the ICP instrumented piles and experimental procedures. Multiple ICP tests and other experiments were then performed at the Building Research Establishment's (BRE) Canons Park test site. The research was summarised by Bond (1989) and Bond and Jardine (1990, 1991).

Figure 2. Locations of ICP test sites in UK and France

The scope was broadened in Phase 2 to cover tests in sand at the French Ponts et Chaussées' test site at Labenne, the BRE's stiff till site at Cowden, and the Engineering and Physical Sciences Research Council's (EPSRC) former national soft clay test site at Bothkennar. At each location an advanced site investigation was performed, a field pile testing facility established, and a programme of multiple (closed-ended) ICP tests carried out. The Phase 2 work was reported by Lehane (1992) and Jardine and Lehane (1994); clear and striking results emerged from the experiments that allowed new design approaches to be proposed for closed-ended piles (Lehane et al., 1993; Lehane and Jardine, 1994a, b). The tentative proposals of Lehane and Jardine (1994c) and Lehane et al. (1994) provided many of the key elements of the later 'MTD' procedures.

The third phase reported by Chow (1997) and Chow and Jardine (1996) involved:

- Establishing facilities and performing advanced site investigations and multiple ICP tests at the Pentre (clay-silts/laminated clays) LDP research site and at the Dunkirk 'CLAROM' dense sand research site.
- Interpreting and performing tests on full-scale driven open-ended piles (with diameters up to 760 mm) at the ICP sites to assess the effects of scale, installation methods and pile-end conditions.
- Field experiments to assess pile group and ageing effects in dense sand.
- Using the above to refine the new approaches for closed-ended piles and extend the design methods to cover open-ended driven piles.
- Collating an up-to-date and critically approved database of full-scale pile tests that met rigorous quality criteria.
- Using the above to calibrate and validate the new methods for a wide range of practical applications.

Phase 4 (Jardine & Standing, 2000) comprised research on full-sized piles performed at Dunkirk between 1998 and 1999. Eight 456mm OD open-ended piles (six of which were 19m long, two 10m long) were driven to examine the effects of cyclic loading, pile age and base grouting.

The fifth phase of relevant work at Imperial College work involved a number of smaller projects conducted (often in collaboration with other groups) between 1997 and 2003:

- Studies by Thompson (1997) into driven pile capacity in calcareous sands and by Cowley (1998) into the effects of pile shape on axial capacity.
- Field tests with Trinity College Dublin (TCD) on square section concrete piles driven in soft Belfast clay to examine group action, cyclic loading and pile ageing (see Lehane and Jardine 2003 and Lehane et al., 2004).
- Field tests in collaboration with the Building Research Establishment at Canons Park to investigate long-term pile ageing effects in clay (Pellew, 2002).
- Research into the effects of pile shape, clay type and seismic/cyclic action for piles driven in Mexico City (Saldivar-Moguel, 2002).
- Further research into the interface shearing properties of clays and sands.
- Application of the pile design procedures to circumstances and combinations of soil conditions that were not covered by the range of tests collated by Chow (1997), including the reuse of pile foundations in construction projects.

2.2.3 Field tests with instrumented piles

A central feature of the first three phases of research has been the development of the accurate and reliable on-pile Imperial College Pile (ICP) instrumentation to study the pore pressures, radial total stresses, local shear stresses and temperatures developed on pile shafts. Until reliable instruments became available, the stress conditions surrounding driven piles had been open to conjecture. The ICP gauges were mounted on 6 to 20 m long, 102 mm diameter, closed-ended[2] steel pipe piles for intensive testing programmes in the geotechnical profiles summarised in Table 1. The ICPs were installed by fast jacking, allowing comprehensive measurements of the effective stress conditions developed close to the shafts to be made at multiple levels during installation, long-term equalisation and load testing to failure. In particular, it was possible to make direct measurements of the residual loads set up by installation, a feature that is often hard to assess in conventional pile tests.

Detailed site investigations were performed at each site, involving in-situ tests and advanced laboratory experiments. 'Strain Path Method' numerical simulations of the ICP tests performed at Canons Park and Bothkennar were also carried out in conjunction with Professor Whittle from MIT as described by Bond (1989) and Lehane (1992).

Table 1. Summary of Imperial College pile research sites

Site	Soil conditions
1. Canons Park	London Clay: stiff to very stiff, high plasticity, Eocene marine clay; high YSR
2. Cowden	Cowden till: stiff to very stiff, lean, glacial lodgement till; high YSR
3. Bothkennar	Carse clay: soft, high plasticity, moderately organic, Holocene shallow-marine/estuarine clay-silt, lightly cemented: moderate YSR
4. Labenne	Dune sand: loose to medium dense, medium-sized, Holocene; low YSR
5. Pentre	Glacio-lacustrine clay-silt and laminated clays: very soft to firm, low plasticity, low YSR
6. Dunkirk	Marine sand: dense to very dense, shelly medium-sized sand, Flandrian: low YSR

Note: Yield Stress Ratio (YSR) is the apparent OCR

2.2.4 Parallel experiments with field-scale driven piles

As mentioned above, less heavily instrumented open-ended driven tubular piles were driven and tested at four of the ICP sites, providing data with which to check the potential effects on axial capacity of pile tip detail and installation method. Offshore scale open-ended piles had been tested at Pentre as part of the Large Diameter Pile (LDP) project described by Clarke (1993), while those at Dunkirk and Cowden were installed for earlier projects run by the CLAROM group and BRE respectively.

[2] The use of closed-ended piles allowed more accurate and robust instrumentation to be deployed.

The Canons Park driven piles were installed by the Imperial College research team and the same group worked with full-scale driven tubular piles at Dunkirk between 1998 and 1999 to study cyclic loading, pile age and base grouting. Recent research on driven square section solid piles, performed with Trinity College Dublin (TCD), has examined the effects of group action, cyclic loading and pile ageing at the Kinnegar soft clay site in Belfast (see for example Lehane et al., 2004). Other projects have investigated the effects of ageing in London Clay and pile shape, seismic action and cyclic loading in Mexico City clay.

3 DESIGN METHODS FOR PILES IN SILICA SAND

3.1 Introduction

The following paragraphs describe the methods proposed for evaluating the short-term static axial capacity of single displacement piles in silica sands. Shaft friction and end bearing are covered under separate headings. Attention is concentrated first on cylindrical piles, with either closed or open ends, before discussing how capacity may be assessed for rectangular or H section piles. Subsequent sections discuss the predictive methods required for calcareous and micaceous sands.

Recent research and experience shows that pile capacity varies with age and testing style. The methods set out below are intended to predict the capacities that may be mobilised in slow maintained load tests, conducted around ten days after driving[3], on previously un-failed piles. The calculation procedures are intended to be compatible with modern pile testing practice, which includes pause periods that allow creep straining to stabilise between loading increments.

Section 4 sets out the equivalent procedures for piles driven in clay, while Section 5 offers an assessment of how well both sets of the predictive equations compare with an updated assembly of pile load tests. The later Sections (6, 7 and 9) consider the effects of age, group action and cyclic loading. Section 8 comments on the methods' use in micaceous and calcareous sands; silts and low plasticity clays; diatomaceous clays and mudstones; layered soil profiles. Worked examples covering both a sand and a clay site are included in Appendix B.

3.2 Shaft friction

3.2.1 Basic mechanisms

The ICP experiments at Labenne and Dunkirk showed that at failure the local shear stresses acting on the pile shaft, τ_f, follow the simple Coulomb failure criterion:

$$\tau_f = \sigma'_{rf} \tan \delta_f$$

The radial effective stress acting on the shaft at failure, depends on σ'_{rc} the equalised value acting a few days after installation (when pore pressures and radial stresses are relatively stable) combined with any changes developed during pile loading. The δ_f term represents the operational interface angle of friction. With sands this is the ultimate value δ_{cv}, which is developed when the soil at the interface has ceased dilating or contracting. The external shaft capacity, Q_s, is obtained by integrating τ_f over the external pile area.

---

[3] Note that this time is shorter than the 50 days originally specified by Jardine and Chow (1996).

The interpretation of the instrumented pile tests at Labenne led directly to new proposals by Lehane and Jardine (1994c) that gave greatly improved predictions for nine case histories involving closed-ended piles driven in sand. The research by Chow (1997) at Dunkirk covered a wider range of conditions, including large open-ended piles and dense sands, leading to the revised set of recommendations summarised in Table 2. As described later, the experiments at Dunkirk showed that for a given set of conditions, τ_f and σ'_{rf} increased when: (i) other displacement piles were installed nearby, and (ii) the piles were allowed to age in situ. As detailed in Section 6, research at Dunkirk has emphasised that a full failure of the pile shaft leads to a loss in load carrying capacity, with markedly lower τ_f and σ'_{rf} values being available in immediate re-tests. However, the radial effective stresses appear to recover partially with time. Shaft failure and ageing are not thought to affect δ_{cv}. Site specific CPT profiles are vital when applying the ICP approach. While q_c values may be estimated on the basis of SPT or other in-situ test data, the calculations will inevitably be less reliable and consideration should be given to raising design safety margins or performing additional site testing.

3.2.2 Evaluating short-term shaft capacity of single cylindrical piles

Table 2 sets out the key steps required to evaluate shaft capacity, Q_s. Important points to note are:

1. When summing the shear stress contributions as shown in Step A1, the shaft should be divided into sufficiently short sections to cope with the soil layering and variations of the key parameters: σ'_{v0}, q_c, and δ_{cv}. Typical calculations require at least 15 sub-divisions, even when the profile is relatively uniform. Smaller increments are recommended near the pile tip.

2. The local values of σ'_{rc} vary strongly with sand relative density, as reflected by the local CPT tip resistance, q_c. They are also highly sensitive to the relative pile tip depth, h, as defined in Figure 3. The radial effective stresses developed at any given depth decline sharply as the pile tip is driven on past that depth level and h increases. This feature, which may vary with the installation method, pile shape and sand properties[4], is the cause of the well-known tendency (in uniform sands) for the average τ_f to reach a quasi-constant limit once a "critical depth" of around 10D has been exceeded. Quasi-constant average τ_f values can be developed in a uniform layer even though the local values of τ_f applying at any fixed distances above the pile tip increase with penetration depth.

3. The effect of the relative pile tip depth on closed-ended piles is accounted for in Table 2 by the h/R term specified in Step A3. Note that a power function is specified that tends to infinity as h/R tends to zero. It is recommended that σ'_{rc} should be computed assuming a lower limit of h/R = 8, although experiments with small model piles suggest that a lower cut-off point may be justified.

---

[4] The interacting causes of the decay of σ'_{rc} with h are considered to be: (i) the extreme stresses developed near the pile tip (during installation) decaying rapidly with upward distance h along the shaft, (ii) the accumulating effects of load cycling on sand layers above the tip, and (iii) the development of circumferential arching above the tip shielding the shaft from a higher ambient radial effective stress field. It has also been suggested that the outward migration of fines generated by particle crushing may play a role (White and Bolton 2002). Recent centrifuge tests by White and Lehane (2004) have underlined the importance of the load cycling, noting that the radial effective stress distributions may vary systematically with the number of cycles applied by the installation procedure.

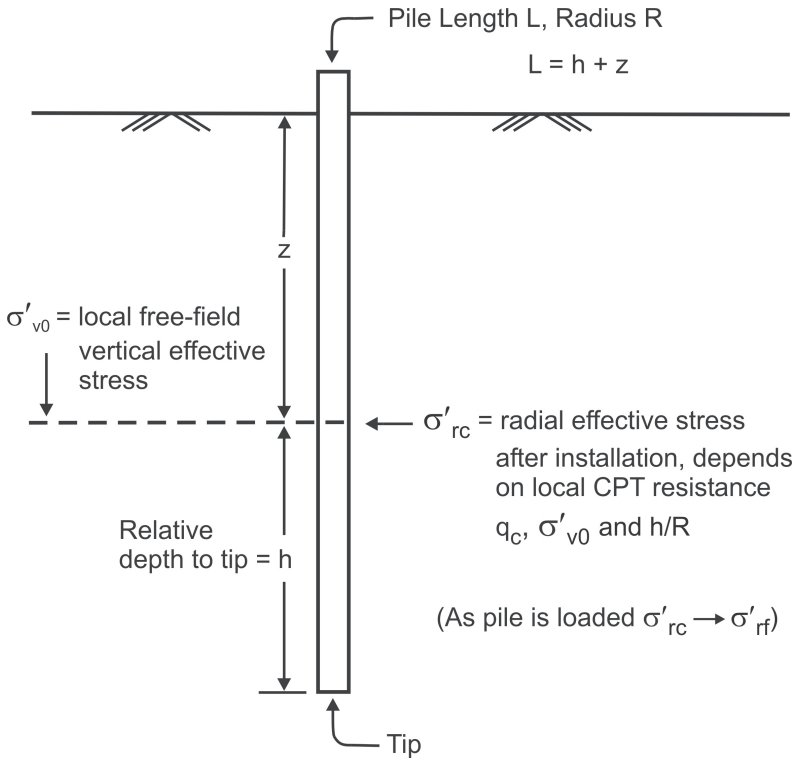

Figure 3. Definitions of parameters for radial effective stress expression

4. Open-ended piles can develop shaft resistance components over their inner surfaces as well as their exterior shaft areas. Our analyses indicate that the inner shaft components are concentrated near to the pile end, and for simplicity we consider these components as contributing to the overall base and external shaft components. These shaft and base contributions are then calculated in a similar way to those applied to closed-ended piles.

5. Tests on open-ended piles indicate a more rapid reduction in σ'_{rc} with h (at any given depth) than expected by Equation A3. The term R^*, defined in Step B3, is substituted for R in the expression for σ'_{rc} leading to a rate of decay with h that depends on the pile wall thickness. As with Step A3, a minimum of eight is specified for h/R^*. R^* is the radius of an equivalent solid pile that has the same solid cross-sectional area as the open-ended pile. The R^* substitution originates from constant volume deep penetration analyses (Chin 1986 and Aubeny 1992) with the Incremental Filling Ratio (IFR, internal core length increment per unit pile penetration) taken as unity. More sophisticated treatments might attempt to account for partially plugging cases where IFR < 1.0, leading to more gentle decays of σ'_{rc} with h. Lehane and Gavin (2001) note that with small diameter piles, driving gives higher IFRs (i.e. less plugging) than jacking. Step B3 was first checked against the stress distributions inferred from tests at Dunkirk on mainly coring open-ended driven piles. It has led since to good shaft shear stress predictions for a wide spread of field data, including the EURIPIDES cases; see Appendix B.

6. The ICP field tests showed that the radial effective stresses, σ'_r, on the shaft undergo changes $\Delta\sigma'_r$ during loading to failure. The main component of change seen in compression tests (on piles in both initially loose and dense sands) was interpreted as $\Delta\sigma'_{rd}$ that is associated with

constrained interface dilation during pile loading, although other changes may be taking place due to the general raising of the ambient stress regime caused by vertical shear stress transfer into the ground and any radial expansion of the pile shaft due to elastic 'Poisson' effects.

7. For slip to occur, a radial displacement, Δr, must develop in the thin interface shear zone that is similar in magnitude to the average peak-to-trough centre-line roughness of the pile surface, $2R_{cla}$. This displacement induces a reactive change in the surrounding soil mass causing a radial effective stress change $\Delta\sigma'_r$ that increases with the sand's global shear stiffness, but is inversely proportional to radius: $\Delta\sigma'_r$ may contribute less than 5% of the capacity for piles with diameters greater than 1m, but is important with medium-scale piles and can dominate the behaviour of small model piles. As specified in Step A4, $\Delta\sigma'_r$ may be estimated by the cavity expansion equation $\Delta\sigma'_r = 2G\,\Delta r/R$. Other procedures may also be applied[5].

8. Sand shear stiffness is known to be non-linear, pressure-dependent and anisotropic. In-situ shear wave velocity measurements, or small-strain laboratory tests, may provide direct information on the maximum values available in situ. In cases where reliable direct measurements of the operational shear modulus, G, are not available, estimates may be made from the CPT resistance, q_c, using an equation such as that specified in Step A4 (after Chow 1997).

9. Smaller values of σ'_r and τ_f develop in tension tests because shear stress transfer reduces the global compressive stress regime around the pile shaft, as do the effects of principal stress axis rotation and any elastic 'Poisson' radial contractions of the shaft under load as illustrated in Figure 4. The latter feature is most significant with tubular piles. Step A6 specifies how to allow for tension loading with closed-ended piles while in Step B3, a further reduction of 10% is recommended for open-ended piles[6].

10. Cowley (1998) developed proposals for how R^* may be defined for other pile geometries including square and H cross-sectional shapes, as described in Section 3.4.

11. The ultimate interface shearing angle, δ_{cv}, depends on the sand's grain size, shape and mineral type, and on the hardness and roughness of the pile's surface: it may also depend on the radial effective stress level. Jardine et al. (1992) investigated a range of clean standard test sands (and a silica silt) in constant normal stress direct shear[7] tests involving steel interfaces prepared with initial R_{cla} values between 6 and 10 μm. They found that δ_{cv} is (i) independent of initial relative density and (ii) increases with the relative roughness of the interface compared to the (current) grain size, which can be expressed for relatively uniform

---

[5] An alternative testing approach is to perform Constant Normal Stiffness (CNS) interface shear tests in which the normal stiffness (relating change in normal stress $\Delta\sigma'_n$ to change in sample height) is set at $2G/R$. However, it is necessary to know the design values of G, which will vary with depth and strain level, as well as the pile's radius R before performing the experiments.

[6] The actual 'Poisson effect' on σ'_r may be evaluated by calculating: (i) the profile with depth of pile axial force at full tension capacity, (ii) the corresponding profile of radial contraction, Δr, from the pile dimensions and elastic properties, (iii) the expected value of $\Delta\sigma'_r = 2G\,\Delta r/R^*$ (where $\Delta\sigma'_r$ and Δr are negative and G is found from Step A4, Table 2). The tension capacity may then be re-calculated iteratively.

[7] Conventional shear box interface tests are not reliable at normal stresses below 100 kPa.

sands as R_{cla}/d_{50}, where R_{cla} is the average centre-line roughness. Figure 5 reproduces the trend found for these standard test materials at typical operating stress conditions. Good matches were also found between field measurements made with the ICPs and site-specific direct shear interface tests for the medium-sized sands found at Labenne and Dunkirk. Shell UK Ltd has since conducted a large number of direct shear interface tests on natural sands from the North Sea. The data set of around 150 tests, concentrated in the $0.05 < d_{50} < 0.3$ mm size range, leads to the regression curve plotted on Figure 5 with $28^\circ < \delta_{cv} < 30^\circ$ and a milder dependence on particle size. The standard deviation in these results is around 2°.

12. Measurements on uncoated weathered industrial steel piles have shown R_{cla} values around 5 to 10 μm prior to installation. CUR (2001) note that driving in dense sand abrades the surface of steel piles, greatly reducing their maximum and average roughnesses. Finer particles are also generated through local crushing and CUR argues that all sands will tend to a constant δ_{cv} angle of around 29°. Ring shear interface tests, of the type described in Appendix A, can be used to assess how these processes might be combined in a sealed system, when many metres of relative displacement are imposed under constant normal stress. Coop et al. (2004) found that particle breakage plays a major role in such tests and that large shear displacements are necessary before a stable grading develops. Ring shear interface tests run recently at Imperial College on test sands and similar interfaces to those used by Jardine et al. (1992) show that, with a sealed system, prolonged shearing under high stresses reduces the dependence of δ_{cv} on initial particle size that was seen in the direct shear tests, giving a narrower spread of ultimate angles (around 26 to 30°). However, White and Bolton (2002) report from model pile tests that fines generated by crushing tend to migrate away from the sand-shaft interface zone as the pile is driven on. With relatively open coarse grained soils this process could lead to lower δ_{cv} values developing than expected from ring shear tests.

13. Site specific interface shear testing is highly recommended wherever feasible to allow for different stress levels, soil types and pile material characteristics. Pre-cast concrete piles may develop different δ_{cv} values to rusted steel piles, while steel mill-scale varnish, paint or any other coating left on a pile surface can reduce δ_f considerably[8]. Ring shear tests may give more representative pile design values for silts, and fine to medium sands. However, direct shear interface tests may be more conservative (and hence appropriate) for coarser soils. With fine to medium-sized sands the test types may give similar results.

14. As described later (in Section 6.1) the shaft resistance of piles driven in sand both grows and becomes increasingly brittle with time after driving. Repeat tests performed on aged piles show that they cannot mobilise the same peak resistance immediately after they have experienced a large displacement failure followed by unloading.

[8] Because coated piles have lower roughness R_{cla}, their dilatant components of effective stress change $\Delta\sigma'_{rd}$ are also lower than usual, leading to further reductions in shaft capacities.

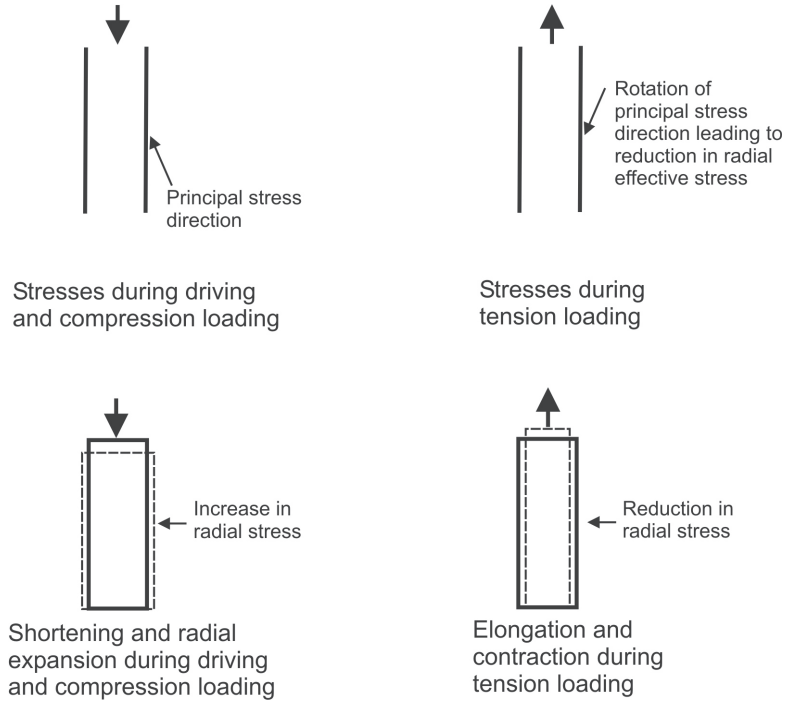

Figure 4. Changes in radial stress due to pile loading

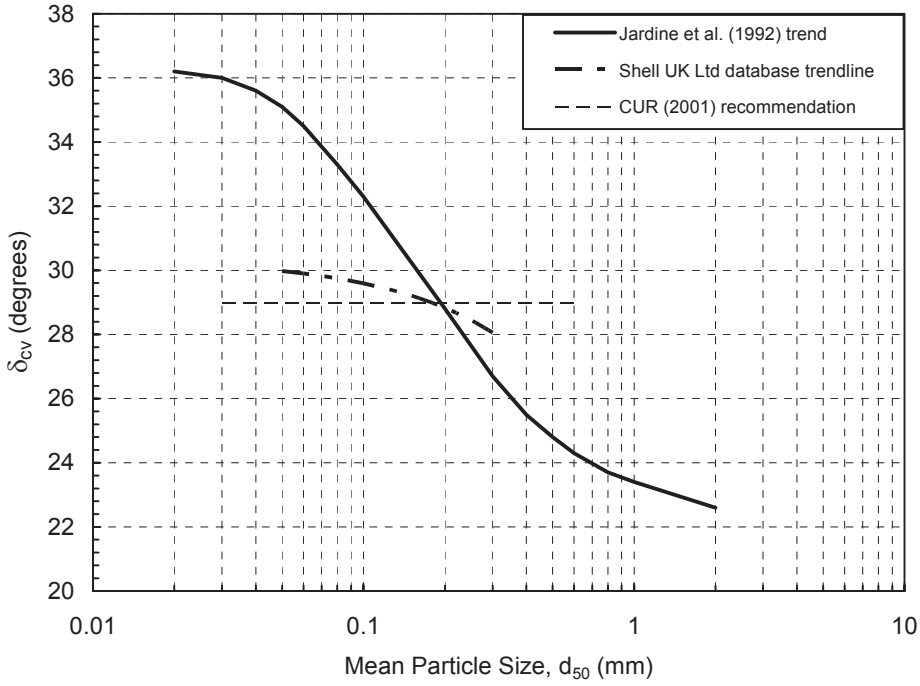

Figure 5. Interface friction angle in sand, δ_{cv}, illustrative trends from direct shear interface tests after Jardine et al. (1992) and Shell UK Ltd

Table 2. Procedures for shaft capacity calculations in sand

A	**SHAFT CAPACITY OF CLOSED-ENDED CYLINDRICAL PILES**	
A1	$Q_s = \pi D \int \tau_f \, dz$	**Shaft capacity** Integral of the local shear stresses along the embedded shaft length
A2	$\tau_f = \sigma'_{rf} \tan \delta_{cv}$ $\sigma'_{rf} = (\sigma'_{rc} + \Delta\sigma'_{rd})$	**Local shear stress** Coulomb failure criterion
A3	$\sigma'_{rc} = 0.029\, q_c\, (\sigma'_{v0}/P_a)^{0.13}\, (h/R)^{-0.38}$	**Local radial effective stress** Function of CPT resistance, free-field vertical effective stress σ'_{v0} (normalised by absolute atmospheric pressure, P_a= 100 kPa) and h/R; q_c is measured (not corrected for OCR) and h/R is limited to a minimum value of 8.
A4	$\Delta\sigma'_{rd} = 2G\, \Delta r / R$ $G = q_c\, [A + B\eta - C\eta^2]^{-1}$ where $\eta = q_c\, (P_a\, \sigma'_{v0})^{-0.5}$ A = 0.0203 B = 0.00125 C = 1.216e-6	**Dilatant increase in local radial effective stress during pile loading** Related to sand shear stiffness, pile roughness R_{cla} and radius. G taken from Baldi et al.'s (1989) correlation with CPT q_c. $\Delta r = 2R_{cla} \approx$ 0.02 mm for lightly rusted steel piles.
A5	δ_{cv} Measure directly in tests. If not feasible estimate from Figure 5	**Interface angle of friction at failure** Equal to constant volume value from interface shear tests, depends on pile roughness and other factors.
A6	$\tau_f = (0.8\sigma'_{rc} + \Delta\sigma'_{rd}) \tan \delta_{cv}$	In **tension loading** Equation A6 should be used in place of Equation A2.
B	**SHAFT CAPACITY OF OPEN-ENDED TUBULAR PILES**	
B3	$\sigma'_{rc} = 0.029\, q_c\, (\sigma'_{v0}/P_a)^{0.13}\, (h/R^*)^{-0.38}$ $R^* = (R^2_{outer} - R^2_{inner})^{0.5}$ **In tension** $\tau_f = 0.9(0.8\sigma'_{rc} + \Delta\sigma'_r) \tan \delta_{cv}$	**Modified radius, R***. Substituted into Equation A3 to give B3; $h/R^* \geq 8$. Shear stresses in tension reduced by a further 10%

Note: Above recommendations apply to (i) silica sands, (ii) piles with circular cross-sections (iii) capacities available in 'first-time' slow maintained loading tests conducted around ten days after driving.

3.3 Base resistance

3.3.1 Introduction

Theoretical investigations of deep penetration problems show that the surface shallow bearing capacity factors and arbitrary upper limits employed in some design codes are unlikely to be representative of field behaviour. Spherical cavity expansion solutions provide more useful analogues for closed-ended piles, indicating how pressure-dependent dilation characteristics, non-linear stiffness behaviour and anisotropic shear strength can all affect ultimate Q_b; particle crushing also plays an important role at the elevated stresses developed by piles in sand. These complex factors make theoretical calculations both difficult to perform and relatively unreliable.

The CPT test produces direct measurements of in-situ resistance under conditions that resemble closely those at a pile tip and this advantage is recognised in the Dutch and French national CPT based design approaches (de Ruiter & Beringen, 1979 and Bustamante & Gianeselli, 1982). The similar contained failure system and boundary conditions allow the CPT data to be used directly, without having to decouple the full set of complex soil parameters that determine both problems. The q_b values (where $Q_b = q_b \pi D^2/4$) observed during penetration in the ICP tests at Labenne and Dunkirk correlated directly with the q_c traces, as did the values developed in static load tests. However, the ICP tests could not show whether q_b/q_c varies with pile scale, or in-situ stress level. Nor could they offer insights into the base resistances of open-ended piles.

3.3.2 Closed-ended piles

Chow's assessment of work completed by others, and interpretation of the limited database of full-scale measurements, led to the provisional recommendations given in Table 3 where q_b is calculated as set out in Step C1. The approach relies on CPT measurements, incorporates a scale effect and distinguishes crucially between open and closed-ended piles. The aim is to predict the tip resistance Q_b available at settlements of up to $D/10$, allowing for its use in simplified calculation procedures that do not account for the different rates of development of shaft and base resistance, or the possibility of progressive failure. Higher base resistances will often be available in load tests that continue until an ultimate 'plunging' failure develops at much larger settlements. With closed-ended piles q_b/q_c is considered to be less than unity, with the ratio falling with pile scale, expressed here by diameter. Continuum based approaches do not predict any such scale effect for ultimate resistance and potential explanations for scale effects involve (i) reference to particle scale processes such as localised crushing zones or shear bands forming within the zone of contained failure beneath the pile tip (which could reduce the global influence of peak strength, stiffness and dilation rates), (ii) the definition of capacity as the load mobilised at a pile head displacement of $D/10$ and (iii) the effects of variations in sand state over short intervals of depth.

The approach taken to select appropriate q_c values from often variable CPT traces can have a considerable influence on the pile capacity calculations. Following from Bustamante & Gianeselli (1982), averaging q_c over 1.5 pile diameters above and below the pile toe is recommended for Steps C1 and D2, provided that (i) the variations in q_c are not extreme and (ii) the depth intervals between the peak and trough q_c values are no greater than $D/2$. A q_c value below the mean should be adopted for design if these conditions are not met as the base capacity may be controlled by a localised failure within any significant weaker layer. Equally, if the pile tip could possibly terminate within 8 pile

diameters of a consistently less competent stratum, then account should be taken of any potential reduction the lower layer might cause to end bearing capacity.

Alternative interpretations have been made of closed-ended driven pile databases assembled by Chow (1997) and others. Randolph, Jamiolkowski and Zdravkovic (2004) propose that q_b/q_c may be taken as 0.4 when designing closed-ended driven piles, the value found from Table 3 (Step C1) when D = 570 mm. Recognising their work, the lower limit given for q_b/q_c in Table 3 has been set at 0.3, corresponding to a 'cut-off' diameter of 904 mm. However, few reliable data points exist for driven piles with diameters greater than 600 mm and we are not aware of any test measurements on closed-ended piles larger than 1.2 m diameter. There is an urgent need for well designed field tests to clarify whether end bearing is affected by pile scale.

3.3.3 Open-ended piles

Open-ended tubular piles develop their base capacities through a combination of:

- The 'internal skin-friction' transferred through the internal soil column.
- Resistance beneath the annular area of the pipe.

The first component can make a substantial contribution (at pile head settlements of D/10) if strong arching develops at the base of the internal pile soil column. The arching action is enhanced by high values of φ', and strong dilation in the sand and at the internal pile interface, both factors correlate with high relative density. However, arching is likely to be less effective as pile diameter increases[9] and a simplified empirical plugging criterion is offered in Step D1, showing the minimum relative density required to achieve a full arch in a pile of given diameter; Figure 6 presents the field data from which this tentative criterion was inferred. The plugging action is likely to be highly sensitive to the soil conditions close to the pile tip and more research is required into the stress regime inside and around the potential pile plug.

The base response developed by a fully arching plugged pile is softer than that of a similar closed-ended pile because: (i) some local settlement is required to establish the arch, and (ii) the soil beneath the soil column has not experienced the same degree of pre-stressing and pre-stiffening during driving. Lehane and Gavin (2001) report that the base response of jacked piles that plugged during driving (giving final Incremental Filling Ratios[10], IFR ≈ 0) was far stiffer than that of similar piles that were driven with final IFRs ≈ 1.0. They argue that a coring penetration mode leads to far smaller residual loads, and that the latter reduce the resistance available at a displacement of D/10. Recording reliable IFR data is recommended: it can prove valuable to any subsequent re-assessment of capacity.

While fully plugged and closed-ended driven piles might develop similar 'plunging' ultimate base capacities after large settlements, Chow's interpretation of the available data shows that the 'fully plugged' end resistance mobilised at a settlement of D/10 is typically around half of that available for a closed-ended pile: Step D2 is therefore recommended when assessing the utilisable open-ended plugged capacity. The lower limit to q_b/q_c has been revised up to 0.15 (applying when D>0.90 m) reflecting the findings of Lehane and Randolph (2002) and Randolph, Jamiolkowski and Zdravkovic

---

[9] This conclusion is reinforced by the CLAROM research at Dunkirk (Brucy et al., 1991) and the GCG/Shell study described by Hight et al. (1996).

[10] IFR = $\Delta H_p/\Delta L$ where ΔH_p is the change in plug height and ΔL is the change in embedded pile length.

(2004) who propose q_b/q_c = 0.2 as a minimum value for open-ended piles. Step D2 also specifies that the fully plugged design capacity should be no less than the unplugged capacity calculated from Step D3.

It is recommended that Step D3 should be adopted if the pile is likely to core during static failure. Note that the full CPT resistance q_c is multiplied by the pile's 'annular area', despite the different shapes of the cone and pile annulus. Numerical analyses indicate that q_b/q_c is less than unity below the annulus and suggest a typical value around 0.7. However, the additional capacity computed by taking $q_b = q_c$ offsets the internal skin friction components that may not be accounted for by Step B3, Table 2. The additional 'end bearing' component is approximately equivalent to applying over the internal pile wall the (maximum) external shaft shear stresses (that apply at the tip) up to a level 30 to 40 wall thicknesses above the toe. Step D3 is considered to be marginally conservative, giving reasonable agreement with both the very sparse field static field test database and driving data obtained with large open-ended piles at several sand sites.

As before, the selection of appropriate q_c values should account for the form of the CPT traces. Because the postulated annular end bearing mechanism can develop over a relatively short depth range of perhaps three pile wall thicknesses, the design value should reflect the weakest sufficiently thick sub-layer within the soil unit in which the pile tip might credibly be terminated. Equally, consideration should be given to the possibility of a more critical fully plugged failure mode developing if a generally weaker layer exists within 8 pile diameters of the expected final tip depth.

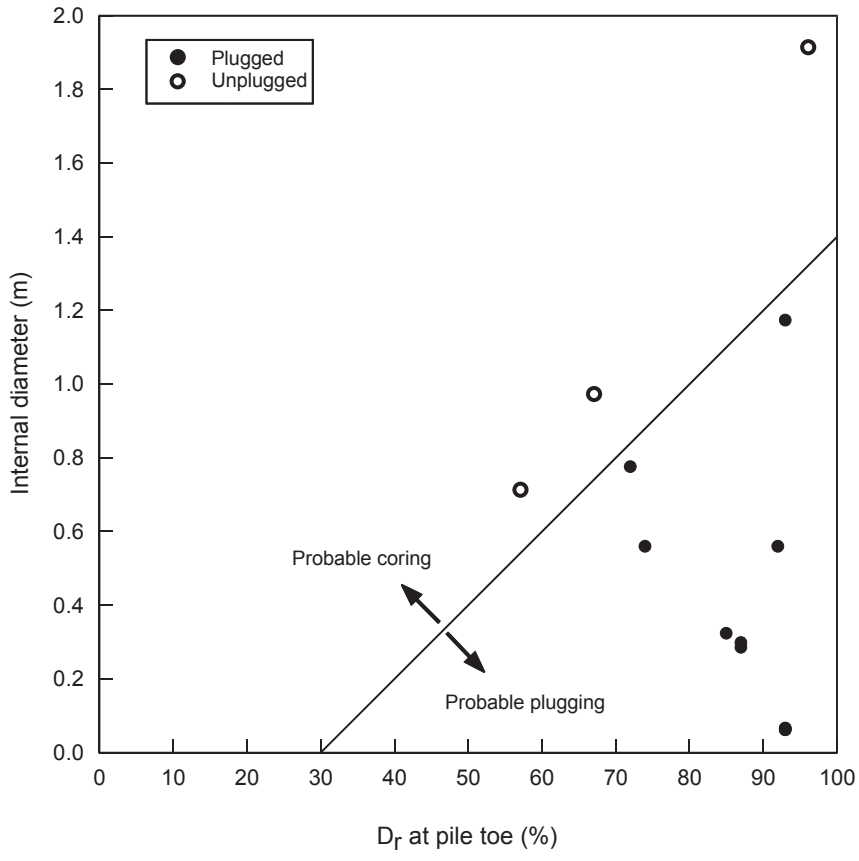

Figure 6. Field evidence for the adopted rigid-plugging criterion in sand

Table 3. Procedures for base capacity calculations in sand

C	**BASE CAPACITY OF CLOSED-ENDED PILES**	
C1	$Q_b = q_b \pi D^2/4$ $q_b = q_c [1 - 0.5 \log (D/D_{CPT})]$	**Pile base resistance** is related to the average CPT end resistance at the founding depth, and the relative pile and CPT diameters. A lower limit of $q_b = 0.30 q_c$ is suggested for piles with $D > 0.90$ m. See text regarding q_c selection $D_{CPT} = 0.036$ m.
D	**BASE CAPACITY OF OPEN-ENDED PILES**	
D1	$D_{inner} < 0.02 (D_r - 30)$ $D_{inner}/D_{CPT} < 0.083 q_c/P_a$	**A rigid basal plug** can develop during static loading if these criteria are satisfied. In the first equation D_{inner} is in metres and D_r in %. Absolute atmospheric pressure, $P_a = 100$ kPa.
D2	$Q_b = q_b \pi R^2_{outer}$ $q_b = q_c [0.5 - 0.25 \log (D/D_{CPT})]$	**Fully plugged piles** develop 50% of the end resistance of closed-ended piles of the same diameter (C1 above) after a pile head displacement of $D/10$. Two lower limits apply: (i) the fully plugged capacity should be no less than the unplugged capacity (D3 below) and (ii) q_b should not fall below $0.15 q_c$ (as predicted for $D > 0.90$ m). See text regarding q_c selection.
D3	$Q_b = q_{ba} \pi (R^2_{outer} - R^2_{inner})$ $q_{ba} = q_c$	**Unplugged piles** are assumed to sustain end bearing on the annular pile base area only with $q_{ba} = q_c$; see text regarding parameter selection. Contributions from internal shear stresses are not considered explicitly.

3.4 Axial capacity of piles with non-circular cross-sections

The ICP methods were originally developed to model tubular steel offshore piles. However, they are fully applicable to driven pre-stressed concrete pipe piles, and closed-ended driven cylinders made from steel or concrete. The rules are likely to be conservative for downwardly tapering, or stepped, driven piles that may develop less marked decays of radial effective stress with h, and hence higher capacities, than prismatic piles with constant cross-sections. However, modifications are required to allow the ICP approach to be applied to other common driven pile geometries such as solid rectangular section pre-stressed piles or H section steel piles.

Cowley (1998) considered how the ICP procedures might be applied to square and H section piles, and also to sheet piles. His approach was to assemble databases of reliable load tests from the literature and assess how well calculations predicted on alternative hypotheses corresponded to the available field data. His database for square piles amounted to a total of 16 tests in sand and clay, with a further 16 tests on H piles. These data populations are too low to define reliable statistics for particular cases and Cowley considered it appropriate to seek rules that were:

- compatible with the thrust of the ICP work;
- as simple as possible;
- equally applicable to sands and clays.

3.4.1 Recommendations for rectangular piles

Cowley's proposals for rectangular piles are set out in Table 4 in which equivalent effective shaft perimeters P and base areas A_b are defined that may be used in combination with the ICP rules for solid cylindrical piles. He found that R^*, the term that determines the rate of decay in σ'_{rc} with h in the shaft calculations could be calculated (as with open-ended tubular piles) as $R^* = [A_b/\pi]^{0.5}$. Note also that his database included no pile wider than 500 mm and that his base capacity formula includes no scale effect, but takes an average $q_b/q_c = 0.7$, which is equivalent to the ratio found from Table 3 Step C1 for $D = 143$ mm.

The proposals set out in Table 4 consider the general case of rectangular section piles (where breadth b may not be equal to width d), involving a slight extension of Cowley's results. As with cylindrical piles, the calculations are intended to predict the capacities mobilised in slow maintained load tests performed around ten days after installation. As detailed later in Section 5.6.1, the design rules provide a generally good fit to the load test database.

3.4.2 Recommendations for H section piles

Table 4 also summarises Cowley's proposals for H piles, defining their equivalent shaft perimeter P and base area A_b in terms of the geometry shown in Figure 7, following from De Beer et al. (1979). As before, R^* is calculated as $[A_b/\pi]^{0.5}$. None of the H section piles was wider than 535 mm and the base capacity formula assumes $q_b/q_c = 1$ with no scale effect. The expressions apply equally to sands and clays. As discussed later in Section 5.6.1, the recommendations give a satisfactory degree of fit to the database of 16 tests covering all material types.

Table 4. Recommendations for ICP method application to rectangular and H section piles: applies to both sands and clays; after Cowley (1998)

Parameter	Square or Rectangular piles	H piles
Dimensions Width	d	Geometry shown in Figure 7
Breadth	b	
Pile perimeter	$P = 2(d+b)$	$P = 2(D+B)$
Base Area	$A_b = d\,b$	$A_b = A_s + 2X_p(D-2T)$
		Where: A_s = Area of H section steel
(A_b definition for H piles after De Beer et al., 1979)		$X_p = B/8$ if $B/2 < (D-2T) < B$
		$X_p = B^2/[16(D-2T)]$ if $(D-2T) \geq B$
Shaft capacity Evaluated as specified in A1 to A6, Table 2, but with Modified Radius R^*	$R^* = [A_b/\pi]^{0.5}$	$R^* = [A_b/\pi]^{0.5}$ (A_b as defined above)
Base capacity Base capacities evaluated from local CPT resistance q_c, as shown opposite. q_c selection criteria as for cylindrical piles	$Q_b = 0.7 q_c A_b$	$Q_b = q_c A_b$

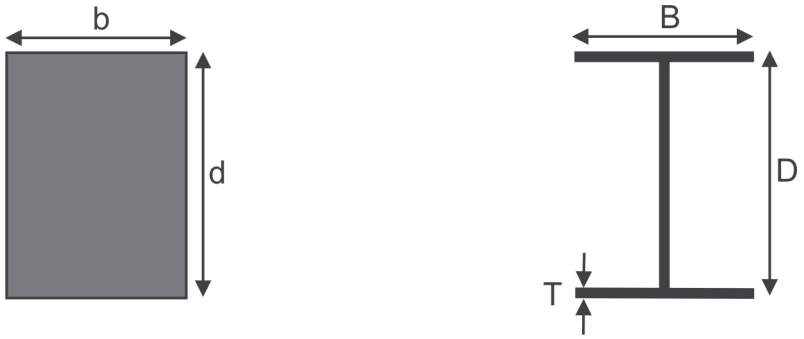

Figure 7. Geometry for rectangular and H piles

4 DESIGN METHODS FOR PILES IN CLAY

4.1 Introduction

The design methods for displacement piles in clay are set out below, following the format adopted earlier for sands.

4.2 Shaft friction

4.2.1 Basic mechanisms

Experiments at the four clay sites identified in Table 1 demonstrated that the conventional total stress 'alpha' methods of pile design are fundamentally flawed: local shaft failure is not controlled by the initial undrained shear strength (S_u) characteristics. The four sets of ICP tests proved that in clays, as well as sands, local shaft failure is governed by the simple Coulomb effective stress interface friction law:

$$\tau_f = \sigma'_{rf} \tan \delta_f$$

σ'_{rf} is the value of σ'_r developed at failure, and it differs slightly from the equilibrium value acting prior to loading: pile installation and subsequent equalisation lead to σ'_{rc} values that usually exceed 'free-field' horizontal effective stress σ'_{h0}; σ'_r can vary considerably during the potentially lengthy equalisation period.

Pile installation modifies the S_u profiles at points close to the pile and creates a generally weaker interface zone; the operational δ_f values bear no relation to the intact soil's S_u or S_u/σ'_{v0} values and the σ'_{rf} profiles are affected by parameters other than S_u/σ'_{v0}. As a result, the local ratios of $\alpha = \tau_f/S_u$ vary considerably with soil type and position on the pile shaft; values exceeding unity are possible under some conditions. While many practitioners choose to work with average 'alpha' ratios found from pile load tests, a wide range of local values may develop over the shaft of a single pile. It is difficult to apply the average ratio deduced from any particular test to other cases where the layering, length or diameter may be different.

A second problem with the conventional 'alpha' methods is the difficulty in defining S_u. Design profiles are usually developed from Unconsolidated Undrained (UU) triaxial tests, even though these may be severely affected by sampling disturbance, especially in some low plasticity, sensitive or cemented clays. Percussively taken samples are more affected than pushed, and thin-walled, sharp-edged, samplers induce less disturbance than thick-walled tubes. S_u is affected by re-consolidation procedure and K_0 reconsolidated triaxial compression (CAU) tests on high quality samples provide a more representative estimate of in-situ shear strength under triaxial compression conditions. Simple shear and triaxial extension tests on K_0 consolidated samples usually provide different S_u values due to

anisotropy and other factors. A strong strain-rate dependency affects CPT, field vane and T-bar tests, as do stress non-uniformity, soil brittleness and anisotropy, giving rise to considerable uncertainty in the choice of the N_k values (applied to CPT q_c values) or vane S_u correction factors μ_{vane}. Different q_c and μ_{vane} values apply to correlations made with either UU or CAU S_u values and different techniques can lead to very widely dispersed S_u profiles, and hence capacity estimates. The fundamental advantage of the approach described below is that it allows the local profiles of τ_f to be predicted reliably from effective stress principles, and the input parameters can be cross-checked in several ways.

Research by Lehane (1992) and Chow (1997) identified the factors that most affect the profiles of long-term, fully equalised, radial effective stresses σ'_{rc} expected on pile shafts. These profiles are expressed most easily in terms of the ratio $K_c = \sigma'_{rc} / \sigma'_{v0}$ expected at any given level. K_c was found to depend primarily on (i) the clay's local Yield Stress Ratio (YSR, or apparent OCR), (ii) its sensitivity and (iii) the relative pile tip depth, h. The latter dependency can be explained partially through two-dimensional strain path analyses of continuous penetration; the effects of extreme undrained cyclic loading during installation are also likely to be important contributors. Chow (1997) noted that piles jacked into the relatively permeable Pentre clay-silt underwent significant pore pressure equalisation during pauses in installation. Her investigation indicated that the decay of K_c with h increased with the number of installation 'dissipation' cycles. Randolph (2003) argued that the '*h/R*' dependence seen in the other ICP tests may have been affected by the ICP installation procedures. However, the same '*h/R*' dependency can be interpreted from driving records made during rapid continuous driving with larger piles at strongly layered clay sites. It is generally not possible to match the field capacity of driven piles through assessments that consider no '*h/R*' effect.

The peak and ultimate interface friction angles (δ_{peak} and $\delta_{ultimate}$) are measurable material parameters that cover a wide range (from 8° to 36°), depending on the soil type, prior shearing history and interface properties. Pile installation modifies the fabric of the soil around the shaft considerably and a ring-shear procedure that simulates these changes and gives appropriate design δ values is set out in Appendix A. Some clays show a ductile pattern of interface failure with little difference between δ_{peak} and $\delta_{ultimate}$. In other cases driving leaves the clay fabric close to the shaft in an imperfectly re-oriented state and δ_{peak} can be significantly greater than $\delta_{ultimate}$. Progressive failure can affect the capacity of long or compressible piles installed in such strata, with layers near the pile head reaching ultimate conditions before those near the toe approach their peaks. The latter feature can be accounted for in numerical procedures such as 'falling branch' *T-Z* calculations or strain-softening Finite Element analyses.

Allowance may also be made in simplified calculations by assessing the elastic shortening or extension of the pile under load. As failure is approached the pile shortening calculated at any given level provides an approximate estimate for the local pile-soil slip. Comparing the expected profile of axial pile movements with those required to progress from peak to ultimate conditions in site-specific ring shear tests allows the potential for progressive failure to be assessed in an approximate way. A safe lower limit approach is to adopt $\delta_{ultimate}$ along the whole pile shaft.

4.2.2 Evaluating shaft capacity of single piles after pore pressure equalisation

The first two phases of ICP research (at Canons Park, Cowden and Bothkennar) were used by Lehane (1992) and Lehane et al. (1994) to develop an ICP design method for fully equalised closed-ended piles in clay. A limited series of checks suggested that similar rules should apply to open-ended

driven piles. Chow's research at Pentre and re-analyses of other full-scale pile tests allowed a wider range of conditions including open-ended piles to be considered as outlined below.

The steps required to calculate the shaft resistance, Q_s, of displacement piles in clay after full equalisation are set out in Table 5. The main points to note are:

1. When summing the shear stress contributions as shown in Step E1, the shaft should be divided into sufficiently short sections to cope with the soil layering and variations of the key parameters: σ'_{v0}, YSR, S_t , h/R (or h/R^*) and δ. Typical calculations require at least 15 sub-divisions, even when the profile is relatively uniform. Smaller increments are recommended near the pile tip where K_c can vary rapidly with depth.

2. The ICP tests in clay showed that pore pressures and total stresses can vary during load tests, usually leading to reductions in σ'_r. In most cases σ'_r reduced by approximately $0.2\sigma'_{rc}$, or less. This factor is specified in Step E4 and is kept equal for tension and compression loading.

3. Laboratory ring shear interface tests that model the expected normal effective stress level, pile interface roughness, shearing history and rates of shearing provide the best means of predicting δ_{peak} and $\delta_{ultimate}$. Provided the procedures recommended by Ramsey et al. (1998) are followed, good agreement is typically found between results obtained with similar samples in different centres and with different apparatus. The scatter plots shown in Figures 8 and 9 (covering mainly inorganic clays) show that there is no universal or systematic link between PI and δ. We re-emphasise that site-specific ring shear interface testing is recommended for practical design and that predictive reliability is greatly reduced if these tests are not performed.

4. The ICP field measurements indicated that local δ values reduced from peak to ultimate conditions after 5 mm, or less, of local pile-soil slip displacement. With short rigid piles, capacity is dominated by δ_{peak} while the upper sections of long compressible piles may well develop sufficient slip to reach $\delta_{ultimate}$ over a considerable proportion of their shaft length. As mentioned above, T-Z, finite element or simplified elastic shortening analyses may be used to assess the potential degree of progressive failure.

5. The main factors that affect the profile of σ'_{rc} over the shaft of any proposed pile are the initial vertical effective stresses, σ'_{v0}, and the Yield Stress Ratio (YSR) = $\sigma'_{vy} / \sigma'_{v0}$. Care should be given in reviewing all the available geological, laboratory and in-situ test data when evaluating YSR. The vertical yield stresses σ'_{vy} may often be gauged from oedometer tests on good quality samples, provided these include a sufficient number of load steps and involve loading to a maximum stress greater than $5\sigma'_{vy}$. High-pressure tests may be needed to achieve such levels when dealing with stiff clays. Gently curving conventional e-log σ'_v plots[11] can lead to anomalous interpretations and natural scale, or log-log scale, data plots often provide clearer indications of yielding. If CRS oedometer tests are performed rather than 24 hour stage loading tests, account should be taken of the effects of strain rate on the recorded σ'_{vy} values.

6. Under-consolidated clays can be encountered where consolidation resulting from prior loading by man or nature is incomplete. In these cases YSR should be taken as unity and σ'_{v0} be evaluated from the total stress (computed from the bulk unit weights) minus the measured in-

[11] Such trends are often found with high YSR samples.

situ pore pressures. Yield stresses from high quality oedometer tests may also help in assessing the degree of potential under-consolidation.

7. With most low YSR deposits, and some high YSR clays, YSR may be estimated on the basis of the ratio of the undrained shear strengths developed in CAU compression tests (conducted under in-situ stress conditions) to the in-situ vertical effective stress σ'_{v0}. CAU S_u/σ'_{v0} ratios determined at suitable depth intervals can be expected to be related to YSR by relationships of the form:

$$S_u/\sigma'_{v0} = [S_u/\sigma'_{v0}]_{nc}\ YSR^{0.85}$$

Where $[S_u/\sigma'_{v0}]_{nc}$ is the value found from CAU compression tests on (K_0) normally consolidated samples and falls between 0.25 to 0.35 for a wide variety of soil types. Figure 10 illustrates such trends for two clays that did not form residual shear bands after developing moderate strains.

CAU tests on 'plastic' clays that can develop brittle shear bands (such as the London, Gault, Lias and Oxford Clays found in the UK) develop quite different patterns at YSRs greater than around 3. The shear bands truncate any dilatant behaviour and lead to lower than expected peak S_u values, causing the S_u/σ'_{v0} - YSR relationships to break down. Any such tendency can be diagnosed from the effective stress paths recorded during undrained shear tests on overconsolidated samples as illustrated in Figure 11.

8. UU triaxial tests are more commonly specified than CAU tests in practice but care is required when using them to determine YSR. The S_{u0}/σ'_{v0} values so obtained are more susceptible to sampling disturbance, the impact of which depends strongly on the clay's fabric and consistency. However, the shape of the UU S_{u0} depth profile developed in uniform, low YSR, strata can give useful information. Extrapolating the profile to project the distance above ground surface at which S_{u0} would equal zero can indicate the equivalent effective stress offset [σ'_{vy} - σ'_{v0}], that would match the combined effects of any prior erosion and/or cementing. The profiles of σ'_{vy} and YSR may then be evaluated for all depths within the linear profile. Following from (5) above, such an approach is not suitable for high YSR clays that develop residual strength.

9. In-situ CPT or field vane test profiles may also be used to estimate YSR. Where linear profiles are found in low YSR deposits, a similar projection to that described above may be employed. Alternatively, the more detailed recommendations of Lunne et al. (1997) may be applied to interpret CPT data. Provided the soil does not develop brittle shear bands, local calibrations between strength tests and either (i) total (or net) q_c values or (ii) field vane or other S_u data can be used to deduce S_u/σ'_{v0} ratios and the relationships plotted in Figure 10 applied to determine the YSR profile[12].

10. The remaining soil property terms required to complete Step E3 relate to the clay's sensitivity, S_t. The K_c values developed against piles driven in high sensitivity, low YSR clays may be half those developed in comparable, but insensitive, soils. The sensitivity of clays reflects their depositional conditions and post depositional history. Deepwater marine deposits often have sensitivities between 4 and 8, while clays deposited particularly rapidly or in higher energy tidal estuarine environments may be less sensitive. Glacial tills can show sensitivities around

[12] A more direct CPT based approach has been proposed by Lehane et al. (2000) for use when laboratory test data are sparse. This procedure is however generally less reliable than that of principal approach described above.

unity, or lower. In contrast, still-water glacio-lacustrine deposits can have sensitivities between 10 and 100, while 'quick' leached uplifted marine clays can develop still higher values.

11. Step E3 offers two ways of taking account of sensitivity, considering S_t up to ≈ 50. It is generally preferable to use the first K_c expression that includes the oedometer property ΔI_{vy}. Alternatively, the second expression involving the related parameter ΔI_{v0} may be used. Slightly different values may be predicted by the two expressions with the second typically leading to marginally lower values of K_c (around 4% lower on average; Chow, 1997).

12. The oedometer test 'sensitivity' parameters ΔI_{vy} and ΔI_{v0} are defined, as shown on Figure 12, in terms of the oedometer compression curves of: (i) undisturbed intact samples, and (ii) reconstituted samples undergoing virgin compression. The latter curve forms the Intrinsic Compression Line (or ICL, as defined by Burland, 1990) and C_c^* is the slope of the ICL in an e – $log\ \sigma'_v$ plot over the range 100 kPa < σ'_v < 1 MPa. The oedometer parameters ΔI_{v0} and ΔI_{vy} are less prone to error than direct strength measurements of S_t, although it can be useful to check design parameters by both strength and oedometer procedures.

13. Burland (1990) recommended that the ICL curve should be established directly by oedometer tests on reconstituted soil mixed from slurry at a water content of 1.25 times the liquid limit. If such tests are not available two empirical correlations exist between e^*_{100}, the void ratio at σ'_v = 100 kPa, and C_c^* (where e_L is the void ratio at the liquid limit):

$$e^*_{100} = 0.109 + 0.679e_L - 0.089e_L^2 + 0.016e_L^3$$

$$C_c^* = 0.256e_L - 0.04$$

Profiles of ΔI_{v0} can be derived from σ'_{v0} and soil index tests using the relationships given on Figure 12, recalling that $e_0 = w_0.G_s$ for saturated samples. Similarly profiles of ΔI_{vy} can be obtained if YSR and C_s are known.

14. Alternatively, the approximate relationship $\Delta I_{vy} = \log_{10} S_t$ can be substituted in Step E3. S_t is defined conventionally as the clay's peak intact (UU) S_{u0} value divided by its remoulded undrained shear strength, S_{ur}. It can be difficult to remould very stiff or hard specimens and, with low plasticity clays, S_{ur} may be affected by drying during remoulding. S_{ur} can be checked by reference to water content (w) and Atterberg liquid and plastic limit measurements (LL and PL) through the Liquidity Index LI correlation given by Wroth (1979), where:

$$LI = (w - PL) / [LL - PL]$$

$$S_{ur}\ (in\ kPa) = 1.7\ [10^{2(1\ -LI)}]$$

We recall from (6) and (7) above that peak S_{u0} values from UU tests are affected by disturbance and that high YSR 'plastic' clays tend to show S_{u0} values that are anomalously low; S_t values deduced from UU tests are as variable as the peak UU S_{u0} values. Uncertainties in S_t can be reduced by adopting peak S_u values from either CAU data or calibrated in-situ test data.

15. The reliability of the YSR and S_t design profiles can be maximised by synthesising all the available data, assessing the alternative interpretations critically, considering any anomalies carefully and ensuring that the overall interpretation is physically feasible and consistent with the site geology. Conservatism should be exercised in cases where the interpretation is insufficiently clear.

16. As in sand, open-ended piles driven in clay typically develop less shaft capacity than closed-ended piles. The substitution of R^* for R in the K_c equation, as set out in Step F3, models this trend by generating a steeper decay of K_c with relative pile tip depth, h. Square piles and H piles may be dealt with following the modifications specified earlier in Table 4 and Section 3.4.

Table 5. Procedures for long-term shaft capacity calculations in clay

E	**SHAFT CAPACITY OF CLOSED-ENDED PILES**	
E1	$Q_s = \pi D \int \tau_f \, dz$	**Shaft capacity** is found by integrating local shear stresses along the embedded shaft length.
E2	$\tau_f = \sigma'_{rf} \tan \delta_f = (K_f/K_c)\, \sigma'_{rc} \tan \delta_f$	**Local shear stress** is expressed using the Coulomb failure criterion, expanded in terms of loading factor, K_f/K_c and σ'_{rc} the local radial effective stress after equalisation.
E3	$\sigma'_{rc} = K_c\, \sigma'_{v0}$ $K_c = [2.2 + 0.016\, YSR - 0.870\, \Delta I_{vy}] YSR^{0.42}\, (h/R)^{-0.20}$ and $\Delta I_{vy} = log_{10}\, S_t$ or: $K_c = [2 - 0.625\, \Delta I_{v0}]\, YSR^{0.42}\, (h/R)^{-0.20}$	**Local radial effective stress after equalisation** σ'_{rc} is found from K_c and σ'_{v0}; K_c depends on Yield Stress Ratio (YSR), normalised distance from the pile tip (h/R) and sensitivity S_t expressed by ΔI_{vy} The alternative ΔI_{v0} expression is marginally less conservative. h/R is limited to a minimum of 8.
E4	$K_f/K_c = 0.8$	The **Loading Factor** is constant regardless of the direction of loading or drainage conditions.
E5	δ_f between δ_{peak} and $\delta_{ultimate}$	The **peak and ultimate interface angles of friction** are measured in interface ring shear tests as specified in Appendix A. The operational value depends on the degree of progressive failure, pile roughness, clay type and shearing history.
F	**SHAFT CAPACITY OF OPEN-ENDED PILES**	
F3	$K_c = f(h/R^*)$ where $R^* = (R^2_{outer} - R^2_{inner})^{0.5}$	K_c can be taken from either of the expressions in Step E3, with the substitution of the **equivalent radius, *R****, in the h/R term. A lower limit of $h/R^* = 8$ applies.

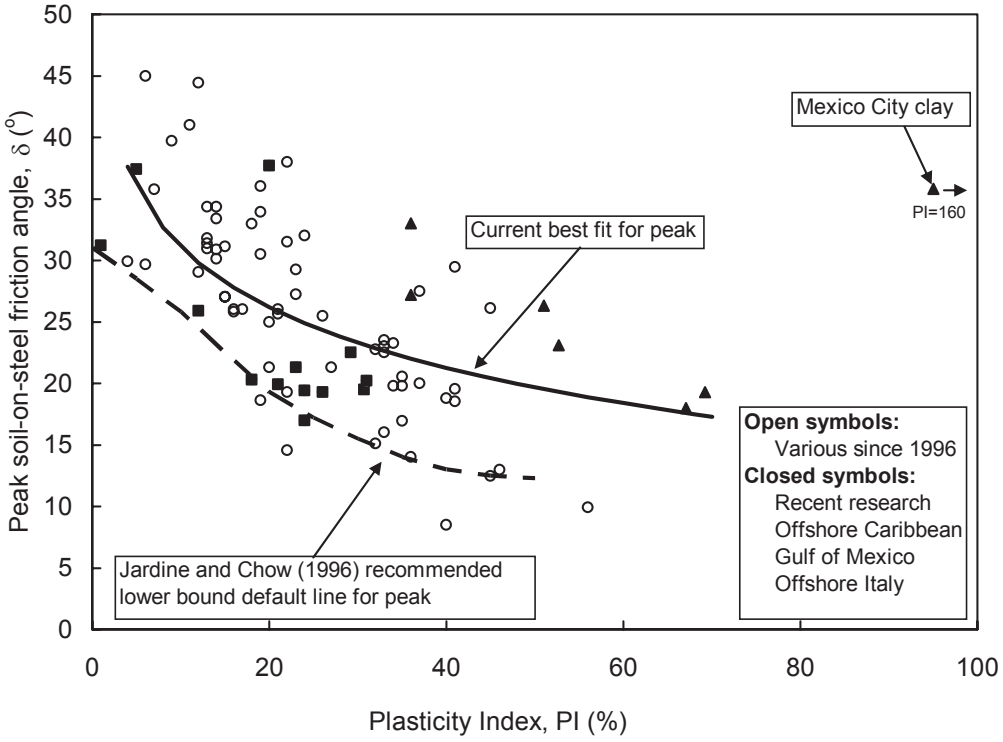

Figure 8. Ring shear interface results for δ_{peak} in clays after Saldivar-Moguel (2002)

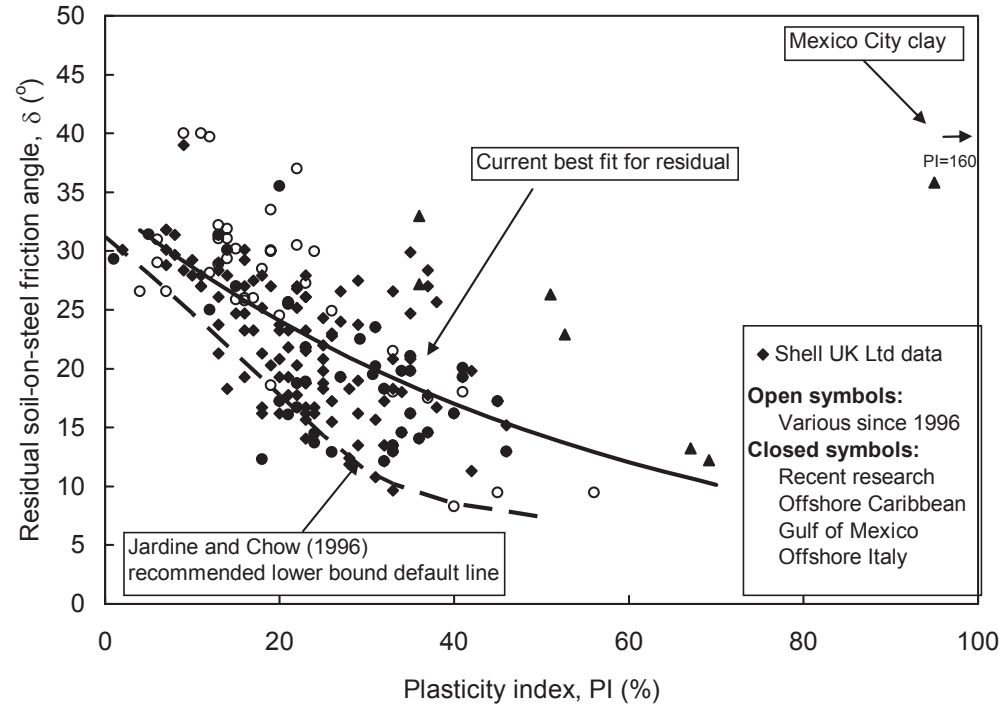

Figure 9. Ring shear interface results for $\delta_{ultimate}$ in clays after Saldivar-Moguel (2002) and Shell UK Ltd

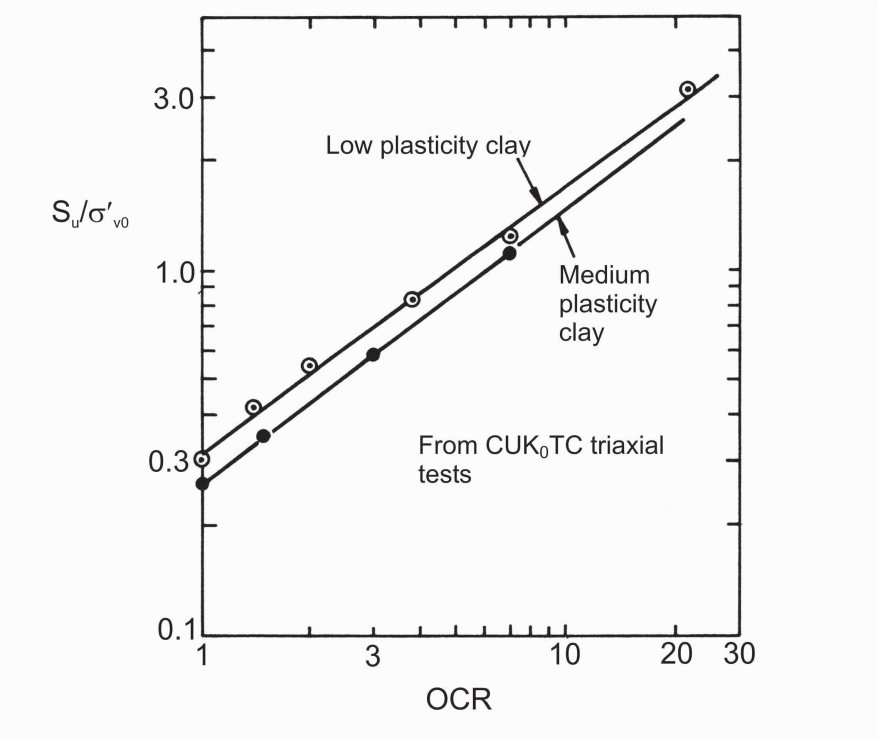

Figure 10. S_u/σ'_{v0} versus OCR for K_0 consolidated non-brittle clays in triaxial compression (Jardine 1985)

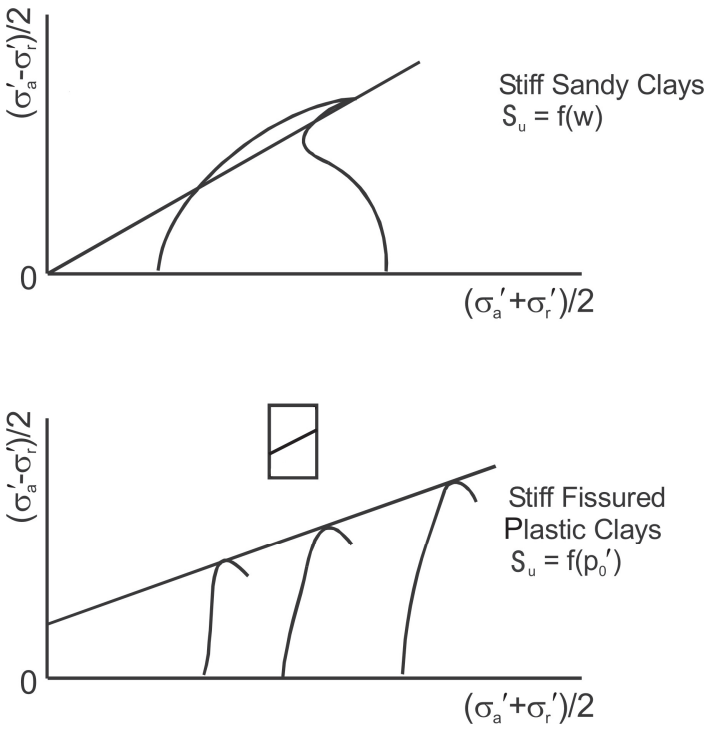

Figure 11. Undrained triaxial effective stress paths of (a) stiff clays that tend to critical state (above) and (b) those that develop residual shear strength (below)

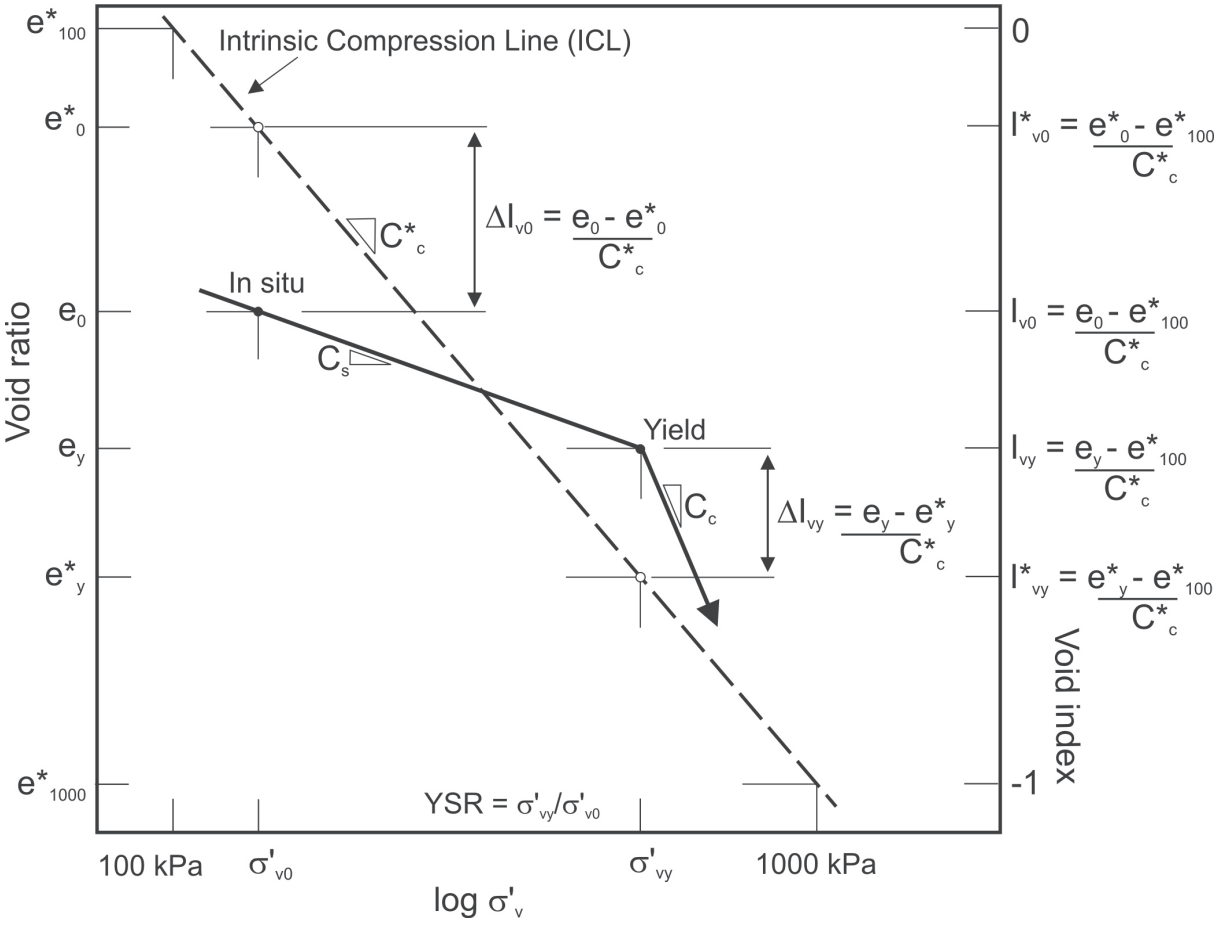

Figure 12. Definitions of intrinsic properties of clay relating to oedometer behaviour

4.3 Base resistance

As with sands, base resistance is mobilised in clays through a contained failure mechanism that depends on the pile geometry, the in-situ stress conditions and the soil's behaviour at both small and large strains.

Base resistance comprises a relatively minor part of the total capacity of most driven piles in clay[13] and is often mobilised at greater displacements than the shaft capacity, and so complex calculations that model the detailed soil response are rarely justified. With closed-ended piles Q_b is traditionally calculated assuming that a bearing pressure $q_b = N_c S_u$ (with $N_c = 9$) acts over the full base area. The 'internal shaft capacity', is also calculated for coring open-ended piles, and this value is adopted in design when it is less than Q_b.

However, the recent research demonstrates that the existing methods are far from ideal. No unique N_c value was found to apply and values far above nine were developed in all of the closed-ended ICP tests. Instead, q_b was found to be closely related to the CPT resistance developed at the pile tip level.

[13] On average, Q_b amounted to approximately 20% of Q_{total} in the authors' pile load database for clays.

Unlike shaft resistance, a clear trend was found for higher q_b values to be developed in experiments where loading was applied under effectively drained conditions.

The research also included an analysis of end bearing data from other high-quality field measurements, including large open-ended piles. While the conventional $q_b = N_c\ S_u$ approaches appeared to be reasonable on average, they led to a considerable degree of scatter. Applying the observations made in the ICP tests in an interpretation of the database led to the alternative design rules given in Table 6 that distinguish between drained and undrained loading and rely on CPT parameters being measured or projected from other test data. The end bearing rules developed to deal with H and square section piles driven in sand (see Table 4) are considered equally applicable to clays.

Table 6. Procedures for base capacity calculations in clay

H	**BASE CAPACITY OF CLOSED-ENDED PILES IN CLAY**		
H1	$q_b = 0.8\ q_c$	Undrained loading	**Pile base resistance** is controlled by CPT resistance at the founding depth and the drainage conditions during loading. q_c is averaged 1.5 pile diameters above and below the founding level.
	$q_b = 1.3\ q_c$	Drained loading	
J	**BASE CAPACITY OF OPEN-ENDED PILES**		
J1	**Plugging** during static loading can occur if: $[D_{inner}/D_{CPT} + 0.45\ q_c/P_a] < 36$ D_{CPT} = 0.036 m. Atmospheric pressure P_a = 0.1 MPa or 100 kPa.		
J2	$Q_b = q_b\ \pi\ D^2/4$		**Fully plugged piles** develop half of the end resistance of closed-ended piles given by Equation H1 after a pile head displacement of D/10.
	$q_b = 0.4\ q_c$	Undrained loading	
	$q_b = 0.65\ q_c$	Drained loading	
J3	$Q_b = q_{ba}\ \pi\ (R^2_{outer} - R^2_{inner})$		**Unplugged piles** sustain end bearing on the annular area of steel only. Base resistance is equal to average CPT end resistance at the founding depth. This may be increased by a factor of 1.6 for drained conditions. No specific allowance is made for the shear stresses developed on the pile's inner wall.
	$q_{ba} = q_c$	Undrained loading	
	$q_{ba} = 1.6 q_c$	Drained loading	

The alternative methods outlined in Table 6 represent provisional best estimates and the tentative plugging criterion given in Step J1 is wholly empirical. Further research is required to explore the basic mechanisms of internal shaft friction development and plugging. However, the remaining uncertainties are unlikely to have a major impact on practical design and the lower limit recommendation given in Step J3 should offer safe estimates for Q_b.

5 RELIABILITY OF THE DESIGN METHODS

Jardine and Chow (1996) assessed the ICP method's ability to predict medium-term, single pile shaft capacity against a large database of high-quality tests on piles driven at either sand or clay sites. Chow (1997) describes the database assembly, the site details and the quality criteria applied to the tests and associated site investigations. The exercise provided the key data from which provisional base capacity recommendations were developed. Shaft capacity predictions were made using a range of methods including the API (1993) recommendations[14], and the results were compared with the field load tests. The study showed that the ICP approach offered considerably better reliability and accuracy; it also provided a fully independent validation for the new shaft capacity procedures.

Naturally, new load test data have been generated since 1996, or made available to the public. We summarise below a number of significant new cases that have been considered by the Authors and added to Chow's original databases, including two cases where site re-assessments have been made on the basis of new site investigation data. The combined data sets are used to provide the Authors' updated assessment of the ICP procedures' predictive reliability. Consideration is then given to assessments by others of the ICP method's reliability before considering the choice of appropriate Factors of Safety for WSD (Working Stress Design) or Resistance Factors for LRFD (Load and Resistance Factor Design) approaches.

5.1 Additional entries to the Chow pile load test database

New load test and site investigation data are constantly being gathered and published. Tables 7 and 8 summarise nine cases where 'new' tests on piles driven in sands, gravels and clays have been evaluated by the present authors and their co-workers. In each case outline details are offered of the soil and pile types, of the capacity predictions offered by the ICP and API (1993) procedures and references to more detailed publications. Points to note in connection with the sand cases in Table 7 include:

1. The table does not include the Jamuna Bridge pile load tests involving micaceous sands that are described by Tomlinson (1996) and CUR (2001), or make any reference to calcareous sands. Pile capacity in these 'special' sands is discussed in later sections.
2. The table does not incorporate any of the tests on square piles identified by Cowley (1998) in his research on the effects of pile shape. However, as noted later (in Section 5.6.1) his proposals provide a marginally conservative fit to the available data.
3. The Leman case entry refers to the updated analysis given by Jardine et al. (1998b).

[14] The American Petroleum Institute (API) 1993 recommendations have been considered generally as the international standard method for designing large driven piles.

4. The recent pile tests at Dunkirk (Jardine and Standing, 2000) focused on the strong effects of time on shaft capacity. Attention is concentrated in Table 7 on tests conducted at relatively early ages, more discussion is offered later on the time effects shown by tests on aged piles.
5. The important EURIPIDES research tests (Zuidberg and Vergobbi, 1996; CUR, 2001) in dense sand are considered in more detail as worked calculations in Appendix B. Several independent workers have reported ICP calculations that match the EURIPIDES field data well, demonstrating that the ICP approach is not unduly 'operator dependent'.

Table 8 summarises the additional clay case histories and references, showing predictions from the ICP and API (1993) methods. One factor that has restricted the size of the available clay data set for the ICP evaluation is the lack of site-specific ring shear interface tests, along with reliable YSR and sensitivity data. Points to consider in connection with the new and modified entries include:

1. Saldivar-Moguel (2002) included suites of ring shear, oedometer and other tests in his evaluation of the ICP's applicability to square concrete piles driven in Mexico City clay, working with four sets of samples covering a typical range of plasticity indices (between 150 and 240%). His combined data set comprised 26 pile tests taken from many different sites on four major projects. Partial pre-boring to reduce driving disturbance is common in Mexico City foundation engineering and Saldivar-Moguel used model test results to estimate the effects on shaft capacity. Checks with the ICP and API procedures, applying the same pre-boring corrections, led to generally good agreement with the ICP and a relatively low mean Q_c/Q_m with the API.
2. We are not aware of any other field data on the potential effects of pile geometry or pre-boring and site-specific pile load tests are recommended whenever such non-standard pile installation techniques are employed.
3. Interface ring-shear experiments and index tests have been carried out recently at Imperial College to help apply the ICP approaches to pile load tests conducted at the Gulf of Mexico (WD58A), Norwegian (Onsøy) and Northern Irish (Kinnegar) sites listed in Table 8. Appropriate spreads of samples were available for the WD58A and Kinnegar cases, while the Onsøy tests had to concentrate on a single depth[15].
4. New laboratory tests have also been performed on samples from the Norwegian Geotechnical Institute's Lierstranda site. As discussed by Karlsrud et al. (1993) and Clausen and Aas (2001) the shaft capacities developed in this very low plasticity, low YSR, clay-silt are exceptionally low; Lierstranda is considered separately in Section 8.3.2.

[15] The sample's Atterberg limits (*LL* and *PL* at 70% and 30%) fall slightly above the mean for the deeper Onsøy layers. The measured ring-shear interface δ, of 28.5º, is higher than expected. An average δ of 23º is required to give $Q_c = Q_m$.

Table 7. New sand data considered by Authors: total capacity

Site: Hound Point Jetty				**Reference:** Williams et al. (1997) Stratigraphy: Very soft clay over medium dense/dense gravel and cobbles					
Pile type	2 steel pipes			Predictions	ICP			API	
No. of tests	3			Q_c/Q_m mean	1.02			1.68	
Pile OD, m	1.22			Q_c/Q_m range	0.89 to 1.19			1.17 to 2.25	
Pile Lengths, m	26, 34 & 41			COV	0.15			0.32	
Site: Sungai Perak Bridge				**Reference:** Williams et al. (1997) Stratigraphy: Medium dense gravelly sand					
Pile type	2 steel pipes			Predictions	ICP			API	
No. of tests	4			Q_c/Q_m mean	1.11			2.08	
Pile OD, m	1.5			Q_c/Q_m range	0.82 to 1.50			1.64 to 2.89	
Pile Lengths, m	33 & 38			COV	0.31			0.34	
Site: EURIPIDES Research Tests				**Reference:** Zuidberg & Vergobbi (1996); CUR (2001) Stratigraphy: Loose sand & clayey sand over very dense sand					
Pile type	2 steel pipes			Predictions	ICP			API	
No. of tests	8			Q_c/Q_m mean	0.97			0.58	
Pile OD, m	0.763			Q_c/Q_m range	0.78 to 1.12			0.43 to 0.89	
Pile Lengths, m	30.5, 38.7, 47 & 46.7			COV	0.13			0.26	
Site: Dunkirk Research Tests				**Reference:** Jardine & Standing (2000); Jardine et al. (2001) Stratigraphy: Medium dense to dense marine sand					
Pile type & OD	Steel pipe 0.457m			Predictions	ICP			API	
Test	C1	R1	R6	Test	C1	R1	R6	C1	R1	R6
Test delay, day	68	9	80	Q_c/Q_m	0.57	0.91	0.54	0.39	1.01	0.54
Pile Length, m	10	19	19	Q_c/Q_m age adjusted	0.85	1.0	1.0			
Site: Leman BD Platform, North Sea				**Reference:** Jardine et al. (1998b) Stratigraphy: Medium dense to dense marine sand					
Pile type	Steel pipe			Predictions	ICP			API	
No. of tests	1			Q_c/Q_m	1.05			0.94	
Pile OD, m	0.66								
Pile Length, m	38.1								

Table 8. New clay data considered by Authors: total capacity

Site: Mexico City Database Partial pilot hole pre-bores Calculated base resistance deducted		**Reference:** Saldivar-Moguel (2002) Soil Conditions: Diatomaceous high plasticity low YSR clays; low unit weights and high ring shear δ angles		
Pile type	Concrete square	Capacity Predictions	ICP	API
No. of tests	26	Q_c/Q_m mean	1.06	0.91
Pile width, m	0.3 to 0.5	Q_c/Q_m range	0.69 to 1.28	0.51 to 1.31
Pile length, m	10 to 38	COV	0.16	0.21
Site: West Delta 58A, Gulf of Mexico Offshore pile tests		**Reference:** Bogard & Matlock (1998); Jardine & Saldivar (1999); Saldivar-Moguel (2002) Soil Conditions: Underconsolidated plastic clays		
Pile type	Steel pipe	Capacity Predictions	ICP	API
No. of tests	1	Q_c/Q_m	0.97	0.96
Pile OD, m	0.762			
Pile length, m	71.3			
Site: Onsøy Research Tests Pre-bored and cased starter-holes Soil plug removed for pipe pile		**Reference:** Karlsrud et al. (1993); Clausen & Aas (2001); Ridgway (2004) Soil Conditions: Medium plasticity low YSR clay		
Pile type	6 steel closed-end	Capacity Predictions	ICP	API
No. of tests	6	Q_c/Q_m mean	1.43	1.37
Pile OD, m	0.219	Q_c/Q_m range	1.26 to 1.63	1.16 to 1.76
Pile length, m	10 to 32.5	COV	0.09	0.16
Pile type	Steel pipe	Capacity Predictions	ICP	API
No. of tests	1	Q_c/Q_m	1.19	1.03
Pile OD, m	0.812			
Pile length, m	10			
Site: Kinnegar Research Tests Calculated base resistance deducted		**Reference:** Lehane et al. (2004); Strick van Linschoten (2004) Soil Conditions: Low YSR clay-silt Belfast "Sleech" (Vane S_u tests)		
Pile type	2 concrete square	Capacity Predictions	ICP	API
No. of tests	1 comp & 1 tens	Q_c/Q_m comp	1.08	1.64
Pile width, m	0.250 square	Q_c/Q_m tens	0.86	1.30
Pile length, m	6			

5.2 Reliability of shaft capacity predictions in silica sand

5.2.1 Shaft capacity database for silica sand

The expanded database of pile tests that was used to assess the shaft capacity calculations is summarised in Table 9. Note that in several cases piles tested in tension had been pre-tested in compression, or vice versa. As discussed later in Section 6, depending on the times allowed for recovery, the second test on each pile may have developed a capacity lower than that available to a fresh pile. In order to eliminate any over-dependence on a single test site a limit of ten was placed on the number of tests included from any single site. The ten tests chosen in such cases were selected to be as representative as possible.

Table 9. Summary of shaft capacity database: sand

	Closed	Open	All
Number of piles	41	40	81
Steel	30	39	69
Concrete	11	1	12
Tension tests	21	20	41
Compression tests	20	20	40
Average length (m)	14.0	26.4	20.1
Range of lengths (m)	1.8 - 34.3	5.3 – 47.0	1.8 – 47.0
Average diameter (m)	0.34	0.76	0.55
Range of diameters (m)	0.10 -0.61	0.32 - 2.00	0.10 - 2.00
Average sand density, D_r (%)	62	65	64
Range of D_r (%)	31 - 97	34 - 100	31 - 100
Average test time after installation	-	-	~25 days

5.2.2 Reliability of the ICP shaft method in sand

Table 10 summarises the $Q_{calculated}/Q_{measured}$ (Q_c/Q_m) statistics found for the ICP approach and the more routinely applied API (1993) methodology; the Coefficient of Variation (COV) is defined as the standard deviation, s, divided by the mean, μ. Ideally the mean of Q_c/Q_m should be close to unity and the COV (or s) should be as low as possible; the ICP method meets these aims far better than the API procedures. Figures 13 to 16 show scatter diagrams of (Q_c/Q_m) against D_r, and normalised pile length for the updated database. As in the 1996 evaluation, the ICP method eliminates the strong skewing produced by the API method and is equally reliable for open-ended and closed-ended piles. While the ICP method can be applied confidently to a wide range of conditions, the variability is likely to reduce when considering a sub-set of similar piles, as shown in Table 10 for open-ended piles driven in North Sea sands.

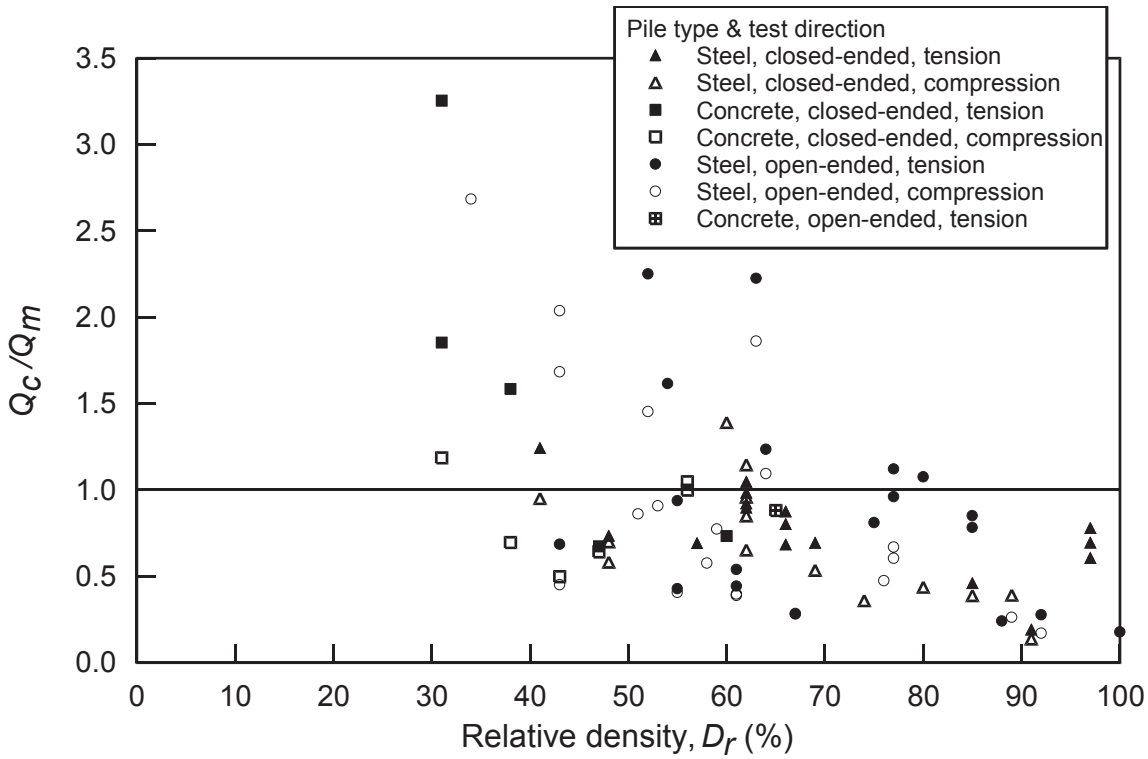

Figure 13. Distribution of Q_c/Q_m with respect to relative density, D_r : API (1993) shaft procedure for sands

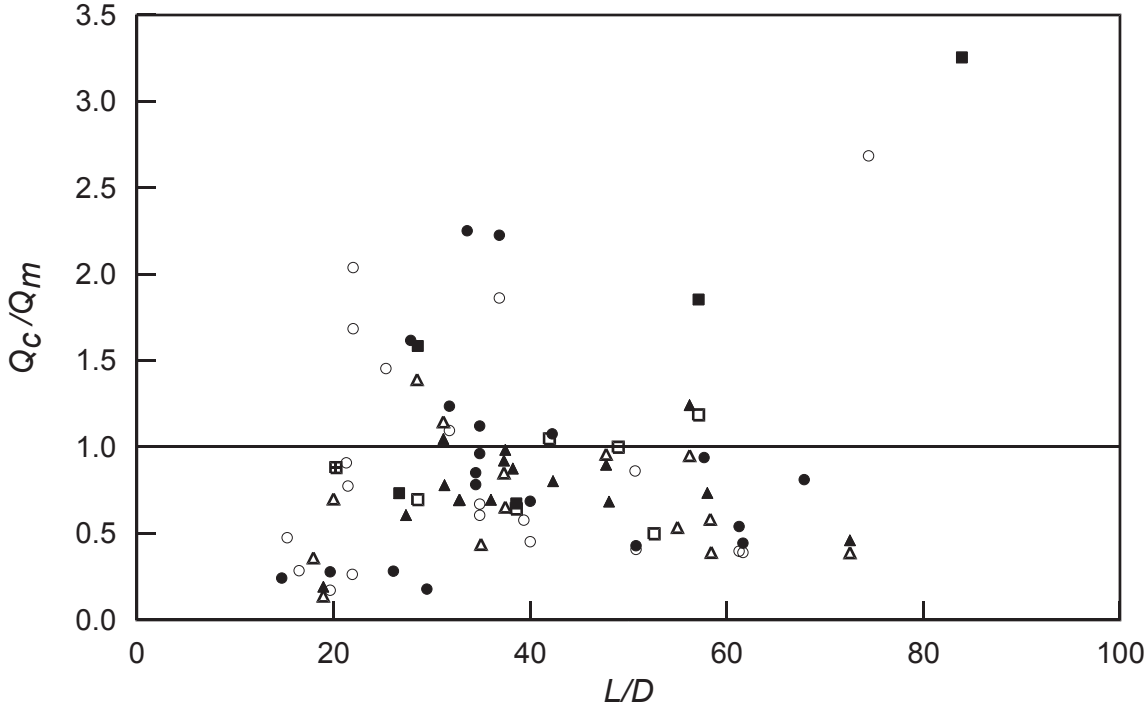

Figure 14. Distribution of Q_c/Q_m with respect to pile slenderness ratio, L/D : API (1993) shaft procedure for sands

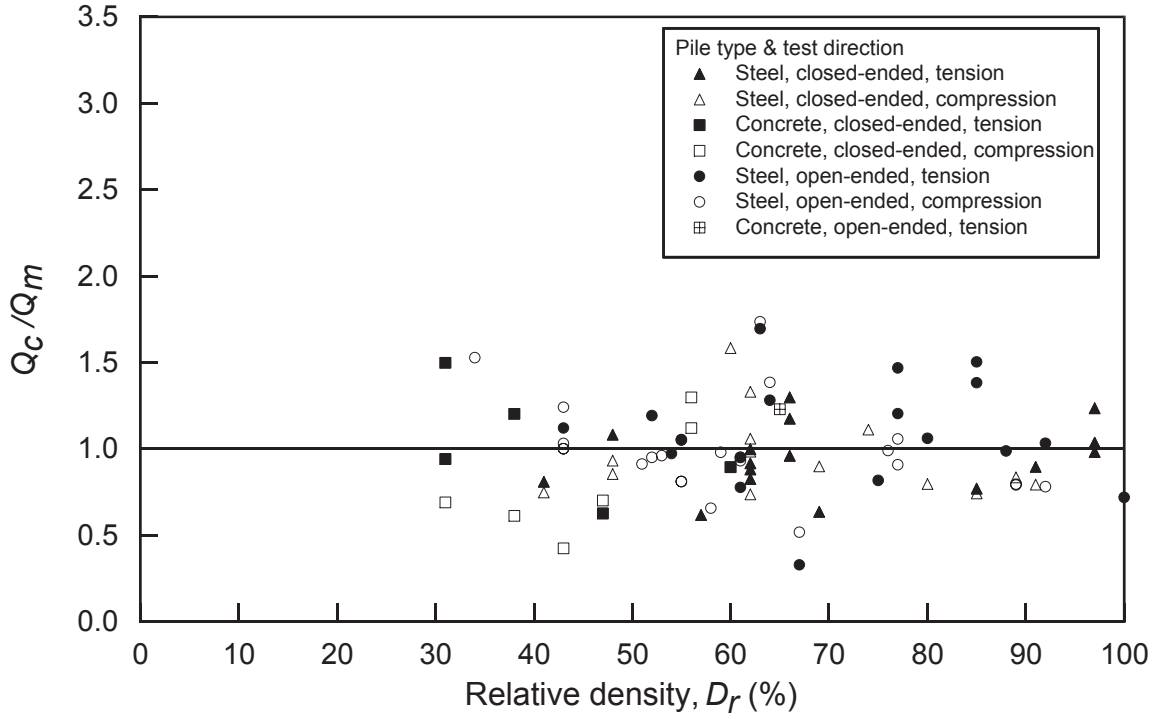

Figure 15. Distribution of Q_c/Q_m with respect to relative density, D_r : ICP shaft procedure for sands

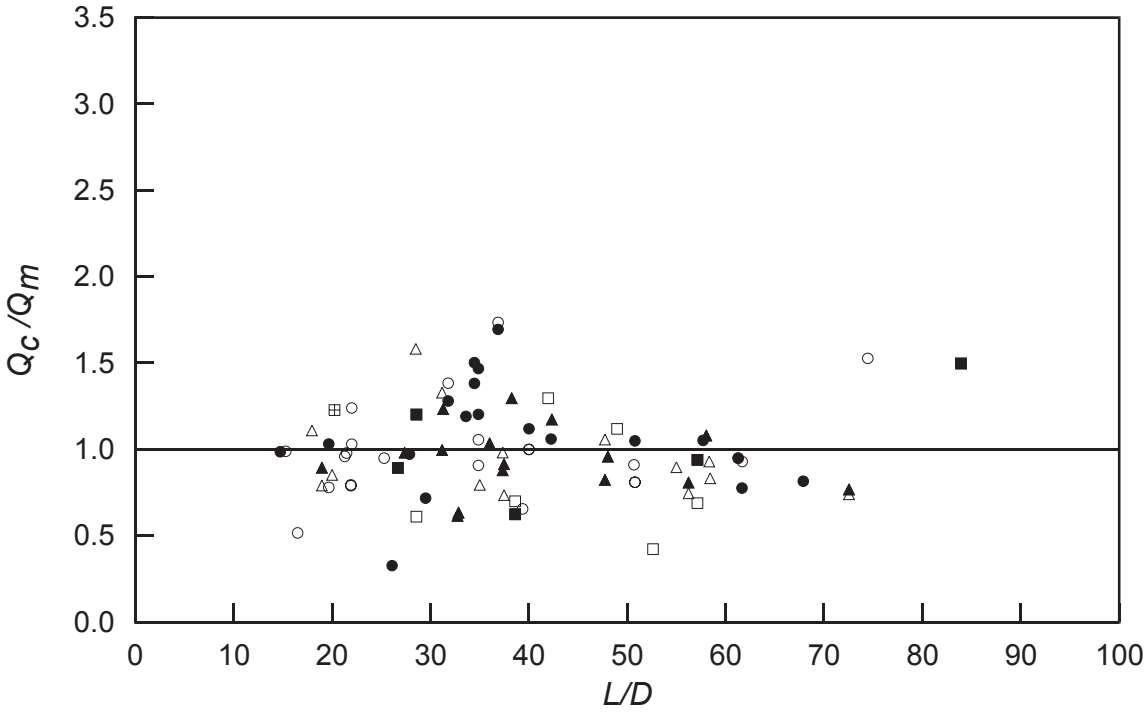

Figure 16. Distribution of Q_c/Q_m with respect to slenderness ratio L/D : ICP shaft procedure for sands

Table 10. Assessment of shaft capacity predictions: Q_c/Q_m in sand

Method	Mean (μ)	Standard deviation (s)	Coefficient of Variation (COV)
ICP, all piles	0.99	0.28	0.28
ICP, all open-ended piles	1.05	0.30	0.28
ICP, open-ended piles (Dense North Sea sand sub-set, comprising EURIPIDES, Dunkirk, Leman BD and Hoogzand)	0.99	0.17	0.17
API RP2A(1993); all piles	0.87	0.58	0.60

The expanded database allows some aspects of pile behaviour in sand to be reviewed more critically. Noting the potential for changes in pile capacity and stiffness with time and on reloading, the statistics have been re-calculated considering only the first tests performed within a month of driving (ranging from 2 hours to 31 days). Data obtained in subsequent tests after driving to greater penetrations have also been excluded and the results are presented in Table 11. The average age at first-time testing is 10 days and the means and coefficient of variations are similar to those obtained using the expanded database given in Table 10. The marginally non-conservative bias seen in Table 10 for open-ended piles is reduced in the above assessment.

Table 11. ICP assessment of shaft capacity for restricted database of first-time tests on 'fresh' piles in sand

Database	No. of tests	Average Length (m)	Average time after installation (days)	Mean Q_c/Q_m (μ)	Coefficient of Variation Q_c/Q_m (COV)
All fresh piles	41	19	10	0.98	0.31
All open-ended fresh piles	18	28	12	1.02	0.35
Dense North Sea sand sub-set	5	28	12	0.97	0.12

Fresh piles with ages greater than 30 days indicate significantly larger capacities than the ICP predictions. Further consideration of the effects of extended ageing after driving in sand is given later in Section 6, while the application of the ICP approach to micaceous and carbonate sands is discussed in Sections 8.1 and 8.2.

5.3 Shaft capacity in clay

5.3.1 Shaft capacity database for clay

Chow (1997) checked the applicability of the ICP method to large open-ended piles driven in clay against the Pentre and Tilbrook Grange 'LDP' tests described by Clarke (1993) before assessing her reliability parameters with a more general database of 55 medium-term, high-quality field tests. We repeat the exercise below, referring to the recently augmented data summarised in Table 12. Shaft capacity calculations were made with both the ICP and API (1993) procedures and statistical summaries made of the ensuing Q_c / Q_m results and their potential skewing with a variety of parameters. As with sands, over-dependence on particular sites and materials was avoided by limiting the number of tests included from any single source. For example, ten representative entries were selected from Saldivar-Moguel's set of 26 Mexico City tests.

Table 12. Summary of shaft capacity database: clay

	Closed	Open	All
Number of piles	43	25	68
Tension tests	21	20	41
Compression tests	22	5	27
Average embedded length (m)	13.7	19.6	15.9
Range of lengths (m)	3.5 - 57	3.0 - 71	3.0 - 71
Average diameter (m)	0.27	0.67	0.42
Range of diameters (m)	0.10 - 0.57	0.10 - 1.5	0.I0 - 1.5
Average YSR	8	25	14
Range of YSRs	1.1 - 43	1.0 - 100	1.0 - 100
Average *PI* (%)	27	32	29
Range of *PI* (%)	12 – 45	15 - 84	12 - 84

5.3.2 Reliability of ICP shaft method in clays

Table 13 summarises the Q_c / Q_m statistics applying to the clay shaft capacity database. Figures 17 to 20 present the corresponding plots of Q_c / Q_m against YSR and pile slenderness, *L/D*, ratio. As with the sands, data points from the recent case histories reported in Table 8 are reported along with the 1996 database. Unlike the API RP2A procedures, the ICP approach shows no sign of skewing with YSR or *L/D* and appears to be equally reliable under a wide range of circumstances.

Other checks on the above database show no skewing with regard to plasticity index. However, Karlsrud et al. (1993) and Clausen and Aas (2001) identified a strong bias in certain tests on very low plasticity, low YSR, Norwegian deposits such as the Lierstranda clay-silt, and this feature is discussed further in Section 8.

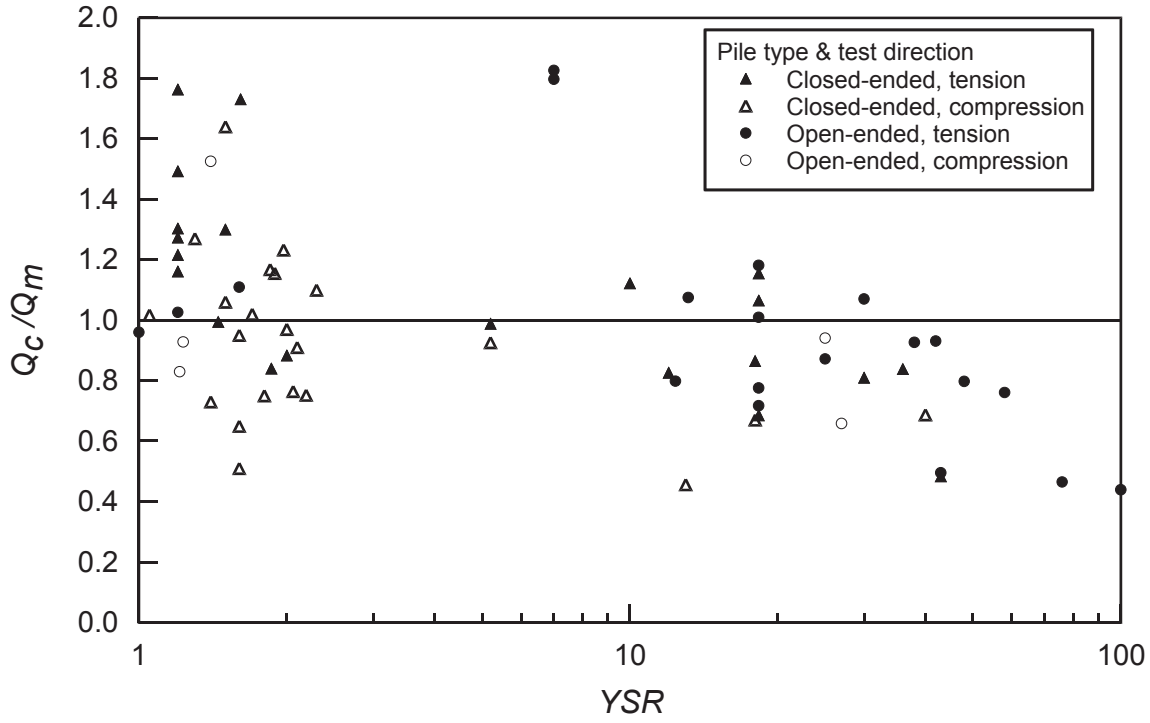

Figure 17. Distribution of Q_c/Q_m with respect to yield stress ratio, *YSR* : API (1993) shaft procedure for clays

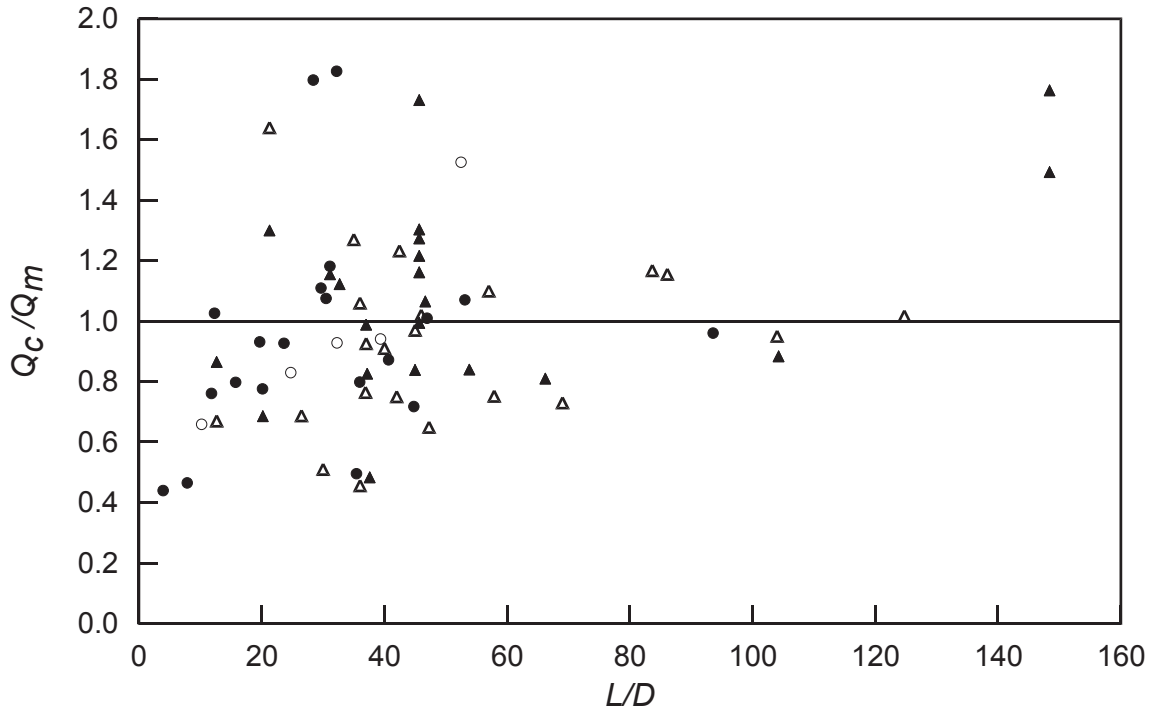

Figure 18. Distribution of Q_c/Q_m with respect to pile slenderness ratio, *L/D* : API (1993) shaft procedure for clays

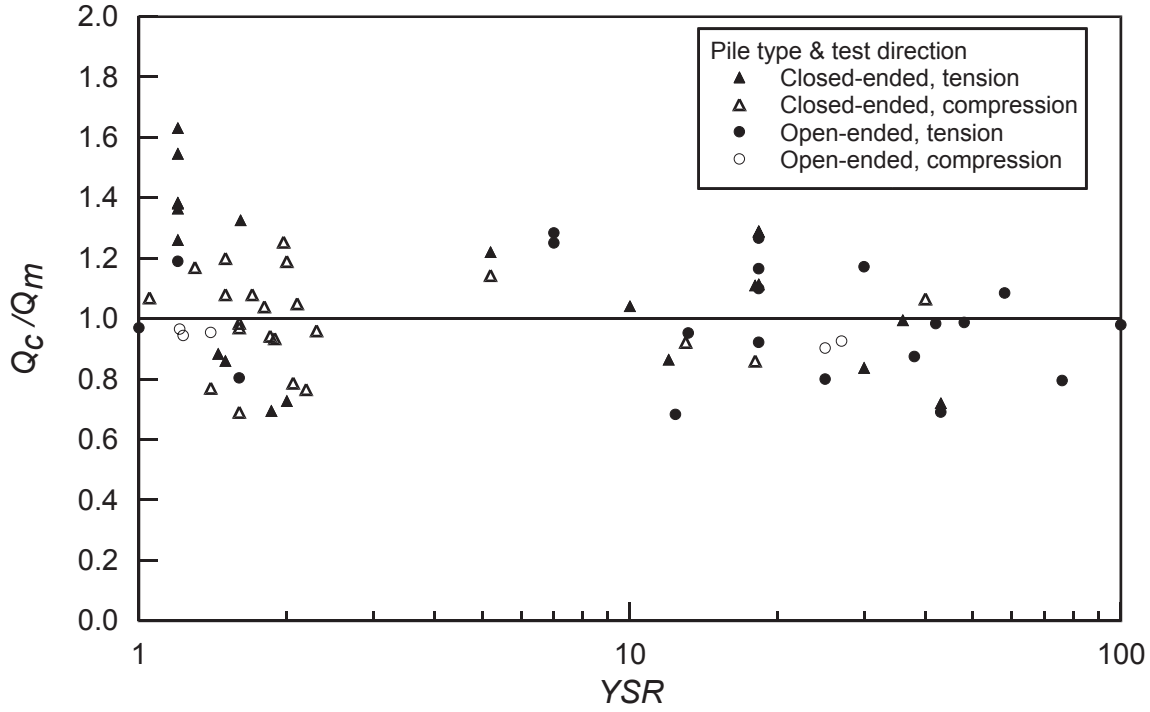

Figure 19. Distribution of Q_c/Q_m with respect to yield stress ratio, *YSR* : ICP shaft procedure for clays

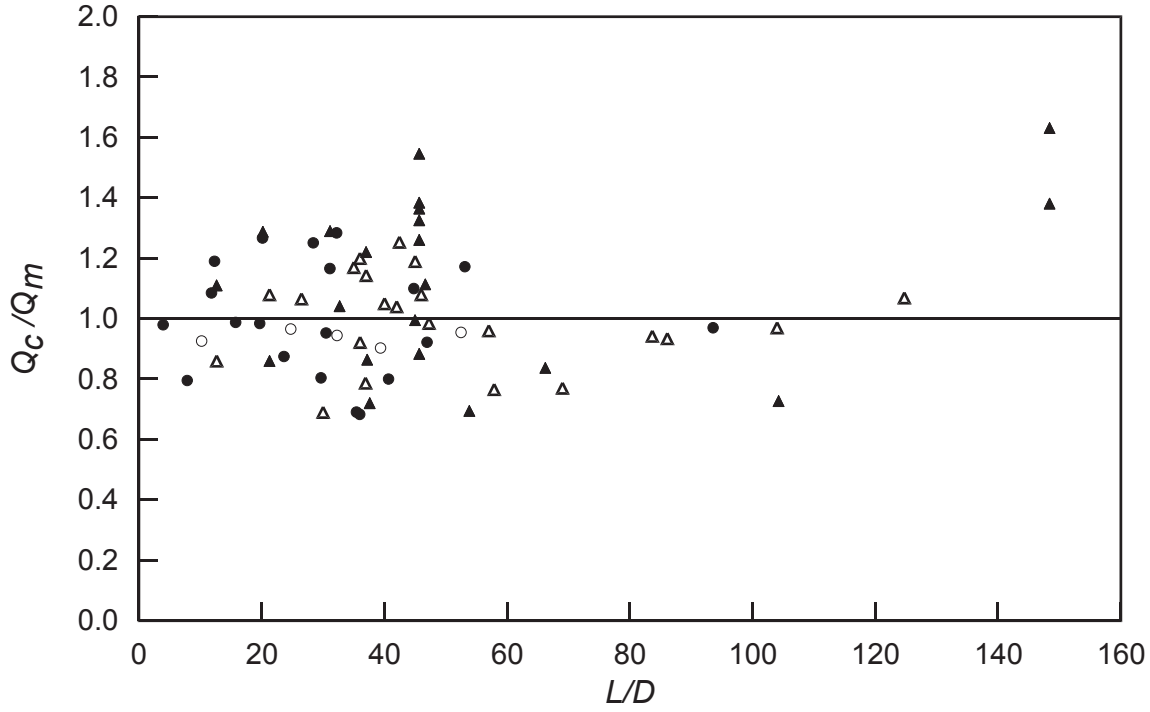

Figure 20. Distribution of Q_c/Q_m with respect to pile slenderness ratio, *L/D* : ICP shaft procedure for clays

Table 13. Assessment of peak shaft capacity predictions: Q_c /Q_m in clay

Method	Mean (μ)	Standard deviation (s)	Coefficient of Variation (COV)
ICP; all piles	1.03	0.21	0.20
ICP; open-ended piles	0.99	0.17	0.17
API RP2A (1993); all piles	0.99	0.32	0.33

5.4 Base resistance in sand

5.4.1 End bearing database in sand

Studies described by Hight et al. (1996) combined with the insights offered by the ICP tests led Chow (1997) to make a fresh interpretation of the available pile test database, leading to new quantitative design recommendations. The ICP end bearing rules relied more heavily on the field test database than the shaft recommendations and were put forward more tentatively. As mentioned earlier alternative interpretations of the same database have been made by others and further reliable data are needed to check the recommendations, particularly for large diameter piles. Bearing in mind the recent work, the lower limit values of q_b/q_c that apply to large diameter piles have been raised marginally in this document. The change affects only one of the closed-ended piles entered into the database: a Franki pile with an expanded concrete base. The Franki pile diameter (0.908m) is close to the limiting diameter above which the lower limit of q_b/q_c applies, hence this change has little effect on the statistical analysis of the database for closed-ended piles. Of Chow's ten open-ended piles with diameter greater than 0.90 m, only seven were tested in compression and, of these, only one (Kimitsu) is predicted to plug during static loading. The new limits result in a 25% increase in predicted base capacity for this pile.

Table 14. Summary of base capacity database: sand

	Closed	Open	All
Number of piles	28	20	48
Steel	16	20	36
Concrete	12	0	12
Average length (m)	11.3	21.4	15.5
Range of lengths (m)	1.1 – 45.4	2.0 – 47.0	1.1 – 47.0
Average diameter (m)	0.40	0.65	0.50
Range of diameters (m)	0.10 - 0.91	0.07 - 2.00	0.07 - 2.00
Average relative density at base, D_r (%)	69	85	76
Range of D_r (%)	25 – 95	57 - 96	25 – 96

Chow (1997) describes how the base and shaft components were separated for her original study. Of the 'new' tests summarised in Table 7, only the EURIPIDES instrumentation system is considered sufficient to isolate end bearing with reasonable accuracy[16]. The end resistance database is summarised in Table 14. It comprises the 40 compression tests from Table 9 and eleven supplementary tests.

5.4.2 Degree of fit for the ICP end bearing method in sand

Table 15 quantifies the degree of fit offered by the updated ICP base resistance procedures for sand, offering also comparisons with the API (1993) procedure. A wider spread could be expected if the method were tested using data that were completely independent of those used in its derivation. Figures 21 to 24 (which combine the 1996 data set and the new data from Table 7) show that the new method eliminates the strong skewing of Q_c/Q_m with D and D_r that appears to be associated with the API recommendations. Figure 6 shows how the 'rigid-plug' formation criterion given in Table 3, Step D1, was established from the open-ended steel pile test data.

Table 15. Assessment of base capacity predictions: Q_c/Q_m in sand

Method	Mean (μ)	Standard deviation (s)	Coefficient of Variation (COV)
ICP; all piles	1.01	0.19	0.19
ICP; open-ended piles	0.98	0.15	0.16
API RP2A (1993); all piles	0.83	0.60	0.73

[16] Tell-tale gauges installed on Dunkirk pile C1 indicated that the shaft contributed around 70% of the total 80 day capacity. However, the potential error in Q_b is large and these values have not been added to the database; the proportional errors in Q_s are naturally far smaller.

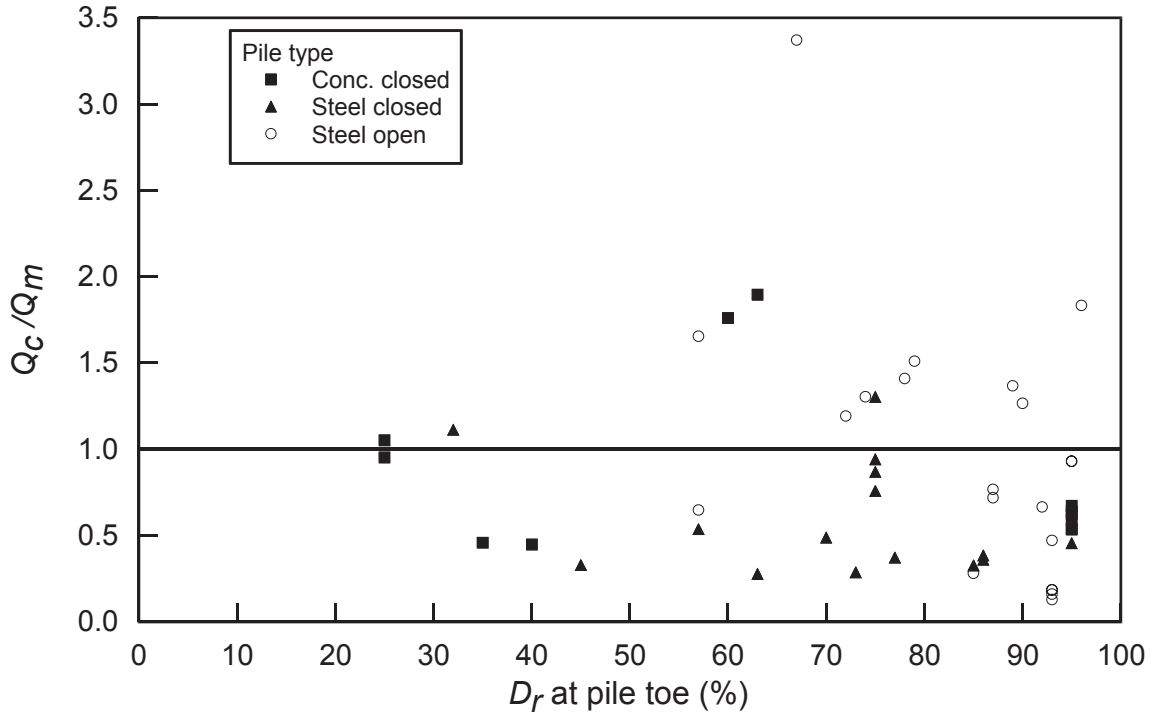

Figure 21. Distribution of Q_c/Q_m with respect to relative density, D_r : API (1993) base procedure for sands

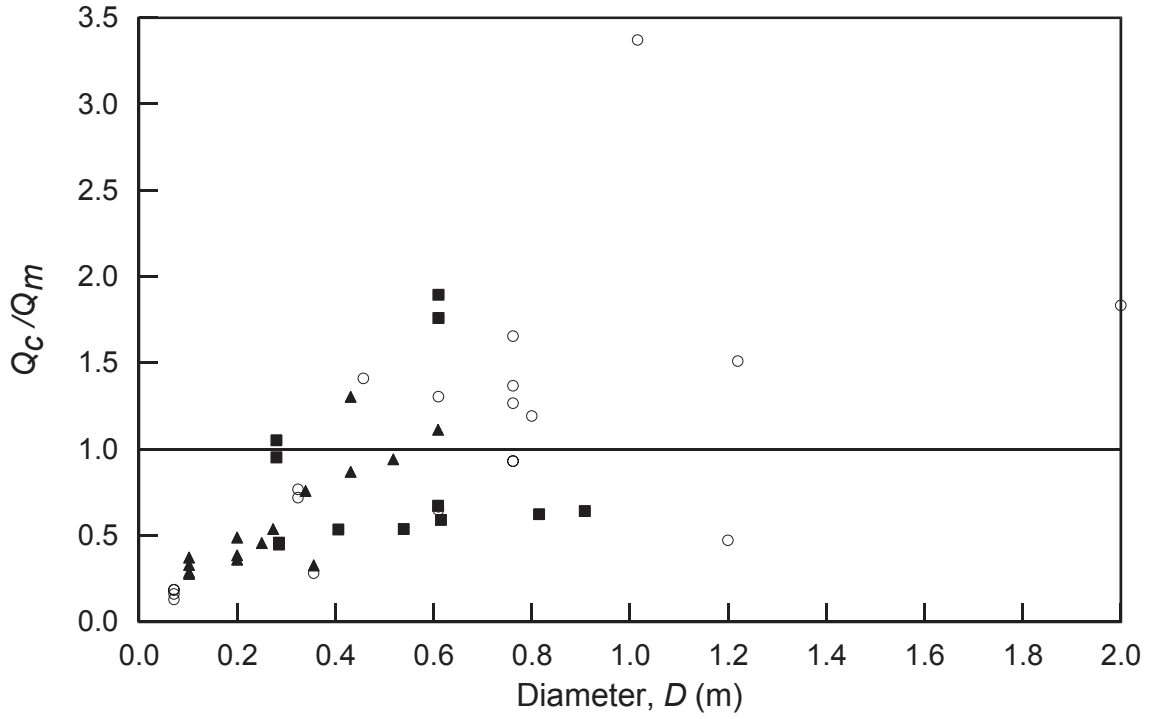

Figure 22. Distribution of Q_c/Q_m with respect to pile diameter, D : API (1993) base procedure for sands

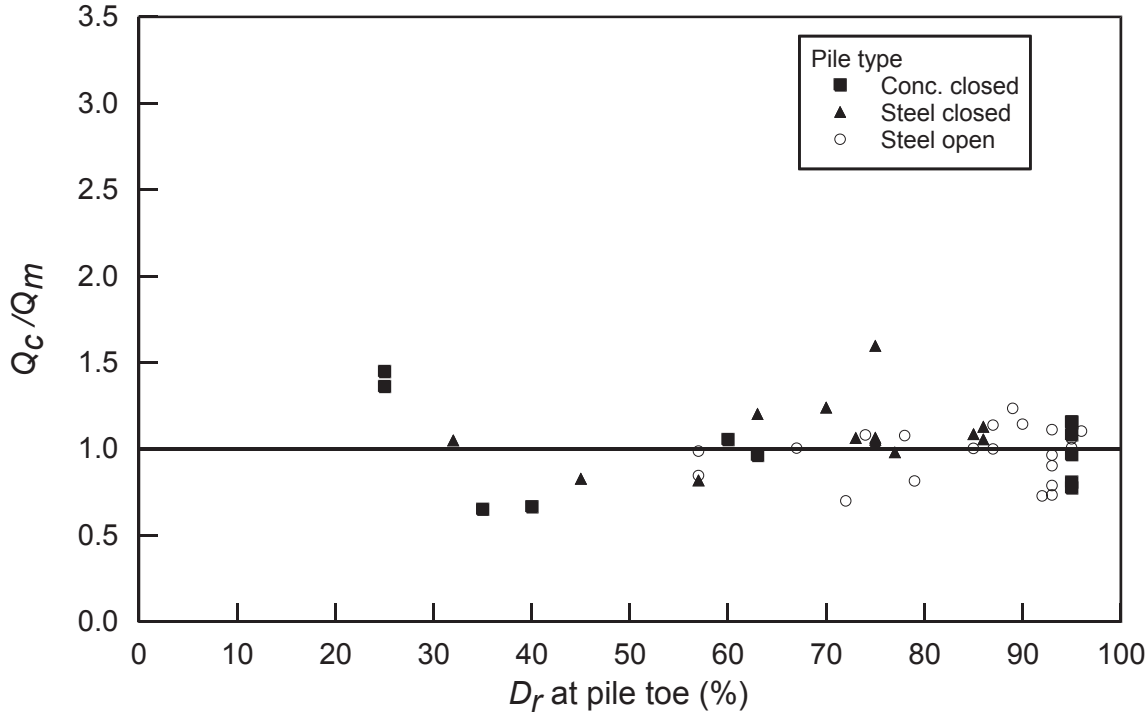

Figure 23. Distribution of Q_c/Q_m with respect to relative density, D_r : ICP base procedure for sands

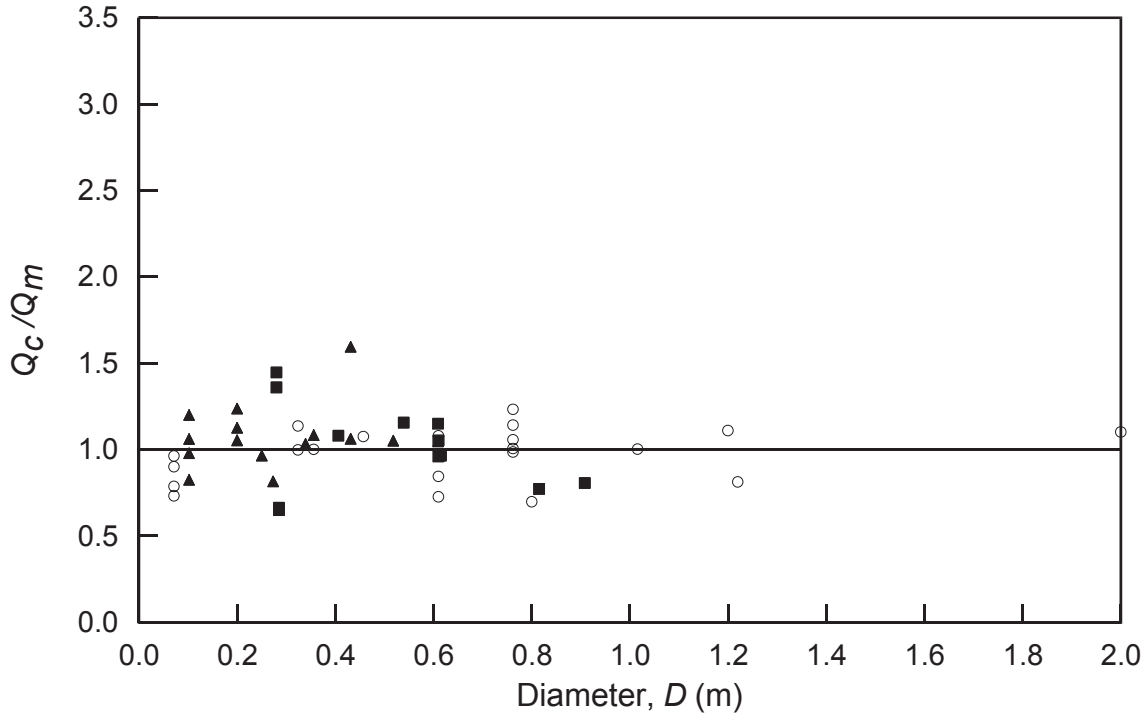

Figure 24. Distribution of Q_c/Q_m with respect to pile diameter, D : ICP base procedure for sands

5.5 Base resistance in clay

5.5.1 End bearing database for clay

The new data assembled in Table 8 do not provide any new reliable entries for the total end bearing database in clay; Chow's original database is re-summarised below. Her interpretation of these field experiments led to the CPT based design rules summarised in Table 5. As with sands, the end bearing approach was proposed tentatively on the basis of the insights offered by the ICP research combined with a re-interpretation of the Table 16 database. As noted earlier, end bearing makes a less important contribution to piles driven in clays than in sands.

Table 16. Summary of base capacity database: clay

	Closed	Open	All
Number of tests	15	16	31
Number of piles with strain-gauges at the base	12	3	15
Average founding depth (m)	10.6	19.1	15.0
Range of founding depths (m)	5.8 - 19	3.0 - 55	3.0 - 55
Average diameter (m)	0.17	0.69	0.44
Range of diameters (m)	0.10 - 0.46	0.20 - 1.5	0.10 - 1.5
Average YSR at founding depth	6	13	10
Range of YSR	1.4 - 24	1.2 - 62	1.2 - 62
Average *PI* at founding depth (%)	24	30	27
Range of *PI* (%)	11 - 50	14 - 84	11 – 84

5.5.2 Degree of fit for the ICP end bearing method in clay

Table 17 summarises the reliability statistics of the ICP and API (1993) methods for end bearing in clay, showing a marginally conservative bias and far lower COVs for the ICP approach. A broader spread might be expected if the method were tested against an independent database.

Table 17. Assessment of base capacity predictions: Q_c/Q_m in clay

Method	Number of piles	Mean (μ)	Standard deviation (s)	Coefficient of Variation (COV)
ICP, all piles	31	0.85	0.26	0.30
ICP, open-ended piles	16	0.75	0.28	0.38
API (1993) RP2A all piles	31	1.06	1.04	0.98

5.6 Independent analyses of ICP methods' predictive reliability

5.6.1 Reliability for square and H section piles

As set out in Section 3.4.2, Cowley (1998) investigated how the ICP approaches might be applied to rectangular and H section driven piles. Evaluating the rules set out in Table 4 against his database of 16 tests covering both sand and clay, his overall recommendations for rectangular piles led to a slightly conservative mean $Q_c/Q_m \approx 0.93$ and COV ≈ 0.35. The results for H section piles were similar, giving a mean $Q_c/Q_m \approx 0.90$, and COV ≈ 0.48 with a second set of 16 tests. These reliability parameters are less satisfactory than those for cylindrical piles, but are far better than those corresponding to more conventional procedures, such as API (1993).

5.6.2 Checks by other organisations on reliability for cylindrical driven piles

Independent database assessments of the ICP methods' ability to predict axial capacity include those made by expert teams from the Norwegian Geotechnical Institute (NGI, Clausen and Aas 2001) and the Dutch Centre for Civil Engineering Research and Codes (CUR, 2001 and Fugro, 2004). The overall assessments made by NGI, CUR and Fugro are summarised in Table 18. Note the NGI assessment only applies to large 'super-piles' while CUR and Fugro excluded sand sites where CPT measurements had not been taken. The Fugro (2004) study revisited the CUR database and focused on a restricted set of pile tests that was particularly relevant to offshore installations.

Considering the sand tests first, it appears from Table 18 that the ICP may be marginally conservative, but with lower COV values than those assessed by the Authors. CUR and Fugro report that the ICP is marginally non-conservative for shaft capacity in sand and conservative for base capacity, although they note that this assessment may be affected by the way in which end bearing is separated from the shaft and by the order in which tension and compression tests were performed on several individual piles. Most of the sand tests considered by CUR were from appropriate sites such as EURIPIDES and Dunkirk, although some tests might be questioned[17]. As noted earlier, the ICP method is intended to predict capacity around ten days after driving in sand and pile age at testing could be a factor in the apparent conservatism, as could the database test selection.

[17] Potentially unrepresentative tests include the Jamuna Bridge mica sand series (from Bangladesh); Leman AD in the North Sea (which had been affected by a gas blow out) and the Saudi Ras Tanajib tests, where hard clay and strong carbonate layers are present.

Table 18. Independent assessments of ICP methods for total capacity: Q_c/Q_m ranges

Case	Number of piles in database	Mean (μ)	Standard deviation (s)	Coefficient of Variation (COV)
Clausen and Aas (2001) 'Super piles' in sand	34	0.93	0.21	0.23
CUR (2001) Open and closed-ended piles in sand All with CPT data	19	0.89	0.24	0.27
Fugro (2004) Open-ended piles in sand All with CPT data	12	0.94	0.23	0.24
Clausen and Aas (2001) 'Super piles' in clay NB Few site specific δ_f measurements	43	0.81	0.28	0.34

The CUR (2001) study did not attempt to apply the ICP approach to piles driven in clays because of a lack of site-specific interface shear test δ_f data. The NGI group did consider clays, applying the illustrative trend given by Jardine and Chow (1996) between δ values and plasticity index when site-specific interface shear information was not available. Figures 8 and 9 show that this curve is generally conservative, but not a true lower limit. Interface shear strength correlates poorly with index tests and an adequate spread of site-specific tests is essential if the ICP is to be applied reliably.

5.7 Selection of safety factors in design

Target levels of reliability are often set for safety critical structures. Designers seek to match these reliability levels when selecting either (i) Factors of Safety, in Working Stress Design (WSD) methods, or (ii) Load and Resistance Factors in 'LRFD' procedures. However, the poor statistical performance of conventional pile design methods makes meaningful reliability analysis difficult to perform. The lack of bias and lower variability offered by the ICP calculation methods makes them more suitable for rational reliability based assessments, provided appropriate site investigations have been performed and the essential soil parameters have been determined correctly. The following paragraphs describe how reliability analysis has been applied practically in conjunction with the ICP methodology.

Figure 25 shows sketches of the probability density functions of load and resistance (f_L and f_R) expected for a foundation supporting a hypothetical structure. These functions are defined by their mean and COV values and the corresponding cumulative probability functions F_L and F_R may be defined from the same data. The separation between the peaks of the expected design load and resistance distributions is a measure of the foundation's safety margin. This can be judged against an appropriate target failure probability when setting, or judging, appropriate Load and Resistance factors as the area of the overlap between the distributions is related to the probability of failure. The target probability can be set on the basis of either ALARP (As Low As Reasonably Possible) risk arguments (Efthymiou et al., 1996) or by comparison with well-established design methods that have a history of acceptable safety in the field.

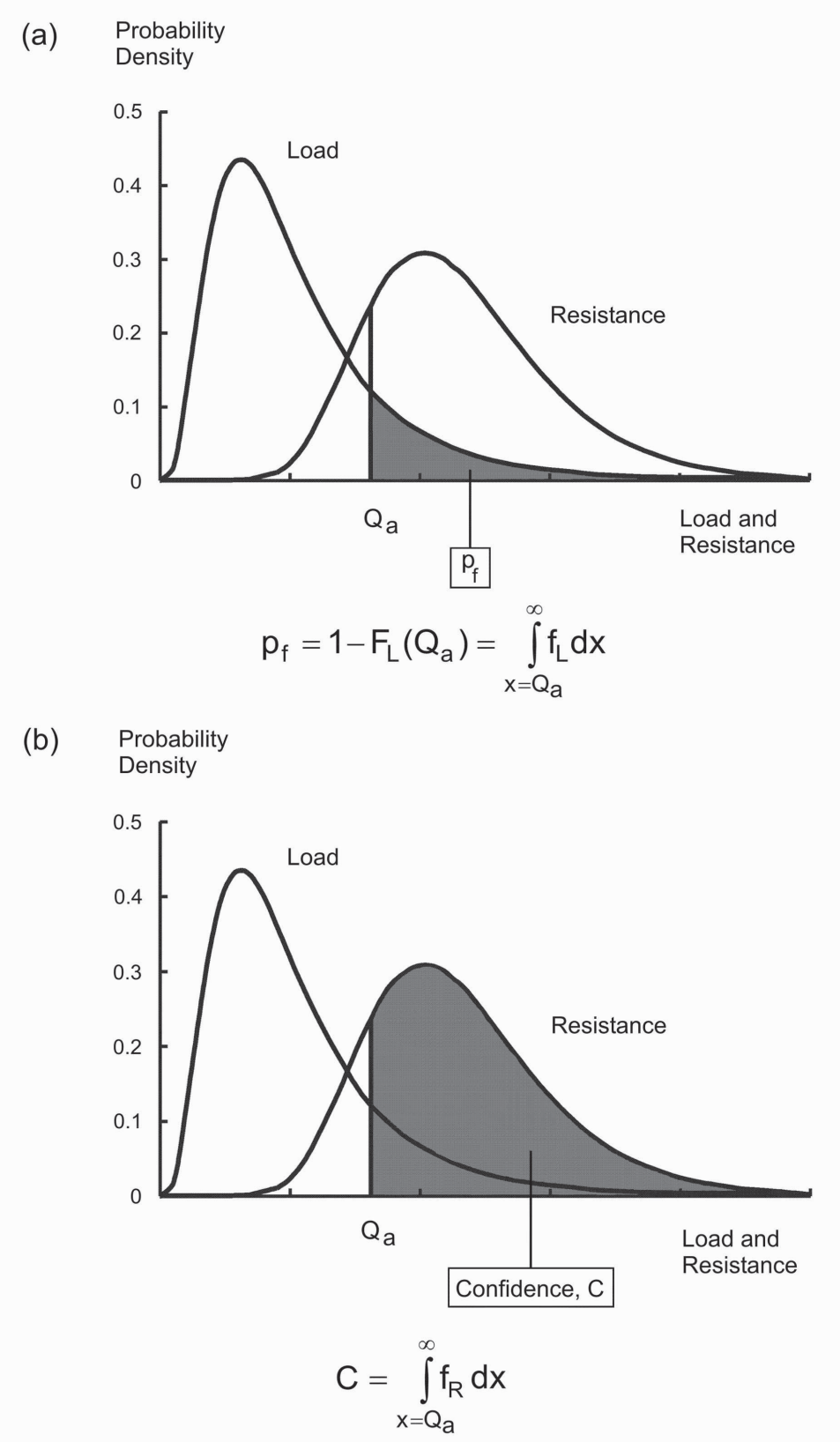

Figure 25. Probability of failure and associated confidence level for a selected resistance Q_a after Langen et al. (1995)

The degree of spread, or uncertainty, in pile capacity predictions originates from model limitations and potential errors in parameter interpretation. Both sources were present (and therefore implicitly considered) in the validation of the ICP methods that was made against pile test data, and the calibrated values have been used to estimate reliability parameters that refer to single pile failures. Most structures rely on multiple piles and their foundations can only fail after developing a complete failure mechanism. However, it is usually conservative to assume that the foundation 'fails' when the load on the most heavily loaded (compression or tension) pile exceeds its axial capacity. Factors that may lead to a higher than calculated reserve strength for the foundation include the possibly ductile failure modes of individual piles, the limited duration of potential extreme design events and potential long-term ageing effects.

5.7.1 Foundation COVs in mixed soil profiles

The ICP method COVs given in Tables 10, 11, 13, 15 and 17 are distinguished by shaft capacity, end bearing and soil type. In normal practice any given pile will derive its capacity from a combination of these elements and its overall COV will vary with the relative contribution each makes to its capacity. As the ICP method's COVs were determined separately it is reasonable to assume the contributions of shaft capacity from sand, shaft capacity from clay and end bearing at any site form three statistically independent variables. In this case the overall foundation COV (COV_f) may be determined from equations involving the sums of the individual components Q_i and the associated uncertainty parameter COV_i as:

$$COV_f = \left[\Sigma(Q_i . COV_i)^2\right]^{0.5} / \Sigma Q_i$$

If further sub-divisions (with multiple layers of clay and sand) are considered it may be necessary to consider them as co-dependent and the overall foundation COV may be determined from equations such as:

$$COV_f = \left[\Sigma(Q_i . COV_i)\right] / \Sigma Q_i$$

5.7.2 Reliability calibrated against well-established design methods

The classical approach to calculating an absolute probability of failure for any combination of f_L and f_R distributions is indicated in Figure 26. The cumulative probability density function for the load (F_L) is used in this method in combination with f_R. The product $(1-F_L)f_R$ is integrated over the full range of possible values (typically zero to infinity) to obtain the probability of failure. The calculation is normally carried out using a First Order Reliability Method (FORM, Madsen et al., 1986).

However, when considering the levels of uncertainty associated with any of the available pile design methods, this classical approach cannot be used to obtain meaningful absolute probabilities of failure. The classical approach is nevertheless useful for determining relative reliability indices that allow one design method to be compared with another, provided the appropriate reliability data exist for both. The interpretation of method error is less critical in such analyses and the sources of uncertainty are best combined in a convolutional integration leading to comparable reliability indices (Langen et al., 1995).

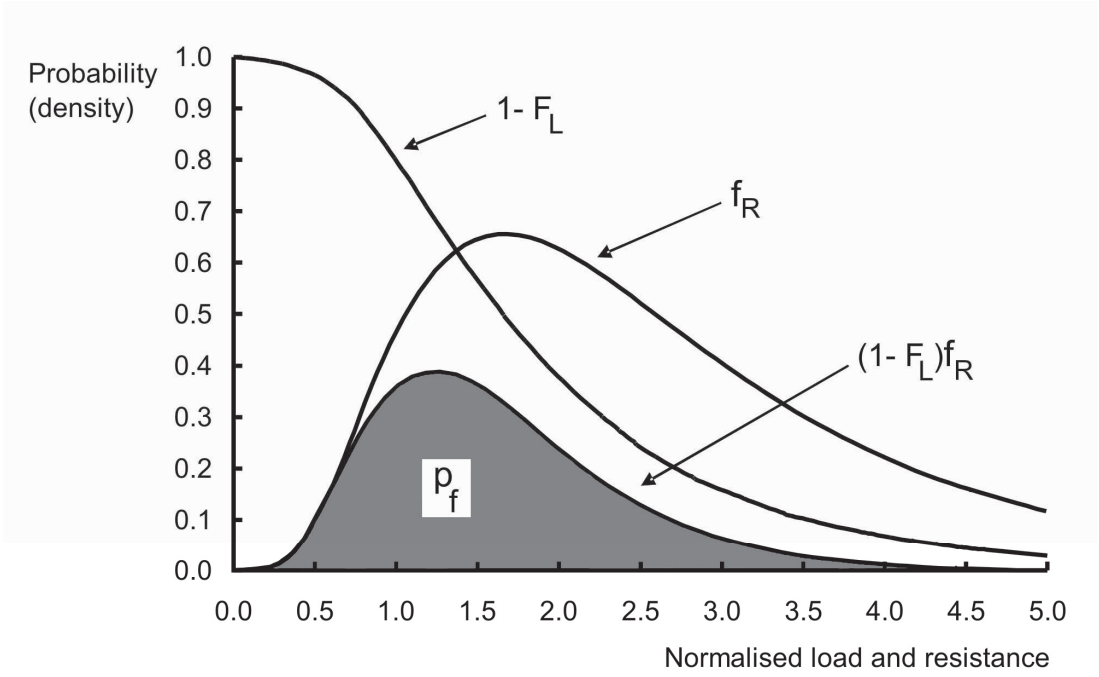

$$p_f = \int_0^{\infty} (1 - F_L) \cdot f_R \, dx$$

Figure 26. Integration of probability distributions to obtain probability of failure after Langen et al. (1995)

5.7.3 Reliability in terms of probability of failure

Langen et al. (1995) show that significant model uncertainty is best treated by translating it into a relationship between (i) any given confidence bound relating to resistance (defined by a suitable fixed percentile point such as 90 or 95% on f_R) and (ii) the absolute probability that the load could exceed the resistance level Q_a defined at this point on the f_R curve. This confidence level is indicated on Figure 25b.

As before, the first step in such a procedure is to establish the pile load and resistance probability density functions f_L and f_R. The absolute probability that the load will exceed the specified resistance Q_a is obtained by integrating f_L between Q_a and infinity. The degree of confidence that the resistance will exceed the specified load Q_a can be evaluated by integrating the f_R function between Q_a and infinity; see Figure 25. The suitability of any Load or Resistance Factor used in the design process can then be tested by considering the calculated probability of pile failure in relation to the explicit target value.

5.7.4 Safety Factors for the ICP methods

Load and Resistance Factors have been developed for many types of Civil Engineering structural design codes that are calibrated to match their Working Stress Design (WSD) predecessors, carrying

over the existing experience base into the newer LRFD code. Calibrated reliability indices are used in such exercises; introducing Partial Factors for Load and Resistance leads to an overall improvement in reliability by eliminating the least reliable elements of WSD practice (CIRIA, 1977).

Site-specific pile tests are often conducted in onshore projects to assess the suitability of a foundation design and failure is often defined by a settlement/deflection limit rather than by an ultimate axial capacity. However, applying a suitable factor of safety against failure can often lead to acceptable displacements.

Settlement criteria are rarely critical in offshore foundation practice and the standard WSD safety factors are often set at levels lower than in onshore practice, with levels between 1.5 and 2.0. These safety factors can be transposed to equivalent LRFD partial safety factors by calculating, as an intermediate step, the probability of foundation failure. It is necessary to know the bias and COV for the capacities and loads developed by the foundations, and the shape of their probability distribution. Proposals have been made for offshore structures by the API PRAC-22 committee that load and resistance uncertainties can be captured by log-normal distributions (having log-normal mean and standard deviations values μ_{lnx} and s_{lnx}, Moses, 1980). The probability density functions f_L and f_R then take the form:

$$f_x = \left[1/\left\{(2\pi)^{0.5} . x . s_{lnx}\right\}\right] . exp\left[-1/2 . \left\{(lnx - \mu_{lnx})/s_{lnx}\right\}^2\right]$$

The values of μ_{lnx} and s_{lnx} are related to the arithmetic means and COVs (μ_x and COV_x) of the f_L and f_R distributions by:

$$s_{lnx} = \left\{ln(1 + COV_x^2)\right\}^{0.5}$$

$$\mu_{lnx} = ln(\mu_x) - 0.5(s^2_{lnx})$$

A summary of the API PRAC-22 committee Load Factor recommendations is given in Table 19 below and it lists the parameters required to calculate the f_L probability density function. Typical LRFD Resistance Factors used with these loads are 0.7, for a pile with a design case dominated by dead loads, (which is equivalent to a WSD FOS of 1.1/0.7 = 1.57) and 0.8 for a pile with a design case dominated by environmental loads, (equivalent to a WSD FOS of 1.35/0.8 = 1.69). Combining these loading data with the reliability parameters associated with the particular pile design method and site soil profile (as set out in Section 5.7.1) leads to the equivalent parameters for the f_R probability density function.

Table 19. Load factors and statistical data for offshore foundations

Load Element	Load Factors		COV	Bias
	Compression	Tension		
Dead Load	1.1	0.9	0.08	1.0
Live Load	1.1	0.8	0.14	1.0
Environmental Load	1.35	1.35	0.08	1.0

The required level of reliability needed for any particular structure must be assessed by the engineer or the asset owner. Efthymiou et al. (1996) suggested that annual probabilities of failure (Pf_a) of 3 x 10^{-5} and 5 x 10^{-4} might be suitable for manned and unmanned offshore structures respectively. The reliability required by any sub-element of the structure (such as a pile) depends on its criticality to the structure and it might be argued that a lower reliability limit could be applied to single piles. However, setting the single pile reliability target to be the same as that of the structure is rationally conservative.

Experience of applying the above approach and criteria to 13 North Sea platforms indicates that target probabilities can generally be achieved with the ICP design methods by adopting the resistance factors given in Table 20.

Table 20. Resistance factors for ICP methods and North Sea foundations

Annual Probability of Failure	LRFD Resistance Factors and (Equivalent WSD Safety Factors)	
	Compression	**Tension**
Pf_a = 3 x 10^{-5}	0.75 (1.5 - 1.8)	0.65 (1.7 - 2.1)
Pf_a = 5 x 10^{-4}	0.85 (1.3 - 1.6)	0.85 (1.3 - 1.6)

6. TIME EFFECTS IN SAND AND CLAY

6.1 Time effects in sand

Jardine and Chow (1996) reported that piles driven in sands experience remarkably strong increases in capacity with time. Chow et al. (1997, 1998) give more details as to how these features were identified by the Imperial College group by retesting piles driven at Dunkirk. A database was assembled covering ten test sets (involving fresh pile tests, re-strikes and re-tests on steel, concrete and timber piles) conducted at a range of times after driving in sands. A tentative trendline was plotted through the highly mixed and broadly scattered data and possible explanations for the time-dependent processes were offered. The relaxation through creep of circumferential arching established around the pile shafts, leading to increases in the local radial effective stresses, was thought to be the dominant process. It was possible that enhanced interface dilation played a role. End bearing capacity was not thought to change significantly with time.

The results obtained at Dunkirk were communicated to the EURIPIDES research group and led to re-tests being performed after extended rest periods at the EURIPIDES, and Jamuna Bridge (mica sand) sites, showing increases in capacity of between 70 and 90% over six months, roughly in keeping with Jardine and Chow's trendline. Other groups have undertaken their own research, a notable example being Axelsson's PhD study (2000), which broadly reinforced the earlier conclusions.

Jardine and Standing (2000) undertook a further research programme into ageing, driving a set of six 19 m long 465 mm outside diameter piles (R1 to R6) and one 10 m long similar pile (C1) at the same Dunkirk test site. They performed multiple first-time tension static and cyclic loading tests on both fresh and pre-tested piles, over several months. CPT tests were conducted in the pile test area allowing the initial conditions at each pile location to be well established, accounting for some spatial variations in the state of the mainly dense marine sands present. Individual ICP capacity calculations were made for each test pile, defining its nominal medium-term tension shaft capacity.

Figure 27 presents the results for first-time slow static tension tests on 'fresh' piles C1, R1, R2 and R6, along with the comparable result obtained by Chow (1997) on a 'fresh' 22 m long 324 mm OD pile driven by the French CLAROM team five years before being load tested. The capacities have been normalised by their respective ICP tension capacities to eliminate the effects of slightly different dimensions and CPT profiles. Also shown is the trendline drawn by Jardine and Chow through their mixed dataset of first tests, re-tests and re-strikes involving a variety of piles and different sands, showing that the 'fresh' Dunkirk piles gained capacity much more quickly than expected. Capacities grow strongly over the first six or so months and the ICP calculations match the field curve around ten days after driving. Values at least twice as high are available in the long term. The curve indicated over the first ten days suggests that End of Initial Driving (EOID) resistance should fall substantially below the ICP assessment. Other data suggest smaller differences over this initial period and further investigation is required.

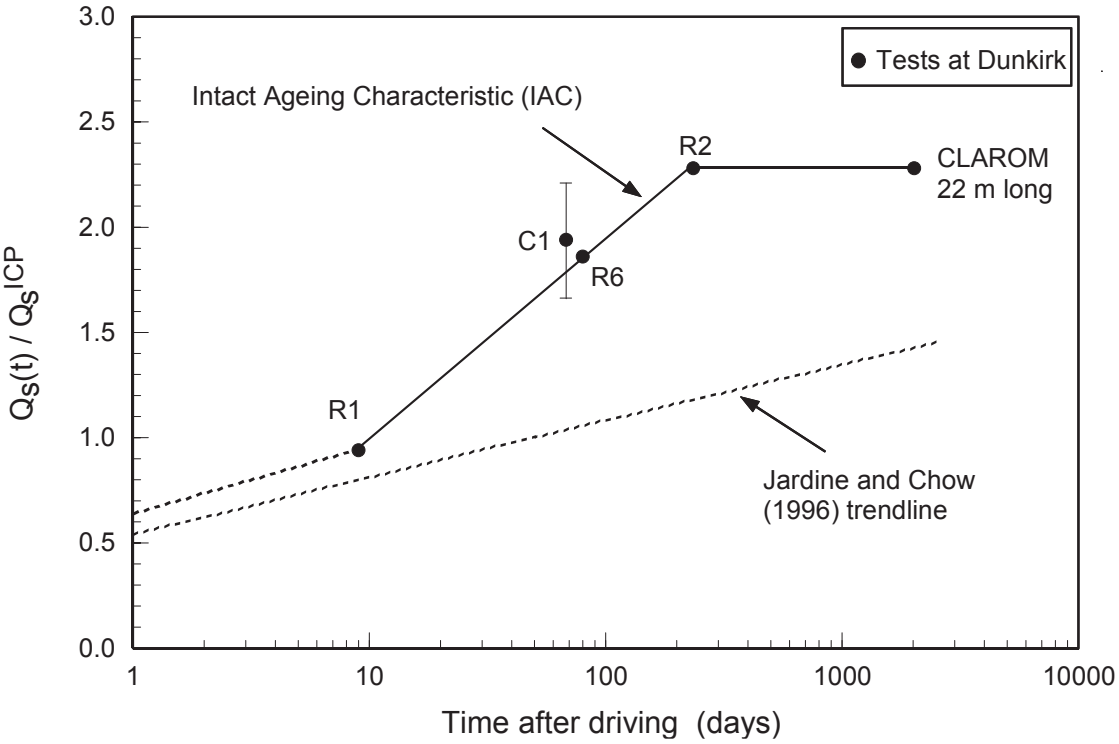

Figure 27. First-time static tension tests on fresh piles, showing strong effects of age on shaft capacity (after Jardine & Standing, 2000)

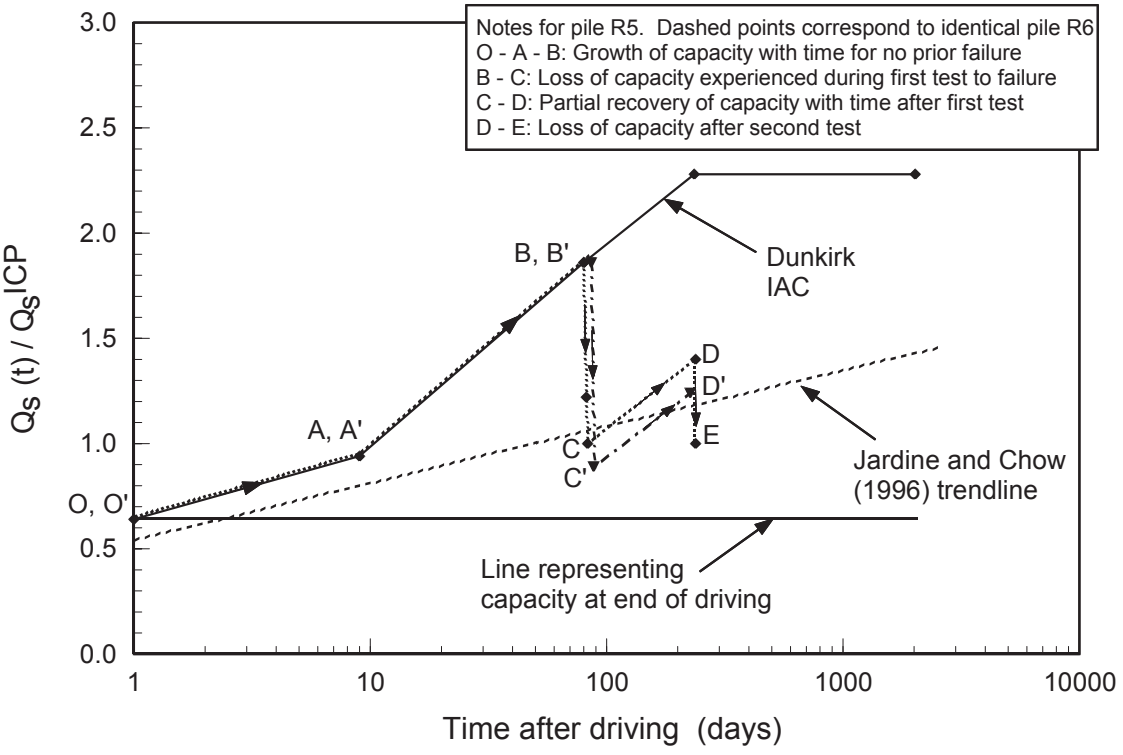

Figure 28. Trends in shaft capacity in sand versus time after driving for multiple tests on single piles (after Jardine, Standing & Chow, 2005)

Repeated tests on Piles R1 and R6 indicate why the original 'mixed data set' trendline falls so far below that for the first time Dunkirk tests. Figure 28 presents the traces of capacity versus time after driving for two piles (R5 and R6) that were subjected to multiple testing. It was found that tension re-tests conducted immediately after unloading from a prior (brittle) failure could not re-mobilise the same capacity. The loss of capacity caused by prior failure, and the subsequent extreme unload-reload cycle, reduce capacity by an amount that increases with the pile age at the time of its first test. Some recovery takes place if the pile is allowed to rest again before being re-loaded, leading to staggering paths that fall closer to the original putative trendline. Returning to the 'mixed' original database, a re-interpretation has been made in which the re-strikes and re-tests have been eliminated, leading to the data set summarised in Table 11. The 'first-time' data are re-plotted on Figure 29 with the shaft capacities available at various times normalised by the values expected one day after driving: the results fall close to the recent Dunkirk tests.

A sustained duration low level cyclic test performed at Dunkirk indicated that the ageing processes can be accelerated by low level agitation. Gentle vibration is likely to accelerate creep in granular media (Jardine et al., 2002), and this observation further supports the argument that the time effects are related to a gradual breakdown in the circumferential arching action that develops when the pile undergoes an extreme load cycle and develops a large displacement, either during driving, or as a result of shaft failure.

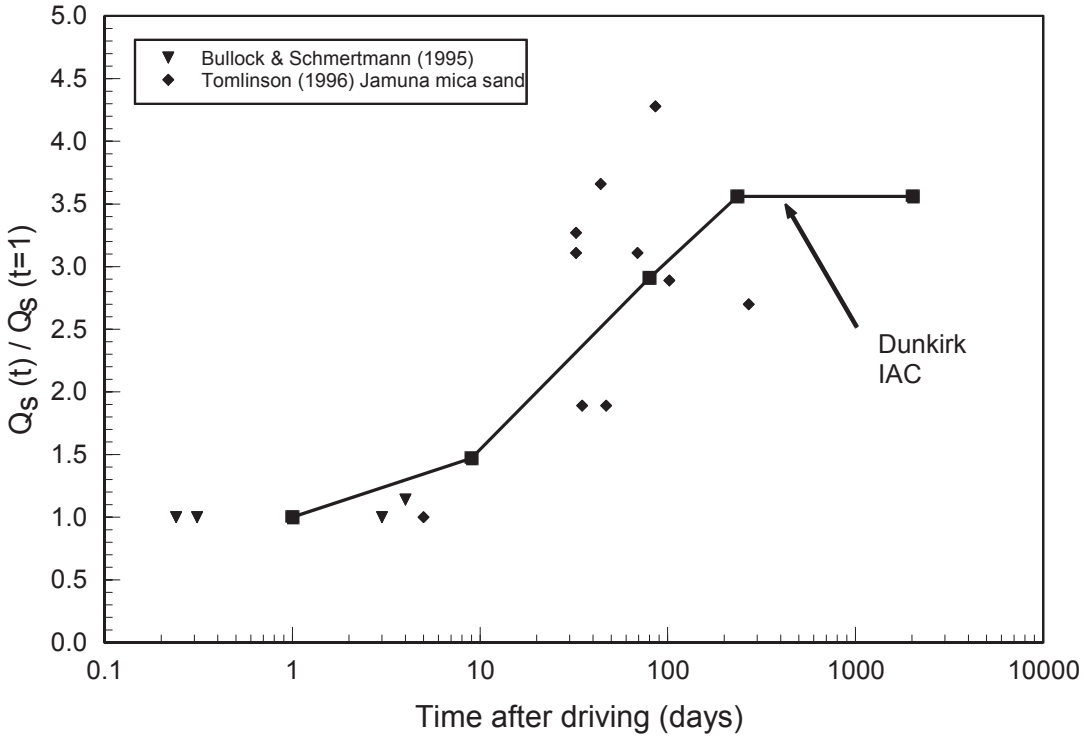

Figure 29. Normalised trends in shaft capacity with time, fresh piles from database of Chow (1997)

6.2 Time effects in clay

Shaft capacity can change greatly in clays during the equalisation period following driving. When the YSR is low and the soil is sensitive, large gains may be expected over the pore pressure equalisation stage (set-up), while insensitive high YSR clays can even show reductions in capacity with time. Such changes are correlated closely with the variations in σ'_r with time.

Figure 30 summarises the σ'_r trends seen in the ICP experiments, plotting the trends for the values of $K = (\sigma'_r / \sigma'_{v0})$ divided by their final K_c values. Points to note are:

1. K increases steadily during equalisation in the low YSR Bothkennar and Pentre clays.
2. At Cowden, a pronounced short-term minimum was seen in the time curves, while the overall changes between installation and full equalisation were practically neutral.
3. A significant net reduction of K with time developed in the London Clay.
4. The Pentre clay-silt is much more permeable than the other three clays and consolidation occurs rapidly.

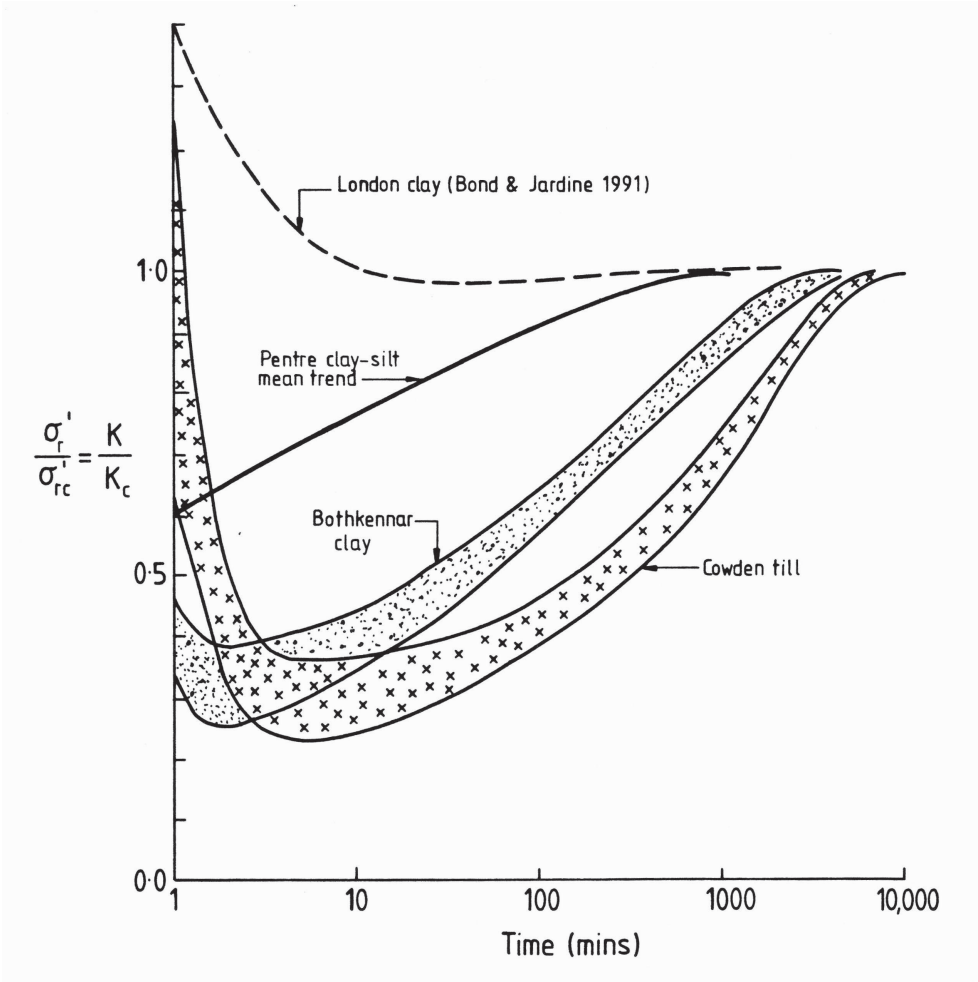

Figure 30. Variations with time of radial effective stresses at four ICP clay test sites

With closed-ended or fully plugged piles, the equalisation process was, for practical purposes, 70% complete when the non-dimensional time factor, T, defined below reached ten (when evaluated using a consistent system of units). The process was effectively complete when $T = 100$.

$$T = c_{vr}\, t/R^2$$

The operational c_{vr} value matched that for swelling or re-compression with radial drainage conditions. The equalisation process is far more rapid with open-ended coring piles that affect a smaller volume of clay during their installation. Field data indicate that pipe piles driven in high YSR clays may develop different set-up characteristics to closed-ended piles, showing short to medium-term capacity increases rather than temporary reductions in axial resistance.

Steel piles driven in clays may be subject to time-dependent processes that develop long after all pore pressures have equalised fully. Pellew (2002) found that the axial capacity of steel piles driven or jacked into London Clay (at Canons Park) had increased significantly over a 17 year period (following from full equalisation) and found evidence that the gains were due to redox reactions involving Sulphate Reducing Bacteria (SRB). The SRB reactions appeared to have increased the shear resistance available on the principal displacement shear surfaces formed during installation and prior load testing.

6.3 Implications

The implications of time effects on pile capacity are numerous:

- Soil resistances measured during pile driving are unlikely to equal those available in short to medium-term tests.
- Pile test interpretation has to account for age since driving; the strong effects of age with piles driven in sand have not been appreciated until recently.
- Pile loading styles (constant rate of penetration or maintained load) and loading rates affect capacity and load-displacement behaviour.
- Prior testing of piles to failure affects their capacities. Re-testing of the same pile at different ages can lead to misleading trends for ageing effects. It could also introduce false biases between compression and tension capacities, or between cyclic and static behaviour.
- In many cases aged existing piles may have higher capacities than expected. These capacities might be available in cases where additional loads were to be applied, or the piles re-used in a new or modified project development.

The reuse of existing foundations is becoming more commonplace as sites become more congested and space for new piles becomes restricted. In this respect, increases in driven pile capacity with time could provide the justification for higher working loads or else deliver a larger factor of safety against failure. The re-assessment of the Leman BD North Sea platform foundations is described by Jardine et al. (1998b), while the re-use of piles for buildings in city centres, and the steps required to confirm durability and load capacity, are described by Chapman et al. (2002).

7. GROUP EFFECTS IN SAND AND CLAY

7.1 Group effects in sand

The stress regime developed around a single driven pile is changed by the installation of a neighbouring pile. Such effects were investigated in field experiments at Dunkirk where a closed-ended pile was installed at a centre-to-centre distance of nine radii from a pre-installed ICP pile (Chow, 1995). Subsequent isolated load tests showed both the piles' Q_s values increasing by 50% due to gains in shaft radial effective stresses that were particularly high towards the pile tip. However, uplift caused by the neighbouring pile's installation softened the ICP's base response and the tip capacity mobilised Q_b, when the shaft was at its maximum, fell by 43%. Similar conclusions were drawn from an instrumented field pile group study described by Briaud et al. (1989). Open-ended piles are likely to be less strongly affected than closed-ended piles, but group effects are also likely to increase individual shaft capacities and lower utilisable base resistances.

Gains in individual piles' shaft capacities, however, will be partially offset under group loading by the effects of the overlapping vertical shear stress fields generated when neighbouring piles are loaded at the same time. These interactions dominate large groups of piles, which can tend to behave as an equivalent block or caisson. However, the interactions between small groups of piles can be estimated through the simplified geometrical approach proposed by Lehane et al. (2004).

Further research into the effects of group action on capacity is required, but it is provisionally recommended that the lower limit base capacity expressions given in Table 3 should be adopted when dealing with small groups of piles. Assuming the shaft components remain equal to those of isolated piles should be conservative; larger group capacities are more likely to be mobilised in the field.

7.2 Group effects in clay

The combined effects of group action on pile capacity in clay have been investigated at Kinnegar, Northern Ireland, by Trinity College Dublin and Imperial College. Field tests included static and cyclic tests on 6 m long (250 mm square) prestressed concrete piles driven in soft Belfast 'Sleech' clay; Lehane and Jardine (2003). Two isolated single piles and three groups were tested, with the groups being set out as 1 m by 1 m square grids with one additional central pile in each, giving a centre-pile to edge-pile spacing (s) to pile width (D) ratio $s/D \approx 2.8$. In contrast to the individually loaded piles driven in sands, the combined effects of group installation and simultaneous loading were found to be negative, with interaction leading to an overall group capacity that was interpreted to be less than the sum of the individual piles' capacities by around 16% in a tension test (performed with a relatively flexible pile cap) and 12% in a compression test involving a rigid cap. Group action also exacerbated the effects of cyclic loading, leading to a more marked degradation of axial capacity under comparable cyclic loading levels. The effects on axial capacity were in keeping with simple estimates made by considering the overlapping and compounding vertical shear stress fields generated by the piles;

(Lehane et al., 2004). The empirical Converse-Labarre equation, which is given below, provided reasonable estimates for the Kinnegar group factors[18]. The efficiency ξ that relates the overall capacity of a group (with m by n rows of piles) to that of the sum of the individual piles is given by:

$$\xi = 1 - \theta\,[(n-1)m + (m-1)n]/[90\,mn]$$

Where the groups contain n rows, and m columns of piles of diameter, D, set at spacings, s. The angle θ is taken as $\tan^{-1}(D/s)$ in some codes and $\tan^{-1}(D/2s)$ in others. Tests by Whitaker (1957) on solid model piles installed in remoulded London Clay indicated that it may be reasonable to take $\theta = \tan^{-1}(D/1.5s)$, and this rule applied at Kinnegar.

[18] Substituting $m = n = \sqrt{5}$, $s = 0.707$ m and $D = 0.25$ m gives $\xi = 0.84$, which falls close to the field measurements.

8. EXPERIENCE WITH OTHER SOIL PROFILES

The following sections discuss the applicability of the ICP procedures to an extended range of soil types and layered profiles.

8.1 Micaceous sands

Sands that include a significant content of the flaky mineral mica can develop very high void ratios, and show a flowing behaviour when subjected to shearing disturbance. The presence of mica can lead to unexpected problems in slope stability, foundation settlements and pile capacities. Tomlinson (1996) describes a suite of tests on piles driven in such sands at Jamuna Bridge in Bangladesh. Static tests were performed on two 762 mm diameter reduced scale trial piles that penetrated between 44 and 75 m below ground level. Both were tested first in compression around one week after driving, and then re-tested in tension one or two days later. One of the piles was driven on to the full depth and then re-tested in compression and tension. The shaft capacities were far below those anticipated from the conventional API procedures and significantly less than indicated by the ICP approach, although the base capacities appear to have been under-predicted by the ICP method. Using local CPT penetration tests, Tomlinson found a Q_c/Q_m range of 1.40 ± 0.25 for the shaft capacities assessed with the ICP method, while CUR (2001) found an even broader range for the API (1993) method. The test capacities may have been affected by their 'young' age and the programme of multiple tests on each pile. However, the short-term capacities of piles driven in micaceous sands appear to fall significantly below the ICP predictions. As noted earlier, the Jamuna piles developed very marked increases in capacity with time (see Figure 29) and the shortfall in capacity may be recovered after a relatively brief period of ageing.

8.2 Calcareous sands

Carbonate sands, defined here as having a Calcium Carbonate ($CaCO_3$) content exceeding 50%, can be either tough cemented calcarenites that lead to hard driving and possible pile damage, or highly compressible uncemented deposits that give very low capacities. The latter are composed of weak (often hollow) and brittle grains of organic origin and it has proved difficult to quantify the axial resistance of piles driven in such sands. Kolk (1997) proposed that an approach developed from the ICP methodology might be helpful; Thompson and Jardine (1998) reported a desk study that developed and validated Kolk's suggestion.

Thompson (1997) assembled a database of 34 compression and 5 tension field tests on piles driven to depths of up to 110 m in carbonate sands, with additional Soil Resistance to Driving (SRD) installation data. He sought to find a single set of ICP 'silica-sand' parameters that would provide reasonably

conservative estimates for the axial capacity database. A series of trials led to recommendations that gave safe estimates (Q_c/Q_m < 1) for more than 90% of his test cases.

It is recommended that the carbonate sands be treated as non-dilating sands with a 'typical' critical state interface shear angle $\delta_{ultimate}$ = 25º. The radial effective stresses acting on the pile shaft should vary with vertical effective stress and the relative pile tip depth parameters (h/R or h/R^* for his open-ended piles) as if the pile had been driven in a soil with a uniform and low relative density, having the CPT profile predicted for a normally consolidated silica sand with D_r = 15% by the Lunne and Christoffersen (1983) calibration chamber relationship. The submerged unit weight of the calcareous sand should be taken as 7.5 kN/m^3.

In summary, the recommendation is to take:

$$\tau_f = \sigma'_{rf} \tan 25º$$

$$\sigma'_{rc} = 72\,(\sigma'_{v0}/P_a)^{0.84}\,(h/R^*)^{-0.38} \qquad \text{(with } R^* = R \text{ if closed-ended)}$$

$\sigma'_{rf} = \sigma'_{rc}$ in compression

$\sigma'_{rf} = 0.8\,\sigma'_{rc}$ in tension, if closed-ended

$\sigma'_{rf} = 0.72\,\sigma'_{rc}$ in tension, if open-ended

Applying the above to Thompson's database led to a mean Q_c/Q_m = 0.74, with a standard deviation of 0.40. As noted earlier the aim was to give a conservative approach and a better average fit can be obtained by increasing the scalar term in the σ'_{rf} equation up to 97, giving a mean $Q_c/Q_m \approx 1$. In comparison, when the API variant proposed by Datta et al. (1980) for calcareous sands was tested against the same data set, the statistics (Q_c/Q_m = 1.6 and standard deviation = 1.20) indicated both huge scatter and a strong non-conservative bias.

8.3 Silts and low plasticity clays

8.3.1 Assessing whether to apply clay or sand design criteria

When applying the above methods it is necessary to decide whether a particular soil layer can be considered as an ideal 'sand' in which pile installation is an essentially drained process, or whether driving will take place under the practically undrained conditions that apply to an ideal 'clay'. Piezocone CPTU tests can be very helpful in making this judgement for transitional materials such as silts, clay-sands or other very low plasticity clays. If the CPTU test indicates an undrained response, the same is likely to apply to pile installation and the ICP clay methodology should be applied.

Note should be taken of the relative diameters D_{CPT}/D of the cone and pile when considering whether a fully drained response is to be expected in marginal cases. The rates of consolidation around the pile will tend to be reduced by a factor of around $[D_{CPT}/D]^2$, so an imperfectly drained CPT response may well indicate a predominantly undrained installation. In such cases a check should be made to assess which of the alternative assumptions (clay or sand) leads to the lower capacity for the layer in question, and the safer estimate from the two approaches should be adopted for design.

8.3.2 Low plasticity, low YSR, sensitive clays and clay-silts

Jardine and Chow (1996) found that the ICP procedures did not lead to any bias with plasticity index when checked against multiple tests in glacial soils at four sites[19]. Aldridge (2004) was also unable to find any significant bias with low plasticity in Fugro UK Ltd's database of pile load tests. However, field testing by the Norwegian Geotechnical Institute (NGI) led Karlsrud et al. (1993) and Clausen and Aas (2001) to warn that some low YSR, low plasticity clays and transitional clay-silts may not be able to mobilise the capacities expected by either the standard design API, or newer ICP, procedures. NGI reported lower than expected capacities in tests at the Pentre, Onsøy and Lierstranda sites. The difficulties encountered may have flowed, at least partially, from the following factors:

1. The nature of some of the field pile installations. Low plasticity soils are very easy to disturb and Chow (1997) argues that the pilot holes drilled by NGI at these three sites may have disturbed the ground significantly and so affected pile installation.
2. The difficulties of determining representative parameters. Sampling disturbance can be severe in such soils, leading to potentially misleading oedometer and UU triaxial test data. The effects of anisotropy can be very strong, leading to a wide spread of results between different test types.
3. Selecting representative δ_f values. The low plasticity Pentre samples developed much lower δ values than expected, given the soils' Atterberg limits. Chow (1997) found that a large proportion of the deposits' silt-sized particles were aggregated from active clay plates that broke up and developed low strength residual surfaces within shear zones (see Appendix B).
4. The soils at the three NGI sites are more sensitive than many tills, resulting in lower radial effective stresses on the pile shaft than would be typical of many offshore low plasticity clays.
5. The potential effects of partial dissipation during installation in laminated clay-silts, leading to significant reductions in radial effective stress as noted in the ICP tests at Pentre.

Independent predictions by the Authors of the Pentre LDP and NGI Onsøy tests are given in Appendix B and Table 8, respectively. Working with site specific ring shear test data, good to fair agreement was found with the field measurements, but the authors were unable to approach the low capacities measured at Lierstranda with either the ICP or API methods. Karlsrud et al. (1993) recall earlier work in Norway by Flaate (1968) who identified comparably low capacities in tests on timber, concrete and steel friction piles at some low YSR, low plasticity Scandinavian sites. Flaate reported multiple re-tests on these piles, finding that installations at these lean clay sites showed a remarkable trend for capacity to continue growing long after pore pressure dissipation was likely to have ended.

Driving instrumented piles provides a means to check for any such unusual behaviour when founding in low YSR, sensitive, lean deposits. Re-strike tests or staged load testing provides a way of checking on whether long-term set-up takes place to compensate for any apparent medium-term shortfall in capacity.

[19] Tilbrook Grange, Cowden, Croke Park Dublin and Pentre.

8.4 Diatomaceous clays and mudstones

Diatomaceous soils can show markedly different behaviours to those composed of more ordinary minerals. Their organic origin leaves them with large intragranular void spaces, high water contents and potentially unusually low effective unit weights, γ'. However, experience with two widely different diatomaceous deposits suggests that the ICP approaches may apply reasonably well, provided the requisite parameters are determined as recommended. Jardine et al. (1998a) describe data from a loading test on an 800 mm diameter open-ended steel pile that had been driven 8.2 m into a soft diatomaceous mudstone having γ' = 3.4 kN/m^3. All of the parameters necessary to run the ICP calculations were measured on good quality samples and the ratio of calculated to measured capacity, Q_c /Q_m, was found to be 0.91. As outlined in Section 5.1, Saldivar-Moguel (2002) found that the capacities of square piles driven into soft diatomaceous Mexico City clay can be predicted reasonably well with the ICP approach, finding a mean Q_c/Q_m, of 1.06 and a COV of 0.16 from his set of 26 tests.

8.5 Layered soil profiles

The ICP procedures have been applied successfully to predict pile test results in cases where the ground profiles involve layers of both sands and clays. In the same way the sand and clay procedures work well even when there are considerable variations of the clay or sand properties with depth. It appears that the methods can generally be applied to layered or variable soil profiles without taking any special measures. However, in cases where clays with low δ angles overlie sands, or high δ clays, reduced δ values should be considered over a transitional depth into the stronger underlying layer, as described by Jardine and Overy (1998). Tomlinson (1993) reports that with closed-ended piles, material from the upper layer can be dragged down to a depth of three or more pile diameters and while this has not been confirmed with open-ended piles it may be appropriate to allow for such down-drag when assigning δ values. Tomlinson also suggested rules for assessing base capacity changes at locations close to strata boundaries.

9. CYCLIC LOADING AND SEISMIC ACTION

9.1 General

Field-scale experiments have shown that cycling degrades the capacity of piles driven in clays; Karlsrud & Haugen (1985), Karlsrud et al. (1993) , Ove Arup (1986), Bogard and Matlock (1998) and others. The degree of degradation depends principally on the amplitude of the cyclic loading imposed (compared to the static capacity) and the number of cycles imposed. The most significant effects are found under high-level, two-way, loading: extreme repeated cycling can lead to short-term capacity losses of 50%, or more. Recovery, and in some cases improvement, of static capacity can take place with time after the cyclic loading has ended, although in some cases permanent degradation occurs.

Limited programmes of cyclic loading experiments were included in the ICP research performed at the sand and clay sites listed in Table 1; Bond (1989), Lehane (1992), Chow (1997). These provided insights into the effective stress processes that govern cyclic degradation and Jardine (1991, 1994) described an approach to understanding and predicting the effects of cyclic action. Jardine and Standing (2000) describe multiple cyclic tests on steel pipe piles driven in dense sand at Dunkirk. Lehane and Jardine (2003) and Lehane et al. (2003) report cyclic experiments on single piles and groups driven in the soft Belfast 'Sleech' clay at Kinnegar, Northern Ireland.

Load cycling affects the shaft capacity of driven piles by (i) changing the local radial effective stresses that act on the shaft, (ii) potentially (in brittle clays) degrading the local values of δ in cases where soil-pile slip starts to develop and (iii) transferring shaft load down to greater depths as the upper levels suffer shaft degradation. When considering events such as short duration offshore storms (with wave periods of perhaps ≈ 10 seconds) the soil behaviour close to the shaft is likely to be predominantly undrained in clays and drained in sands. However, conditions close to the shaft are highly constrained kinematically in both cases: circumferential and vertical strains are limited to very small values by the presence of the relatively rigid pile. In clays, the undrained zero volume strain constraint leads to very small radial strains, while in free draining sands the stiffness of the surrounding soil mass limits the radial displacements. The main aspects of load cycling to be considered under these conditions are outlined below.

- Undrained cyclic simple shear tests (involving either pore pressure measurements or a constant height vertical stress control algorithm) provide the simplest means of determining the soil's tendency to generate reductions in σ'_r under the relevant shaft loading regimes. Constant Normal Stiffness (CNS) tests may also be used in sands, in which the stiffness relationship expected at the pile-soil boundary: $\Delta\sigma'_r / \Delta r = 2G/R$ is simulated, taking account of the (pressure and strain- dependent) shear stiffness G and pile radius R.
- Undrained tests impose an infinite CNS, which gives an upper limit to the local losses in σ'_r and hence pile capacity. Cyclic triaxial and hollow cylinder tests can also provide information on the soil response under a variety of conditions; their value is enhanced if local strain measurements are made.

- The local changes in σ'_r are related to the amplitudes of the applied shear stresses and developed shear strains τ_{cyc} and γ_{cyc}. No reduction in σ'_r (causing capacity degradation) occurs below limiting values of γ_{cyc} that might amount to perhaps 0.005% for sands and lean clays. The interface failure mechanism sets an upper limit to $\tau_{cyc} = \sigma'_r \tan \delta_f$ and also to γ_{cyc}. While the latter depends on the soil's shear stiffness response and tan δ, slip is likely to occur before γ_{cyc} exceeds 1%.

- Cyclic laboratory tests on suitably consolidated samples can lead to simple (material and effective stress level specific) power law (or semi-logarithmic) relationships for the effects of cycling on the effective stress σ'_{n0}. Considering the effects of N uniform cycles on a sample initially consolidated to σ'_{n0}, test interpretation can give relationships such as:

$$\Delta\sigma'_n / \sigma'_{n0} = A[B + \tau_{cyc}/\tau_{max\ static}]\, N^C$$

or

$$\Delta\sigma'_n / \sigma'_{n0} = A[B + \tau_{cyc}/\tau_{max\ static}]^C \log_{10} N$$

- In this case $\tau_{max\ static}$ is the maximum shear stress that the soil could withstand when sheared against an interface made of the pile shaft material under the relevant (drained or undrained) conditions, after consolidation to the same σ'_n, so $\tau_{max\ static} = \sigma'_{nf} \tan \delta$. Sufficient tests are needed to confirm which form of relationship is most appropriate for the anticipated range of N, leading to secure estimates for the material coefficients such as A, B and C above. Note that A and B should have negative values.

- The effects of shear stress cycling on the pile capacity may then be predicted by assuming that the same simple relationship applies over the shaft. The capacity reductions are assessed from the changes in the shaft radial effective stress profiles, starting from the initial (radial) normal effective stresses predicted from the ICP approach. Groups of cycles having different amplitudes can be considered by following an approach such as the curve hopping procedure applied to Gravity Base foundations by Andersen and Hoeg (1992). As mentioned earlier, cycling at levels below the critical limit can be beneficial, enhancing for example the medium-term increases in driven pile capacity seen in sands.

- The effects of cycling develop progressively. Degradation spreads downwards from the pile head at a rate that depends on the cyclic loads, the pile's axial stiffness, the initial soil profile and any potential brittleness in δ. The pile base will experience little of the applied cyclic loading until the shaft is nearing cyclic failure. One-way pile head loading leads to two-way local cycling once local slip starts to develop at shallow depth, causing compressible piles to degrade more rapidly than rigid piles. In the same way, piles that rely on end bearing for a significant proportion of their capacities are likely to be more susceptible to cyclic action because the local ratios of $\tau_{cyc}/\tau_{max\ static}$ will be correspondingly higher.

- Quantitative cyclic loading assessments can be developed for single piles using a variety of approaches, including non-linear Finite Element methods or cyclic *T-Z* approaches; see for examples Stock et al. (1993), Randolph et al. (1996) and WS Atkins (2000).

- Simplified calculations may also be performed applying the above expressions to gauge the response at a 'representative' point on the shaft, and then assuming that the cyclic shear stresses and resulting degradation apply at other points on the shaft in proportion to the local shaft resistance.

9.2 Recent cyclic pile testing in sand and clay

Test data from field loading experiments provide graphic illustrations as to the potential response of different soil types to loading. Provided a sufficient number of tests is conducted, the results can be summarised conveniently by plotting interaction diagrams where the load combinations are expressed as the amplitude of the pile head loads Q_{cyclic} and their average values $Q_{average}$ normalised by the static capacity $Q_{max\ static}$. The latter may change during cycling and the value applying just before cycling commences has to be estimated from static control tests, or some other means.

We are not aware of any field investigation of the cyclic response of piles driven in sand being reported in the literature, prior to the account by Jardine and Standing (2000) of cyclic experiments on 10 m and 19 m long, 456 mm outside diameter, steel open-ended pipe-piles driven in dense sand at Dunkirk. Figure 31 summarises the results in a single interaction diagram. Each cyclic failure is characterised by a number of cycles to failure N_f, which is indicated beside each data point. Cases where no failure developed within the test period are also identified. Contours may then be interpreted to show the number of cycles that would be required to cause a failure under any given load combination. One-way loading can cause significant damage; severe two-way loading can easily halve pile capacity. Many of the cyclic tests involved piles that had undergone prior failure. As discussed earlier, capacity recovers partially with time after cyclic failure, but pre-failed piles can never regain the capacity applying to fresh piles. Careful account had to be taken of changes in $Q_{max\ static}$ caused by ageing effects and pre-testing in the interpretation, and it is encouraging that the tests showed broadly compatible trends when interpreted in terms of loads normalised by $Q_{max\ static}$.

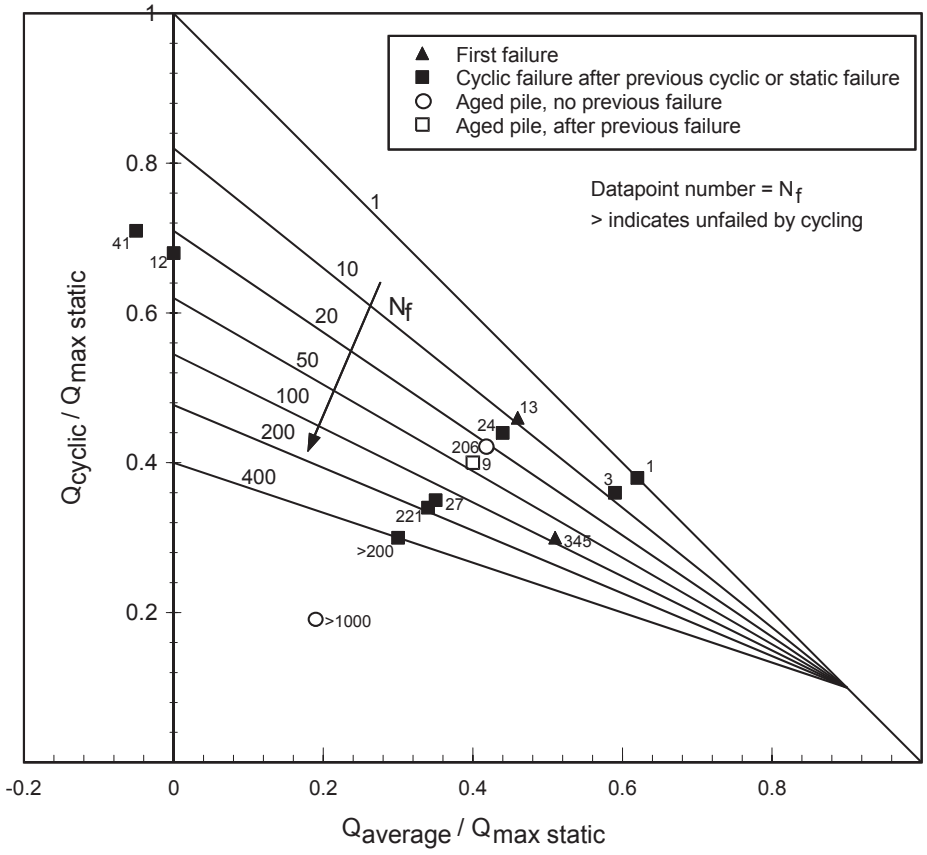

Figure 31. Cyclic interaction diagram for driven pipe piles in dense sand at Dunkirk

Cyclic loading also degrades the capacity of piles driven in clays. Low OCR, sensitive, clays with high δ angles are more susceptible to cycling than insensitive soils. Clays with low (and non-brittle) δ angles that limit the shear stress cycles that can be applied across the pile-soil interface are the least susceptible; Karlsrud et al. (1993); Jardine (1994). Figure 32 shows an interaction diagram taken from recent one-way cyclic tension tests undertaken at Kinnegar on two isolated 6 m long concrete (250 mm square) piles driven in soft Belfast 'Sleech' clay; Lehane and Jardine (2003). As with the sand tests considered above, the cyclic and mean loads are shown normalised by the pile static capacity applying before cycling commenced (with capacities being defined from slow, maintained load, tests on control piles). The response seen during the relatively rapid cycling (with period T = 60 seconds) involves a combination of degradation due to cycling and temporary capacity enhancement due to loading rate effects. It can be seen from Figure 32 that hundreds of cycles were required to cause single pile failure under one-way conditions even when the cyclic amplitude approached half of the static capacity and the maximum loads approached the static capacity. However, static re-tests undertaken after the cyclic failures showed that their static capacities had degraded by around 15%; far greater degradation could be expected under extreme two-way loading conditions.

Three pile groups were installed at Kinnegar, each comprising four piles set out on 1 m by 1 m square grid, plus one additional central pile. Figure 33 presents the results of the cyclic tests on the three installations. Group action clearly exacerbates the cyclic effects: the one-way tension loading levels required to induce failure (in a similar number of cycles) were around 20% lower than in the single pile cyclic tests.

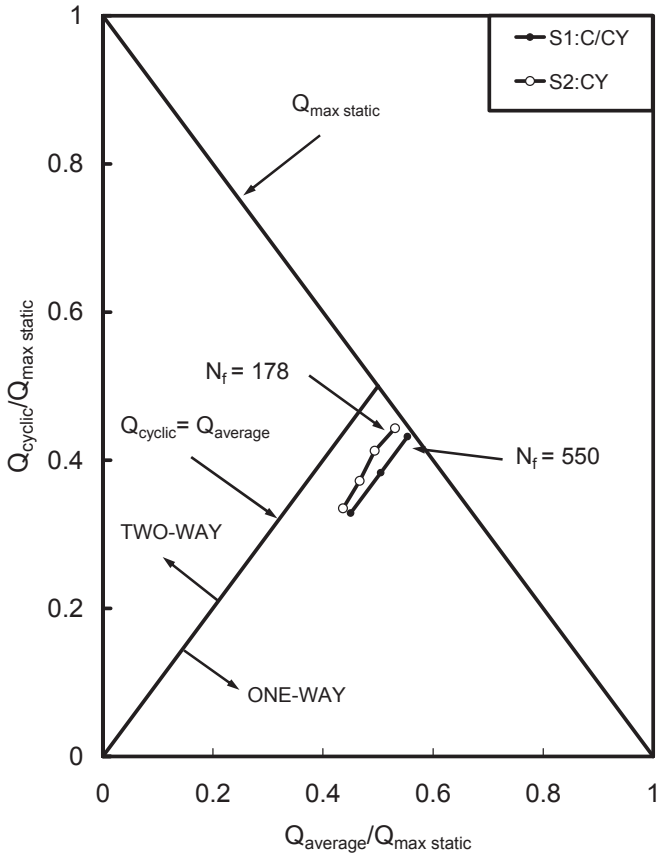

Figure 32. Cyclic interaction diagram for single precast concrete piles in soft clay at Kinnegar (Lehane and Jardine, 2003)

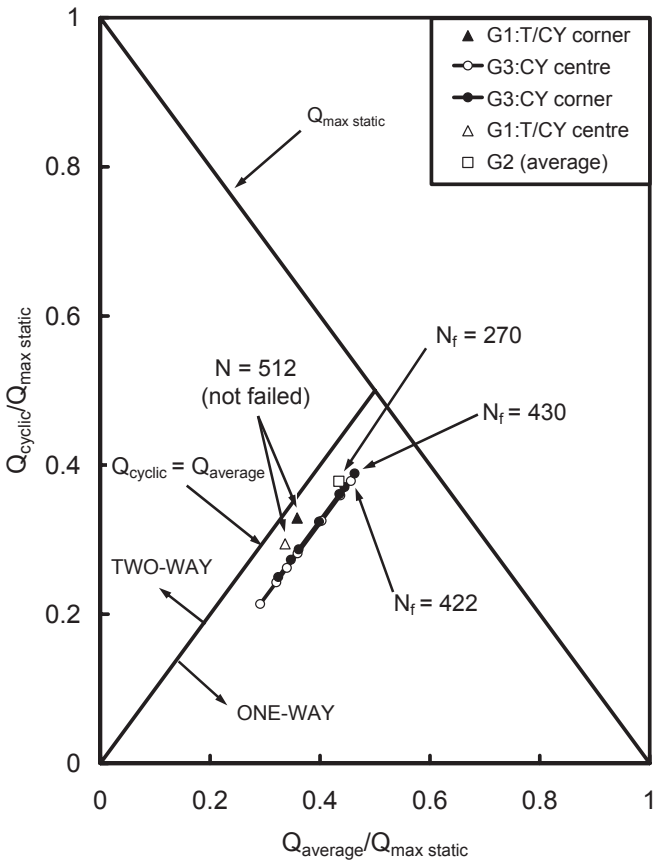

Figure 33. Cyclic interaction diagram for pile groups in soft clay at Kinnegar (Lehane and Jardine, 2003)

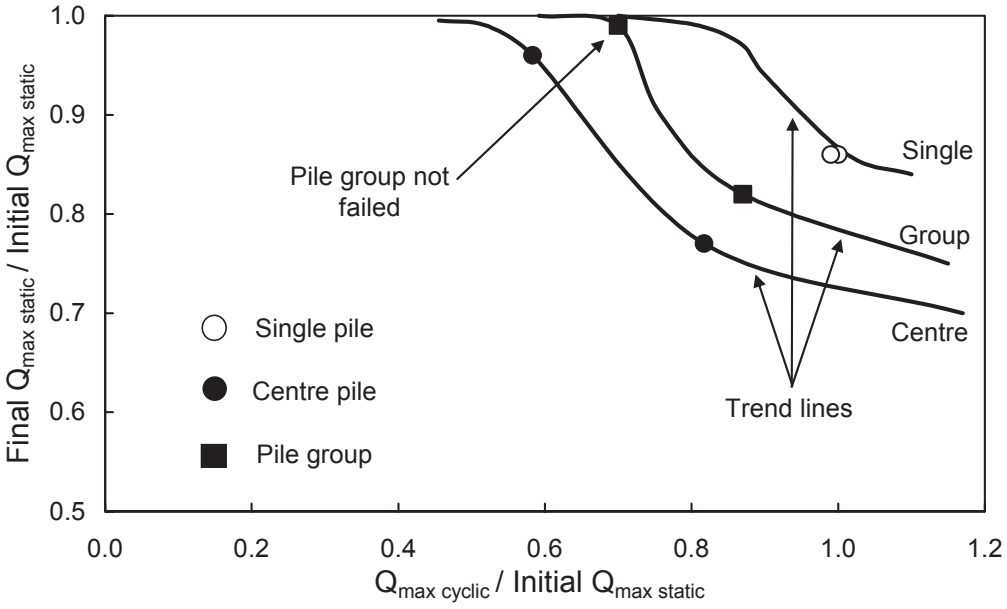

Figure 34. The effects of group action on cyclic loading (Lehane and Jardine, 2003)

Static tests were conducted on the single piles and groups after the end of cycling and the results are summarised in Figure 34, in terms of the ratio of the post cycling 'final' shaft capacity $Q_{max\ static}$ to the initial, pre-cycling, value expected at the same age from control tests. This degradation ratio is plotted against the ratio of the maximum cyclic shaft load ($Q_{max\ cyclic} = Q_{average} + Q_{cyclic}$) to the initial $Q_{max\ static}$. While the single piles lost around 15% of their capacity, greater losses were developed by the group piles, with the central pile being the most affected. As with static group action, the mutual compounding of vertical shaft shear stresses is thought to be main factor that causes the observed group action effects.

9.3 Axial capacity of piles driven in clay under seismic loading

It has been argued that the rate effects referred to above in connection with cyclic loading apply even more strongly under fast acting seismic loading, leading to potentially high bias factors in which seismic capacity might be far greater than the slow static capacity. However, it is recognised that such rate effects may be counteracted by cyclic degradation processes. Recently Saldivar-Moguel (2002) undertook a systematic analysis of the response of structures resting on driven friction piles to shaking during earthquakes in Mexico City, correlating the extreme pile loads interpreted from his analysis with the medium-term capacities expected from site-specific ICP calculations, applying the modest local 'correction factor' that he found applied to the unusual diatomaceous Mexico City clays. His overall conclusion was that, under the mainly one-way cycling imposed in the cases considered, the positive effect of the high loading rates was roughly matched by the cyclic degradation, leading to only modest (10 to 15%) or negligible bias factors. The Kinnegar tests discussed above suggest that the static axial capacities are likely to have been degraded, especially in those cases where slip movements occur during the earthquakes, giving rise to extreme load cycling.

10. CONCLUSIONS

10.1 Main points

1. This document has re-stated, updated and extended the ICP design approaches developed through long-term research programmes carried out by Imperial College in collaboration with other groups.

2. Attention has focused on the axial capacity of driven piles. Load-displacement behaviour has not been considered. Research on this area, including field measurements, has been reported by Jardine and Potts (1988, 1992) and Jardine et al. (2004).

3. Consideration has been given to silica sands, clays and other soil types including calcareous and micaceous sands, as well as diatomaceous clays and silts. The effects of pile shape, group action, time, cyclic loading and seismic action have been discussed, as has the rational choice of Factors of Safety and LRFD factors.

4. Detailed worked examples are set out in Appendix B, showing how the methods can be applied explicitly to sand and clay sites. The two well-known cases cited both involved high quality tests conducted for joint industry research programmes.

5. The new capacity calculation procedures are relatively simple and can be applied easily in practice. Nevertheless, when used correctly they are considerably more accurate than existing procedures. Greatly improved reliability statistics are found when the methods are tested against high quality databases, allowing factors of safety to be selected rationally.

6. The procedures have been developed through a combination of field, laboratory and theoretical research. They have also been checked thoroughly against field performance. Reference was made to around 250 individual pile tests in compiling this document and it has been shown that the ICP procedures provide a good model for nearly all of the field circumstances considered. The procedures have also been applied successfully in onshore and offshore practice for almost ten years, confirming their general fitness for purpose.

7. The methods rely critically on appropriate site investigations being performed. Check lists are given below for the key parameters that must be obtained. Some parameters, such as clay sensitivity and YSR, may be derived by more than one type of procedure, and guidance has been given on how this may be approached.

8. The recommended interface shear tests are often omitted in conventional investigations and CPT testing is not always performed: we recommend that practice should be revised to include these measurements.

10.2 Check list for sands

- Good quality CPT or CPTU tests.
- Laboratory, or in-situ, unit weight measurements.
- Interface shear tests with suitable initial roughness, sand densities and stress levels. Ring shear tests are preferred in cases involving long piles driven in dense sands.
- Undrained or CNS cyclic simple shear tests may be required in cases where cyclic loading action may be important.

10.3 Check list for clays

- Good quality CPT or CPTU tests, or equivalent in-situ measurements.
- Laboratory unit weight measurement.
- YSR measurements from in-situ tests, laboratory CAU or UU triaxial tests, intact oedometer tests and index properties.
- Sensitivity measurements from UU triaxial tests and remoulded strengths, remoulded oedometer tests and index properties.
- Interface ring shear tests with suitable roughness, stress levels and shearing rates.
- Undrained cyclic simple shear tests may be required in cases where cyclic loading action may be important.

11. ACKNOWLEDGEMENTS

The Authors acknowledge the contributions made by many current and former colleagues to the development of the ICP procedures and their recent extension. The most important contributions were made by Drs Andrew Bond and Barry Lehane, and by the technician group at Imperial College: Steve Ackerley, Graham Keefe and Alan Bolsher. As referenced in the text, the studies by Richard Cowley, Steven Everton, Alice Ridgway, Charlie Strick van Linschoten, Giles Thompson and by Drs Bryan McCabe, Emilio Saldivar-Moguel and Adam Pellew have also been highly valuable.

12. REFERENCES

Aas, P.M., Clausen, C.J.F. and Lacasse, S. (2004), Bearing capacity of driven piles in sand based on pile load tests, *Presentation at the API workshop, Capacity of Driven Piles in Sand from CPT Test, Results and Interpretation of Euripides and Ras Tanajib Full-Scale Tests*, Houston.

Aldridge (2004) Personal Communication.

American Petroleum Institute (1993), *RP2A-WSD: Recommended Practice of Planning, Designing and Constructing Fixed Offshore Platforms - Working Stress Design*, 20th edition, Washington, pp. 59-61.

Andersen, K.H. and Hoeg, K. (1992), Deformation of soils and structures subjected to combined static and cyclic loads. *Proc. Xth ECSMFE*, Firenze, Vol. 4, pp. 1147-1158.

Aubeny, C.P. (1992), *Rational interpretation of in situ tests in cohesive soils*. PhD Thesis, Massachusetts Institute of Technology (MIT).

Axelsson, G. (2000), *Long term set up of driven piles in sand*. PhD Thesis, Royal Institute of Technology, Stockholm, Sweden.

Baldi, G., Belottini, R., Ghionna, V.N., Jamiolkowski, N.I. and Lo Presti, D.L.F. (1989), Modulus of sands from CPTs and DMTs. *Proc. 12th ICSMFE*, Rio de Janeiro, Vol. I pp. 165-170.

Bogard, D. and Matlock, H. (1998), Static and cyclic load testing of a 30-inch diameter pile over a 2.5-year period. *Proc. Offshore Technology Conf.*, OTC 8767, pp. 455-468.

Bond, A.J. (1989), *Behaviour of displacement piles in over-consolidated clays*. PhD Thesis, Imperial College, London.

Bond, A.J. and Jardine, R.J. (1990), *Research on the behaviour of displacement piles in an overconsolidated clay*. UK Dept. of Energy, OTH Report, OTH 89296, HMSO, London.

Bond, A.J. and Jardine, R.J. (1991), Effects of installing displacement piles in high OCR clay. *Géotechnique,* Vol. 41, No. 3, pp. 341-363.

Bond, A.J., Jardine, R.J. and Dalton, J.C.P. (1991), The design and performance of the Imperial College instrumented pile. *Am. Soc. for Testing Materials, Geotech. Testing J*, Vol. 14, No. 4, pp. 413-424.

Bond, A.J. and Jardine, R.J. (1995), Shaft capacity of displacement piles in a high OCR clay. *Géotechnique,* Vol. 45, No. 1, pp. 3-23.

Briaud, J-L. and Tucker, L.M. (1988), Measured and predicted axial load response of 98 piles. *J. Geotech. Engn*g., ASCE, Vol. 114, No. 9, pp. 984-1001.

Briaud, J-L., Tucker, L.M. and Ng, E. (1989), Axially loaded five pile group and a single pile in sand. *Proc. 12th ICSMFE*, Rio de Janeiro, Vol. 2, pp. 1121-1124.

Brucy, F., Meunier, J. and Nauroy, J-F. (1991), Behaviour of a pile plug in sandy soils during and after driving. *Proc. 23rd Offshore Technology Conf.*, OTC6514, pp. 145-154.

Bullock, P. & Schmertmann, J.H. (1995), Personal Communications.

Burland, J.B. (1990), On the compressibility and shear strength of natural clays. 30th Rankine Lecture, *Géotechnique*, Vol. 40, No. 3, pp. 327-378.

Bustamante, M. and Gianeselli, L. (1982), Pile bearing capacity by means of static penetrometer CPT. *2nd Eur. Symp. on Penetration Testing*, Amsterdam, pp. 493-500.

Chapman, T.J.P., Chow. F.C. & Skinner, H. (2002). Building on old foundations - sustainable construction for urban regeneration. *CE World, ASCE's First Virtual World Congress for Civil Engineering*, www.ceworld.org

Chin, C. T. (1986), *Open-ended pile penetration in saturated clays*. PhD Thesis, Massachusetts Institute of Technology (MIT).

Chow, F.C. (1995), Field measurements of stress interactions between displacement piles in sand. *Ground Engineering*, Vol. 28, No. 6, pp. 36-40.

Chow, F.C. (1997), *Investigations into displacement pile behaviour for offshore foundations*. PhD Thesis, Imperial College, London.

Chow, F.C. and Jardine, R.J. (1996), *Research into the behaviour of displacement piles for offshore foundations.* UK Health and Safety Executive, OTO Report, HSE Books, London.

Chow, F.C. and Jardine, R.J. (1997), Applying the new Imperial College pile design methods to large open-ended piles in clay and sand. *Proc. 8th Int. Conf. on the Behaviour of Offshore Structures (BOSS)*, Delft, Pergamon Press (UK), pp. 109-124.

Chow, F.C., Jardine, R.J., Nauroy, J.F. & Brucy, F. (1997). Time-related increases in the shaft capacities of driven piles in sand. *Géotechnique,* Vol. 47, No. 2, pp. 353-361.

Chow, F.C., Jardine, R.J., Brucy, F. and Nauroy, J.F. (1998), The effects of time on the capacity of pipe piles in dense marine sand. *ASCE, JGE*, Vol. 124, No. 3, pp. 254-264.

CIRIA (1977), *Rationalisation of Safety and Serviceability Factors in Structural Codes*, Report 63, Construction Industry Research Information Association, London.

Clarke, J. (ed) (1993), *Conf. on Large-Scale Pile Tests in Clay*. Thomas Telford, London.

Clausen, C.J.F. and Aas, P.M. (2001), Capacity of driven piles in clays and sands on the basis of pile load tests. *Proc. Conf. ISOPE*, Stavanger, Vol. 4, pp. 581-586.

Coop, M.R., Sorensen, K.K., Bodas Freitas, T. and Georgoutsos, G. (2004), Particle breakage during shearing of a carbonate sand. *Géotechnique*, Vol. 54, No. 3, pp. 157-164.

Cowley, R.C. (1998), *The effect of pile geometry on the design of piles using the new Imperial College pile design method*. MSc dissertation, Imperial College, London.

CUR (2001), *Bearing capacity of steel pipe piles*. Report 2001-8 Centre for Civil Engineering Research and Codes, Gouda, The Netherlands.

Datta, M., Gulatti, S.K. and Rao, G.V. (1980), An appraisal of the existing practice of determining the axial load capacity of deep penetration piles in calcareous sands. *Proc. 16th Offshore Technology Conf., Houston*, OTC4838, pp. 527-534.

De Beer, E., Lousberg, D., de Jonghe, A., Carpentier, R. and Wallays, M. (1979), Analysis of the results of loading tests performed on displacement piles of different types and sizes penetrating at relatively small depth into a very dense sand layer. *Proc. Recent Developments in the Design and Construction of Piles*, ICE, London, pp. 199-211.

de Ruiter, J. and Beringen, F.L. (1979), Pile foundations for large North Sea structures. *Marine Geotechnology*, Vol. 3, No. 3, pp. 267-314.

Efthymiou, M., van de Graaf, J.W., Tromans, P.S. and Hines, I.M. (1996), Reliability based criteria for fixed offshore platforms, *15th OMAE Conf.*, Florence.

Flaate, K. (1968), Baereevnen av friksjononspeler I leire. *Veglaboratoret*, 1968.

Foray, P.Y. & Colliat, J-L. (2005) CPT-based design method for piles driven in dense sands calibrated on the Euripides pile load tests. Proc. Int. Symp. on Frontiers in Offshore Geotechnics, Perth (in press).

Fugro (2004), *Axial pile capacity design method for offshore driven piles in sand*. Report No. P1003 to API.

Gibbs, C.E., McCauley, J., Mirza, U.A. & Cox, W.R. (1993), Reduction of field data and interpretation of results for axial load tests of two 762mm diameter pipe piles in clay. *Proc. Conf. Large-Scale Pile Tests in Clay*, London, Thomas Telford London, pp. 285-345.

Hight, D.W., Lawrence, D.M., Farquhar, G.B. and Potts, D.M. (1996), Evidence for scale effects in the end bearing capacity of open-ended piles in sand. *Proc. 28th Offshore Technology Conf*, Houston, OTC7975, pp. 181-192.

Jardine. R.J. (1985), *Investigations of pile-soil behaviour, with special reference to the foundations of offshore structures*, PhD Thesis, Imperial College, London.

Jardine, R.J. and Potts, D.M. (1988), Hutton tension leg platform foundations: An approach to the prediction of pile behaviour, *Géotechnique*, Vol. 38, No. 2, pp. 231-252.

Jardine, R.J. (1991), The cyclic behaviour of offshore piles, in *The Cyclic Loading of Soils*, Brown and O'Reilly (eds.), Blackie & Son, Glasgow.

Jardine, R.J., Lehane, B.M. and Everton, S.J. (1992), Friction coefficients for piles in sands and silts. *Proc. Int. Conf. on Offshore Site Investigation and Foundation Behaviour*, SUT, London, Kluwer (Dordrecht), pp. 661-677.

Jardine, R.J. and Potts, D.M. (1992), Magnus foundations: Soil properties and predictions of field behaviour. *Proc. Conf. on Large Scale Pile Tests in Clay*, Thomas Telford, London, pp. 69-83.

Jardine, R.J. (1994), *Review of offshore pile design for cyclic loading: North Sea clays*. HSE Offshore Technology Report, OTN 94 157.85.

Jardine, R.J. and Lehane, B.M. (1994), *Research into the behaviour of offshore piles: Field experiments in sand and clay*. UK Health and Safety Executive, OTH Report, OTH 93 401, HSE Books, London.

Jardine, R.J. and Chow, F.C. (1996), *New Design Methods for Offshore piles*, Marine Technology Directorate, London.

Jardine, R.J. and Overy, R.F. (1996), Axial capacity of offshore driven piles in dense sand, *Proc. 28th Offshore Technol. Conf*, Houston, OTC7973, pp. 161-170.

Jardine, R.J., Overy, R.F. & Chow, F.C. (1998b), Axial capacity of offshore piles in dense North Sea sands. *ASCE, JGE*, Vol. 124, No. 2, pp. 171-178.

Jardine, R.J., Chow, F.C., Matsumoto, T. & Lehane, B.M. (1998a), A new design procedure for driven piles and its application to two Japanese clays. *Soils & Foundations* Vol. 38, No.1, pp. 207-219.

Jardine, R.J. and Saldivar, E. (1999), An alternative interpretation of the West Delta 58A tension pile research results. *Proc. Offshore Technology Conf.*, Houston, OTC10827.

Jardine, R.J. and Standing, J.R. (2000), *Pile load testing performed for HSE cyclic loading study at Dunkirk, France*. 2 Vols. Offshore Technology Report OTO 2000 007; Health and Safety Executive, London.

Jardine R.J., Standing, J.R., Jardine, F.M., Bond, A.J. and Parker, E. (2001), A competition to assess the reliability of pile prediction methods. *Proc. XVth ICSMGE*, Istanbul, Vol. 2, pp. 911-914.

Jardine, R.J., Kuwano, R., Zdravkovic, L. and Thornton, C. (2002), Some fundamental aspects of the pre-failure behaviour of granular soils. *Proc. 2nd Int. Symp. On Pre-failure Behaviour of Geomaterials*, IS-Torino, Balkema, Rotterdam, Vol. 2, pp. 1077-1111.

Jardine, R.J., Standing, J.R. and Kovacevic, N. (2004), Lessons learned from full-scale observations and the practical application of advanced testing and modeling. *Proc IS-Lyon, Deformation Characteristics of Geomaterials*, Eds. Di Benedetto, Doanh, Geoffroy and Sauzeat, Balkema, Vol. 2, In Press, 45p.

Jardine, R.J., Standing, J.R. and Chow, F.C. (2005). Some observations of the effects of time on the capacity of piles driven in sand. Submitted to *Géotechnique*, December 2004.

Kalsrud, K. and Haugen, T. (1985), Axial static capacity of steel model piles in overconsolidated clay. *Proc. 11th ICSMFE*, San Francisco, Vol. 3, pp. 1401-1406.

Karlsrud, K., Nowacki, F. and Kalsnes, B. (1993), Response in soft clay and silt deposits to static and cyclic loading based on recent instrumented pile load tests. *Proc. SUT Int. Conf*, Kluwer, Dordrecht, pp. 549-584.

Kolk, H. (1997), Significant developments in offshore geosciences. Invited Paper. *Proc. 8th Int. Conf. on Behaviour of Offshore Structures (BOSS)*, Delft, Vol. 1, pp. 3-40, Pergamon.

Lambson, M.D., Clare, D.G., Senner, D.W.F.S. & Semple, R.M. (1993), Investigation and interpretation of Pentre and Tilbrook Grange soil conditions, *Proc. Conf. Large-scale Pile Tests in Clay*, London, Thomas Telford London, pp. 134-196.

Langen, H. van, Swee, J., Efthymiou, M. and Overy, R.F. (1995), Integrated foundation and structural reliability analysis of a North Sea structure. *Proc. Offshore Technology Conf.*, Houston, OTC 7784.

Lehane, B.M. (1992), *Experimental investigations of pile behaviour using instrumented field piles*. PhD Thesis, Imperial College, London.

Lehane. B.M., Jardine, R.J., Bond, A.J. and Frank, R. (1993), Mechanisms of shaft friction in sand from instrumented pile tests. *J. Geotech. Engng.*, ASCE, Vol. 119, No. 1, pp. 19-35.

Lehane, B.M. and Jardine, R.J. (1994a), Displacement pile behaviour in glacial clay. *Can. Geotech. J.*, Vol. 31, No. 1, pp. 79-90.

Lehane, B.M. and Jardine. R.J. (1994b), Displacement pile behaviour in a soft marine clay. *Can. Geotech. J.*, Vol. 3l, No. 2, pp. 181-191.

Lehane, B.M. and Jardine, R.J. (1994c), Shaft capacity of driven piles in sand: a new design approach. *Proc. Conf. on the Behaviour of Offshore Structures (BOSS)*, pp. 23-36.

Lehane, B.M., Jardine, R.J., Bond, A.J. and Chow, F.C. (1994), The development of shaft resistance on displacement piles in clay. *Proc. 13th ICSMFE*, New Delhi, Vol. 2, pp. 473-476.

Lehane, B.M., Chow, F.C., McCabe, B.A. and Jardine, R.J. (2000), Relationships between shaft capacity of driven piles and CPT end resistance. *Geotechnical Engineering*, Vol. 143, No. 2, pp. 93-102.

Lehane, B.M. and Gavin, K.G. (2001), The base resistance of jacked pipe piles in sand. *J. Geotech. Geoenviron. Eng. ASCE*, Vol.127, No. 6. pp. 473-480.

Lehane, B.M. and Randolph, M.F. (2002), Evaluation of a minimum base resistance for driven pipe piles in siliceous sand. *J. Geotech. Geoenviron. Eng. ASCE*, Vol. 128, No. 3, pp. 198-205.

Lehane B.M. and Jardine R.J. (2003), *Pile group tension cyclic loading. Field test programme at Kinnegar N. Ireland*. Research Report 101, Health and Safety Executive (HSE) publications, Sudbury. 43pp.

Lehane, B.M., Jardine, R.J. and McCabe, B.A. (2003), One-way axial cyclic tension loading of driven piles in clay. *BGA Int. Conf. on Foundations*, Dundee, Thomas Telford, London, pp 493-506.

Lehane, B.M., Jardine, R.J. and McCabe, B.A. (2004), Response of a pile group in clay to first time one-way cyclic tension loading. Advances in Geotechnical Engineering. *Proc. Skempton Memorial Conference*. Thomas Telford, London, pp. 700-710.

Lunne, T. and Christoffersen, H.P. (1983), Interpretation of cone penetrometer data for offshore sands. *Proc. Offshore Technology Conf.*, Houston, OTC4464, pp. 181-192.

Lunne, T., Robertson, P. and Powell, J. (1997), *Cone Penetration Testing in Geotechnical Practice*, Chapman Hall, 312pp.

Madsen, H.O., Krenk, S. and Lind, N.C. (1986), *Methods of Structural Safety*. Prentice Hall, London, 403pp.

Moses, F. (1980), *Final Report for API PRAC 79-22*. American Petroleum Institute, Dallas.

Ove Arup and Partners (1986), *Research on the behaviour of piles as anchors for buoyant structures.* Dept. of Energy, Offshore Technology Report, OTH 86 215. HMSO, London, 80pp.

Parker, E. J., Jardine, R.J., Standing, J.R. and Xavier, J. (1999), Jet grouting to improve offshore pile capacity. *Proc. Offshore Technology Conf.*, Houston, OTC10828.

Pellew, A. (2002), *Field investigations into the behaviour of piles in clay*. PhD. Thesis, University of London.

Ramsey, N., Jardine, R.J., Lehane, B.M. & Ridley, A.M. (1998), A review of soil-steel interface testing with the ring shear apparatus. *Proc. Conf. Offshore Site Investigations and Foundation Behaviour.* Society for Underwater Technology, London, pp. 237-258.

Randolph, M.F., Joer, H.A., Khorshid, M.S. and Hyden, A.M. (1996), Field and laboratory data from pile load tests in calcareous soils. *Proc. 28th Offshore Technology Conf*, Houston, OTC 7992, pp. 327-336.

Randolph, M.F. (2003), Science and Empiricism in pile foundation design. *Géotechnique*, Vol. 53, No. 10, pp. 847-876.

Randolph, M.F., Jamiolkowski, M.B. and Zdravkovic, L. (2004), Load carrying capacity of foundations. Keynote Lecture, Advances in Geotechnical Engineering. *Proc. Skempton Memorial Conference*, London, Thomas Telford, London, Vol.1, pp. 207-240.

Ridgway, A. (2004), *A re-evaluation of driven pile loading tests at Lierstranda and Onsøy, Norway*. MSc. dissertation, Imperial College, London.

Saldivar-Moguel, E.E. (2002), *Investigation into the behaviour of displacement piles under cyclic and seismic loads*. PhD Thesis, Imperial College, London.

Smith, P.R. (1992), *Properties of high compressibility clays with reference to construction on soft ground*. PhD Thesis, Imperial College, London.

Stock, P.J., Jardine, R.J. & McIntosh, W. (1993). Foundation Monitoring on the Hutton Tension Leg Platform. *Proc. Conf. on Offshore Site Investigation and Foundation Behaviour*, Society for Underwater Technology, London, Kluwer, London, pp. 469 – 491.

Strick van Linschoten, C.J. (2004), *Driven pile capacity in organic clays, with particular reference to square piles in the Belfast Sleech*. MSc dissertation, Imperial College, London.

Thompson, G.W.L. (1997), *The applicability of the new Imperial College Design method to calcareous sands*. MSc dissertation, Imperial College, London.

Thompson, G.W.L. and Jardine, R. J. (1998), The applicability of the new Imperial College Design method to calcareous sands. *Proc. Conf. Offshore Site Investigations and Foundation Behaviour*. Society for Underwater technology, London, pp. 383-400.

Tomlinson, M.J. (1993), *Foundation Design and Construction*. 6th edition, Pitman, London.

Tomlinson, M.J. (1996), Presentation at British Geotechnical Society meeting "Recent Advances in driven pile design". Institution of Civil Engineers, London, reported in *Ground Engineering*, Vol. 29, No. 10, pp. 31-33.

Whitaker, T. (1957), Experiments with model piles in groups. *Géotechnique*, Vol. 7, No. 4, pp. 147-167.

White, D.J. and Bolton, M.D. (2002), Observing friction fatigue on a jacked pile. *In Centrifuge and Constitutive Modelling: Two Extremes*. Ed S.M. Springman, Swets & Zeitlinger, Rotterdam, pp 347-354.

White, D.J. & Lehane, B.M. (2004), Friction fatigue on displacement piles in sand. *Géotechnique*, Vol 54, No. 10, pp 645-659.

Williams, R.E., Chow, F.C. & Jardine, R.J. (1997), Unexpected behaviour of large diameter tubular steel piles. *Proc. Int. Conf. on Foundation Failures*, IES, NTU, NUS & Institution of Structural Engrs, Singapore, 12-13 May 1997.

Wroth, C.P. (1979), Correlations of some engineering properties of soils. *Proc. 2nd Int. Conf. on Behaviour of Offshore Structures (BOSS)*, British Hydromechanics Research Association, Fluid Engineering, Cranfield, UK, Vol. 1, pp. 121-132.

WS Akins (2000), *Cyclic degradation of offshore piles*. OTO Report 2000/013 Health and Safety Executive (HSE) Books.

Zuidberg, H.M. and Vergobbi, P. (1996), EURIPIDES, Load tests on large driven piles in dense silica sands. *Proc. Offshore Technology Conf.*, Houston, OTC7977.

APPENDIX A

RING SHEAR TESTING METHODOLOGY

Standard test procedure for soil-steel interface ring shear tests

A1.1 Principle of test

Drained ring shear interface tests may be used to obtain the interface friction angles (δ_f) that govern the shear stress that can be mobilised on the shaft of a driven pile. Fast shearing between the soil specimen and an appropriate interface is initially performed; this is essential to the creation of a fabric on the shearing plane similar to that adjacent to a driven pile. Subsequent drained shearing allows measurement of the peak and ultimate interface friction angles (δ_{peak} and $\delta_{ultimate}$). δ_{peak}, unlike $\delta_{ultimate}$, is affected to some extent by factors such as the precise rate of the prior fast shearing, the loading history, the specimen state and the type of ring shear apparatus.

A1.2 Specimen and interface preparation

a) Ideally, fine-grained soils should not be allowed to air dry[20] and should be placed directly in the ring shear apparatus following remoulding by hand at their natural water content. If it is considered that the coarse fraction of the soil[21] is likely to affect the test results (because of scale effects in the apparatus) then it should be removed prior to remoulding. Fine to medium sized sands may be poured into place; the test is not suitable for coarser materials.

---

[20] Air drying has been shown to alter the nature of the organic fraction present within a soil; interface friction angles can be affected significantly by this fraction (Smith, 1992).

[21] Remove fraction of soil particles larger in size than 425 μm when using the 'Bromhead' apparatus (for which the specimen's initial thickness, H_0, and width, B, are 5 mm and 30 mm respectively) and larger than 2 mm when using the 'Bishop' apparatus (with H_0 = 10 mm and B = 50 mm). These dimensions are in keeping with the commonly applied restriction in laboratory strength tests that the maximum soil particle size should not exceed $H_0/5$. The limiting particle size in the 'Bromhead' apparatus is, however, governed by the need to allow soil particles freedom to move in the gap between the interface (of outer diameter 99.9 mm) and the ring (with internal diameter 100.2 mm).

b) If it is considered that the soil is too hard to be remoulded into the equipment by hand, then it is recommended that the specimen should be "wetted up" to a water content corresponding with a Liquidity Index of between 0.0 and 0.2. The water used in mixing should be distilled (in the absence of the soil's natural pore water).

c) Conversely, if it is considered that the soil may be susceptible to large settlements during consolidation, then the specimen should be allowed to dry in air to a water content corresponding with a Liquidity Index of between 0.0 and 0.2.

d) The annular steel interface should be of same material and roughness as that of the pile; this roughness typically corresponds to a centre-line average value (R_{cla}) of about 10 μm and can most readily be achieved by shot-blasting a fresh interface. Precise roughness measurements can be obtained used a Hobson Taly-Surf profilometer and approximate R_{cla} estimates may be made by simple tactile means using reference blocks of known R_{cla} values. A graphical representation of how R_{cla} is defined is presented on Figure A1 at the end of this appendix.

A1.3 Test procedure

a) The soil is placed in the apparatus in at least two layers, each layer being compacted by a uniform distribution of thumb pressures. Particular care is required to minimise the possibility of entrapping air within fine grained soil. Attention should be given to avoiding any irregularities in the soil at the boundary with the steel interface.

b) A total normal stress (σ_n) representative of the in-situ horizontal effective stress in the ground is applied to the test specimen, which is then allowed to consolidate to achieve this effective stress. If the specimen has been remoulded at a relatively high Liquidity Index, a number of increments of applied stress should be used to attain σ_n (following the procedure used in oedometer tests). No further load increment should be applied in the 'Bromhead' apparatus if the measured vertical strain exceeds 15%[22]. Water is added to the bath after application of the first (or only) increment of normal stress. A minimum σ_n value of 50 kPa is recommended, to reduce errors associated with friction in both the 'Bromhead' and 'Bishop' devices.

c) The specimen is subjected to a series of fast shearing pulses for a total displacement of at least 1 metre; this stage is intended to simulate the displacement history of soil elements adjacent to a pile during driving. The shearing pulses should impose displacements of ≈ 200 mm at a rate of 500 mm/min[23] and should be separated by pause periods (at zero applied shear stress) of ≈ 3 minutes in the 'Bromhead' apparatus and ≈ 10 minutes in the 'Bishop' apparatus. The torque applied to specimens during fast shearing can only be measured reliably by using LVDTs within proving rings or by using load cells. These measurements cannot, however, be related to δ_{peak} or $\delta_{ultimate}$, although they can provide useful information on the uniformity of the specimen/interface and on the fast/undrained shearing characteristics of the soil.

---

[22] Because of the increased effect of friction between the side of the interface and the soil in the gap between this side and the adjacent confining ring, settlement should be limited in the 'Bromhead' apparatus to 0.75 mm (equivalent to 15% vertical strain).

[23] This rate must be applied manually in the Bromhead apparatus.

d) If significant squeezing/loss of soil between the confining ring and interface is observed during the first shearing stage (as indicated by significant change in specimen height), then (i) the rate of fast shearing should be slowed down and/or (ii) the proposed displacement at the fast rate should be reduced or (iii) the gap between the ring and the interface in Bishop's apparatus should be closed. However, it should be noted in the reporting of the results that the accuracy of subsequently measured δ_{peak} values may be compromised.

e) Excess pore pressures induced in the specimen during fast shearing are allowed to dissipate fully, then the specimen is reconsolidated using a vertical stress representative of the equalised effective radial stress acting on the pile wall after the pore-water pressures induced by driving have dissipated.

f) The specimen is then sheared at a slow drained rate of displacement until ultimate residual conditions are established; this usually requires a displacement in excess of 10 mm. Rates of displacement required to ensure fully drained conditions in plastic clays are typically 0.02 mm/min and 0.005 mm/min in the 'Bromhead' and 'Bishop' devices respectively. However, if the total change in specimen height during the slow shearing exceeds 0.75 mm, then it should be noted in the reporting of the results that the accuracy of subsequently measured $\delta_{ultimate}$ values may be compromised.

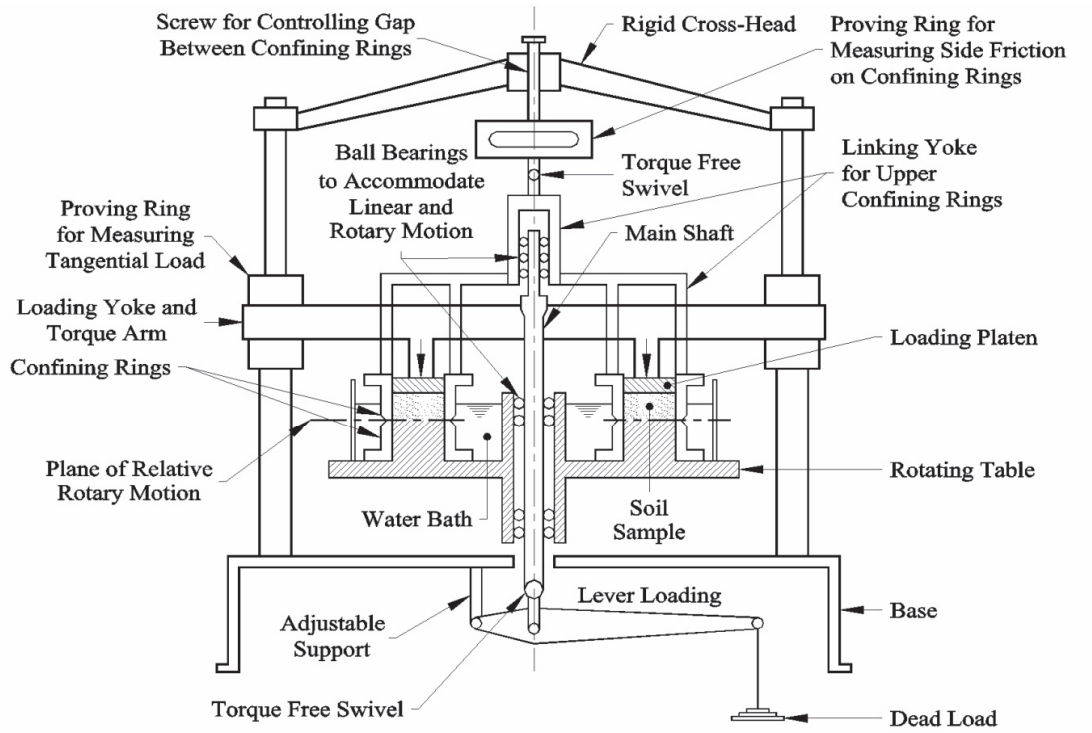

Figure A1. Bishop ring shear apparatus

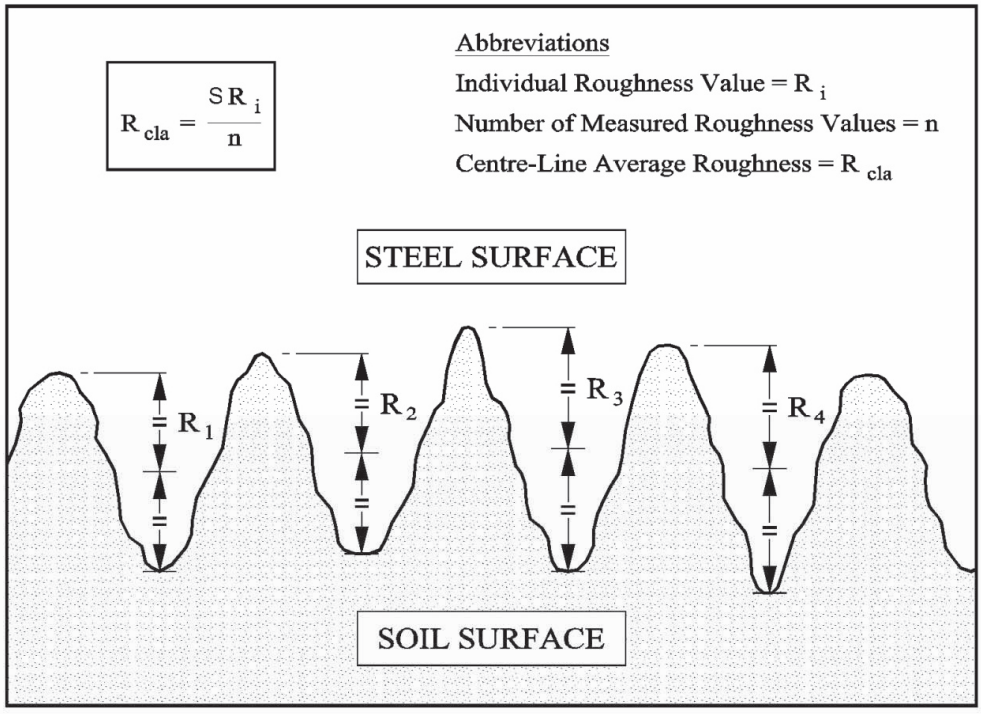

Figure A2. Idealised representation of centre-line average roughness

APPENDIX B

CASE HISTORIES AND WORKED EXAMPLES FOR PILES IN SAND AND CLAY

Since the first publication of 'New Design Methods for Offshore Piles' in 1996 the ICP methods have been applied in a wide variety of ground conditions around the world. The Authors illustrate the methods' application in this Appendix by referring to the detailed analysis of the large-scale EURIPIDES tests in sand (Zuidberg and Vegobbi 1996) and the large diameter Pentre pile test in clay (Clarke, 1993). The Authors' aim in this Appendix is to show explicitly how the methods can be applied in practice.

Chow (1997) gave details of how she applied the ICP approach to more than 100 pile tests in the 1996 database. Tables 7 and 8 in Section 5.1 of this document, referred to some more recent case histories, citing appropriate sources for further information. Additional references to published ICP case histories are given below in Table B1.

Table B1. Published case histories in addition to those cited in Tables 7 & 8 and Chow (1997)

No.	Site	Reference	Dominant soil type
1	Tilbrook, Cambridgeshire, UK	Chow & Jardine (1997)	Hard Lowestoft Till and Oxford Clay
2	Ras Tanajib, Saudi Arabia	Chow & Jardine (1997)	Medium to very dense sand and silty sand underlain by weakly cemented, very dense sand and silty sand
3	Noetsu Bridge, Japan	Jardine et al. (1998a)	Soft diatomaceous mudstone
4	Kansai Bridge, Japan	Jardine et al. (1998a)	Mixed cohesive and cohesionless nearshore deposits

B1 EURIPIDES

A site at Eemshaven, in the Netherlands, was selected by the Joint-Industry EURIPIDES project for large diameter pile tests in dense sand. The programme of work was performed in 1995 and comprised a series of tension, compression and cyclic load tests carried out at two locations. The pile was then left in situ for 18 months before being retested.

B1.1 Site conditions

The site soil profile consists of a sequence of Holocene and Pleistocene fine to medium sands extending from the water table to in excess of 60 m. These soils are overlain by about 5 m of made ground (fine sand). Figure B1 shows a general soil profile through the site and the cone penetrometer tests carried out at the two pile test locations. The worked example is based on the CPT36 profile and this is shown in more detail on Figure B2. Other soil parameters used in the worked example are mostly taken from the Fugro report to API presenting the pile test results (Fugro 2004). Fugro does not report interface shear tests for the soils above 22 m so a value of 29º has been used except between 15 and 22 m where 20º was selected to reflect the soil description of interlayered sand, silt and clay.

B1.2 Test pile

The test pile was a nominal 30”OD x 1.5”WT steel pipe that was driven to various toe penetrations between 30 and 47 m into the ground. The initial pile surface roughness was measured as 31 μm but this had reduced to about 13 μm on extraction. As the laboratory interface shear tests were performed with a surface roughness of 25 μm this value is used in the example.

B1.3 Pile capacity prediction

A worked example for the third test at 47 m, at Location I, is shown in Table B2. Predictions for shallower penetrations can be derived by adjusting the depth and pile length, and a prediction for Location 2 can be obtained by using the appropriate cone penetration test profile.

The relative densities shown in the table were calculated from the calibration chamber relationship between q_c, D_r and σ'_{v0} for a normally consolidated silica sand given by Lunne and Christoffersen (1983). They are not required for the calculation but can be used as a check on the reasonableness of the site interpretation.

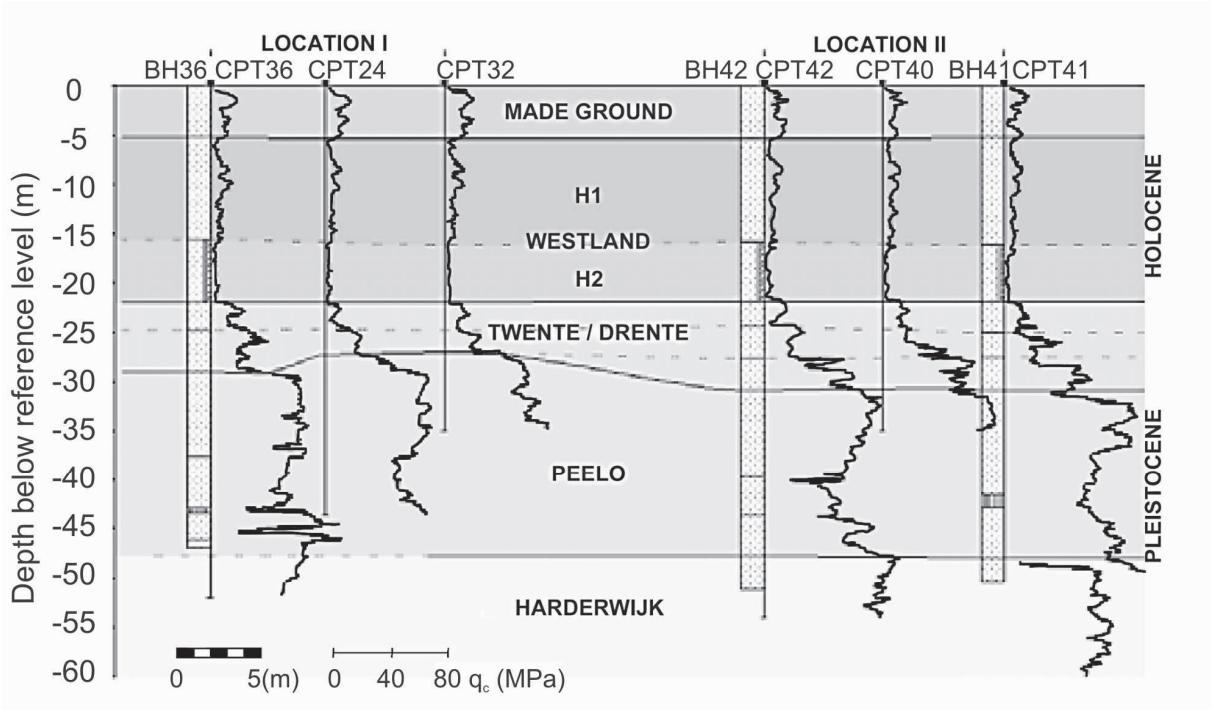

Figure B1. EURIPIDES stratigraphy and CPT q_c profiles (after Fugro, 2004)

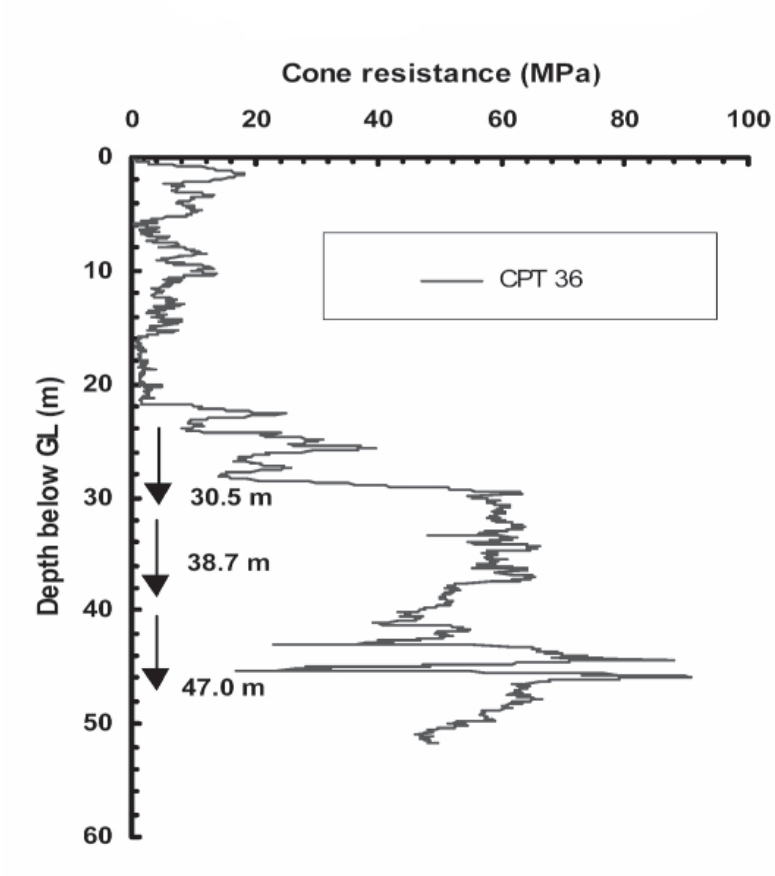

Figure B2. EURIPIDES CPT 36 q_c profile (after Fugro, 2004)

Table B2. EURIPIDES worked example

EURIPIDES Site 1 Test 3

Pile Diameter, D (m)	0.763
Pile Length, L (m)	47
Wall Thickness, t (mm)	36
Pile Roughness, dh (mm)	0.025

Full cross sectional area (m^2)	0.46
Pile displacement ratio	0.18
Annular base area (m^2)	0.08
R* (m)	0.16

Depth, z [m]	dz [m]	Unit Wt [kN/m^3]	σ'_{v0} [kPa]	q_c [MPa]	h/R*	D_r	G [MPa]	σ'_{rc} [kPa]	$\Delta\sigma'_{rc}$ [kPa]	δ_f [º]	Compression τ_f [kPa]	Compression τ_f*dz [kN/m]	Tension τ_f [kPa]	Tension τ_f*dz [kN/m]
0	0.5	15.5	0	0	291	1.06	0	0	0	29	0	0	0	0
1	1	15.5	16	5	284	0.85	31	13	4	29	10	10	7	7
2	1	15.5	31	9	278	0.88	47	26	6	29	18	18	14	14
3	1	15.5	47	10	272	0.82	56	31	7	29	21	21	16	16
4	1	15.5	62	10	266	0.75	63	33	8	29	23	23	17	17
5	1	15.5	78	10	260	0.69	68	34	9	29	24	24	18	18
6	1	9.5	87	2	253	0.11	43	7	6	29	7	7	6	6
7	1	9.5	97	4	247	0.32	58	14	8	29	12	12	9	9
8	1	9.5	106	6	241	0.44	67	22	9	29	17	17	13	13
9	1	9.5	116	8	235	0.52	75	30	10	29	22	22	17	17
10	1	9.5	125	10	229	0.57	82	38	11	29	27	27	20	20
11	1	9.5	135	6	223	0.38	73	23	10	29	18	18	14	14
12	1	9.5	144	4	216	0.22	66	16	9	29	14	14	11	11
13	1	9.5	154	4.3	210	0.23	69	17	9	29	15	15	11	11
14	1	9.5	163	4.7	204	0.25	73	19	10	29	16	16	12	12
15	0.5	9.5	173	5	198	0.26	76	21	10	29	17	9	13	7
15	0.5	7.5	173	2	198	0.00	51	8	7	20	5	3	4	2
16	1	7.5	180	2.15	192	0.00	54	9	7	20	6	6	5	5
17	1	7.5	188	2.3	185	0.00	56	10	7	20	6	6	5	5
18	1	7.5	195	2.45	179	0.00	59	11	8	20	7	7	5	5
19	1	7.5	203	2.6	173	0.00	61	12	8	20	7	7	6	6
20	1	7.5	210	2.75	167	0.00	63	13	8	20	8	8	6	6
21	1	7.5	218	2.9	161	0.01	65	13	9	20	8	8	6	6
22	0.5	7.5	225	3	155	0.02	67	14	9	20	8	4	7	3
22	0.5	10.5	225	10	155	0.43	102	47	13	31	37	18	28	14
23	1	10.5	236	10	148	0.42	104	48	14	31	37	37	28	28
24	0.5	10.5	246	10	142	0.41	105	50	14	31	38	19	29	14
24	0.5	11	246	20	142	0.65	125	99	16	31	69	35	52	26
25	1	11	257	20	136	0.64	127	101	17	31	71	71	53	53
26	1	11	268	20	130	0.63	129	104	17	31	72	72	54	54
27	1	11	279	20	124	0.62	131	106	17	31	74	74	55	55
28	1	11	290	20	117	0.61	133	109	17	31	76	76	57	57
29	0.5	11	301	20	111	0.60	135	112	18	31	78	39	58	29
29	0.5	11	301	30	111	0.74	150	167	20	31	112	56	83	42
30	1	11	312	60	105	0.97	197	344	26	31	222	222	163	163
31	1	11	323	60	99	0.96	199	353	26	31	228	228	167	167
32	1	11	334	60	93	0.95	200	364	26	31	234	234	172	172
33	1	11	345	60	87	0.94	202	375	26	31	241	241	177	177
34	1	11	356	60	80	0.93	204	387	27	31	249	249	182	182
35	1	11	367	60	74	0.93	205	401	27	31	257	257	188	188
36	1	11	378	60	68	0.92	207	416	27	31	266	266	195	195
37	1	11	389	60	62	0.91	208	433	27	31	277	277	202	202
38	1	11	400	50	56	0.84	195	377	26	31	242	242	177	177
39	1	11	411	50	49	0.84	196	396	26	31	253	253	185	185
40	1	11	422	45	43	0.79	191	376	25	31	241	241	176	176
41	1	11	433	45	37	0.79	193	400	25	31	256	256	187	187
42	1	11	444	45	31	0.78	194	430	25	31	274	274	200	200
43	0.5	11	455	45	25	0.78	196	470	26	31	298	149	217	109
43	0.5	11	455	63	25	0.89	222	658	29	27	350	175	255	127
44	1	11	466	63	19	0.89	224	736	29	27	390	390	284	284
45	1	11	477	63	12	0.88	225	862	30	27	454	454	330	330
46	1	11	488	63	8	0.87	227	1021	30	27	535	535	388	388
47	0.5	11	499	63	8	0.87	228	1024	30	27	537	268	389	195
Total	**47**										**Total shaft load [kN]**	**14404**		**10557**
											Total base load [kN]	**5180**		
											Total load [kN]	**19584**		**10557**

D_r at pile tip	0.87
Plugged q_b [MPa]	63

B1.4 Comparison of calculated and measured capacity

Table B3 presents a summary of the first compression and tension test results at each pile penetration, as shown in the API report (Fugro, 2004). The compressive load values quoted correspond to a toe deflection of $D/10$, taken as equal to the pile head deflection plus the elastic shortening of the pile under load. The Q_c values were derived using the calculation set out in Table B2 for Test 1.3. This was modified as described to obtain Q_c values for the other tests.

Table B3. EURIPIDES pile test results

Test	**1.1**		**1.2**		**1.3**		**2.1**	
Toe depth (m)	-30.5		-38.7		-47.0		-46.7	
Test direction	Comp - Tens		Tens - Comp		Comp - Tens		Comp - Tens	
Approx. no. days after driving	7		2		12		6	
Total pile load (MN)	8.4	-2.9	-9.7	13.8	20.4	-13.6	20.0	-11.1
Shaft load, Q_{sm} (MN)	4.4	-2.9	-9.7	10.2	15.5	-13.6	15.1	-11.1
Base load, Q_{bm} (MN)	4.0	-	-	3.6	4.9	-	4.9	-
Pile head displacement (mm)	92	40	60	106	123	80	122	80
Shaft capacity, Q_{sc}/Q_{sm}	1.00			1.05	0.93		0.95	
Base capacity, Q_{bc}/Q_{bm}	1.23			1.13	1.06		1.01	
Total comp capacity, Q_{Tc}/Q_{Tm}	1.11			1.07	0.96		0.97	
Total tens capacity, Q_{Tc}/Q_{Tm}		1.12	0.81			0.78		0.95

The later re-tests of the pile at Location 2.1 did not reach failure. The compression test was terminated at a pile head load of 30 MN. The tension test was terminated at a pile head load of 17 MN. The load-displacement data indicated little plastic straining in either re-test, suggesting that the true capacities rose substantially higher than the maximum applied loads, confirming the earlier discussed beneficial effects of time on shaft capacity (Section 6.1).

Independent pile capacity predictions using the ICP approach have been conducted for the EURIPIDES pile tests by others including the Norwegian Geotechnical Institute (Aas et al., 2004), Randolph (2003) and Foray & Colliat (2005). All of these indicate similar good agreement between predictions and measurements.

B2 Pentre

The Pentre test site in Shropshire was chosen by the Joint-Industry Large Diameter Pile (LDP) Testing Programme for its thick sequence of lightly overconsolidated, low plasticity, glacial lake deposits. The site has undergone three test programmes by:

- the LDP consortium (Gibbs et al., 1993)
- the Norwegian Geotechnical Institute (NGI) (Karlsrud et al., 1993) and
- Imperial College (Chow, 1997)

These tests involved a wide range of instrumented pile types with different diameters, end-conditions and installation methods. This example examines the large diameter pile test performed by the LDP consortium.

B2.1 Site conditions

Figure B3 shows the soil stratigraphy consisting of a thick deposit of Holocene glacial lake sediments overlain by 3.5 m of recent alluvium. The site is fully described by Lambson et al. (1993) and composite plots of the main soil parameters used in the worked example to derive design profiles are found in that publication. Additional test data have been published by Chow (1997) and these are summarised in Figures B4 and B5.

The phreatic surface is 1m below the ground surface, with artesian pressures beneath due to an underlying aquifer. The glacial lake deposits are unusual in that they combine the index properties of a low to medium plasticity silty clay with a coarse silt-sized grading and high permeability and consolidation characteristics. Light apparent overconsolidation has been caused by ageing and changes in water levels; the YSR profile inferred by Lambson et al. (1993) has been confirmed by oedometer tests at Imperial College.

Ring-shear interface tests were performed by both the LDP team (Lambson et al., 1993) and Imperial College. Figure B4 shows the correlation made by Chow (1997) of low residual strength at low PI. The mean trend line from the LDP ring shear test results was adopted for the prediction of the LDP test's pile capacity in the example since they involved the same RQT steel type as the pile. Values of $\delta_{ultimate}$ corresponding to the soil plasticity indices of each main unit were used in the example set out below to model the ultimate load condition of the test. Chow (1997) also computed the peak shaft capacity, noting that her pile elastic compression calculations indicated that peak δ angles were only expected to apply over the bottom section of the LDP pile shaft, giving modest differences between peak and ultimate shaft capacity.

Profiles for the oedometer sensitivity parameter ΔI_{vy} were evaluated as set out in Section 4.2, employing (i) the yield points from intact oedometer tests performed at Imperial College and (ii) the ICL curves expected from correlations with index properties obtained in the LDP investigation. The results are shown in Figures B5(a) and B5(b) respectively.

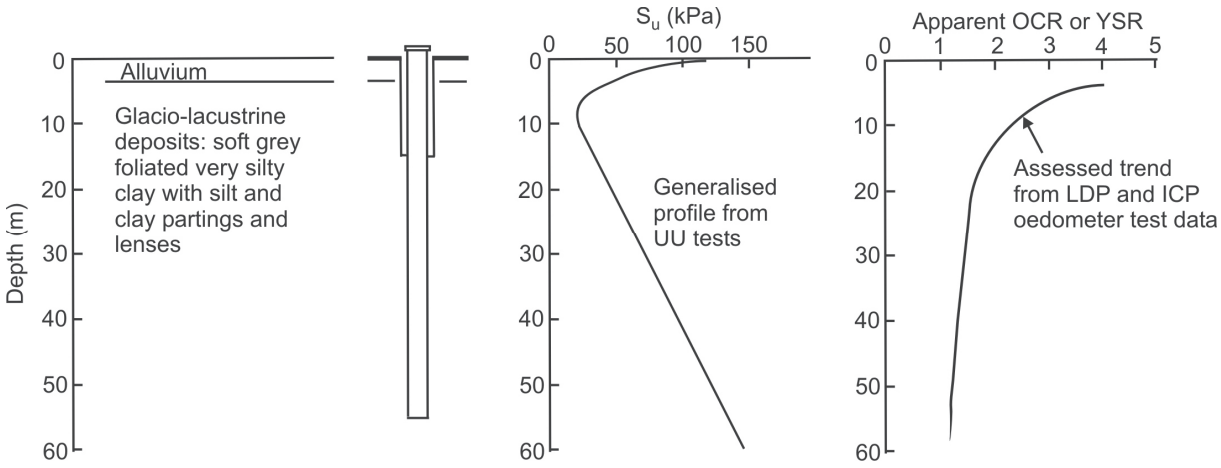

Figure B3. Pentre soil profile

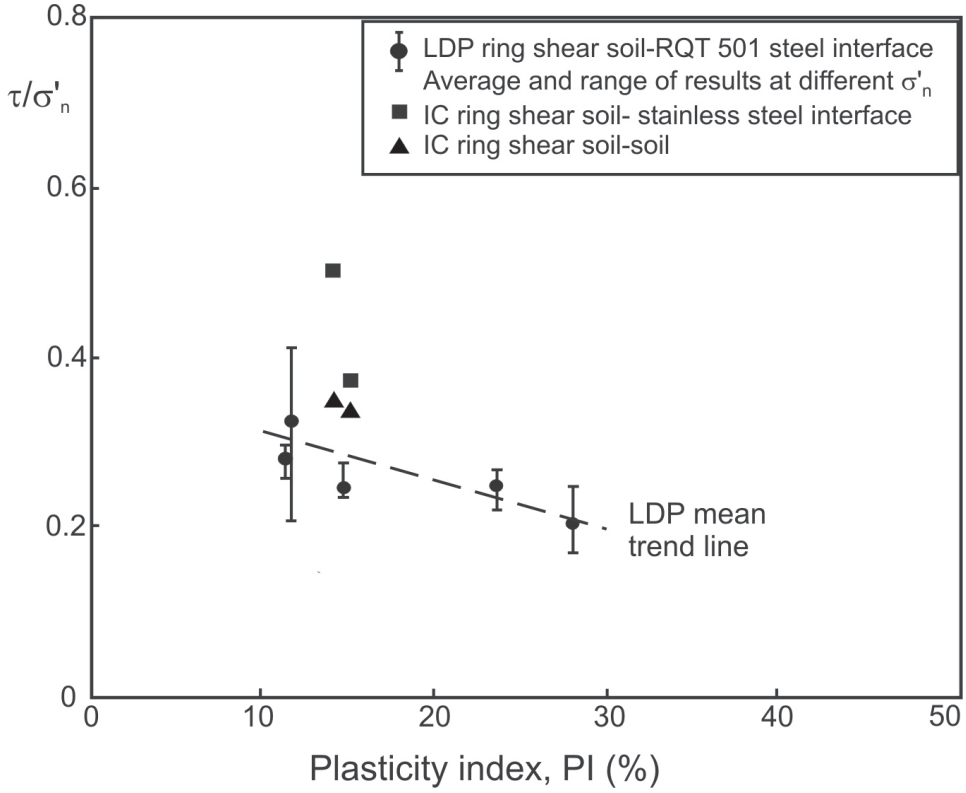

Figure B4. Results for interface angle of friction for Pentre clay-silt

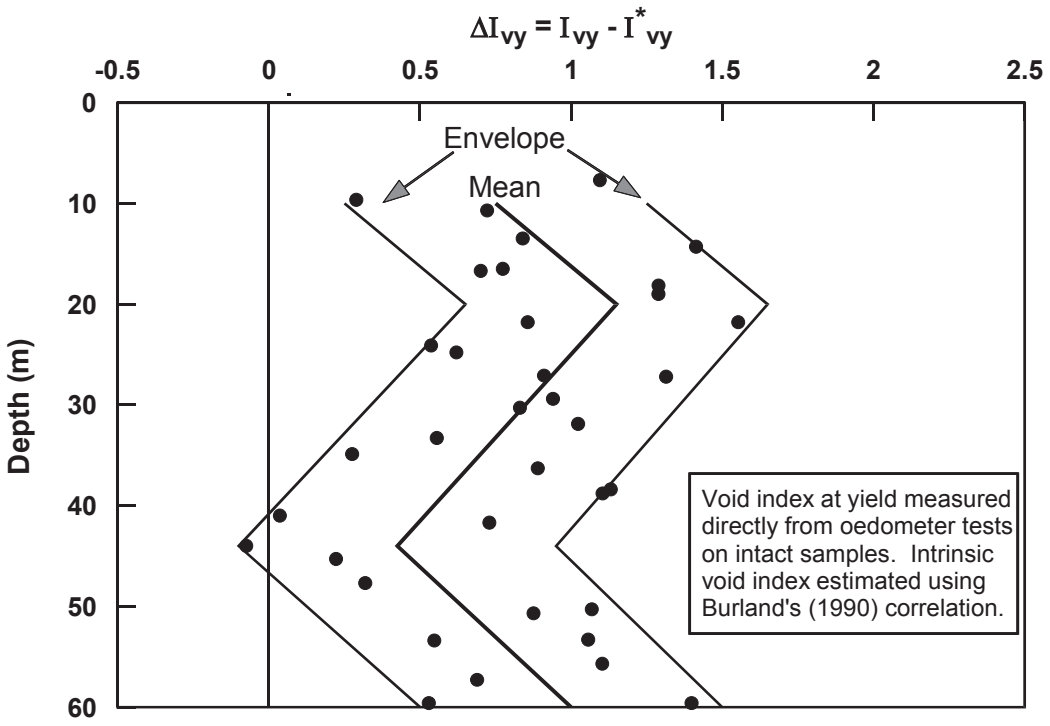

Figure B5(a) Pentre ΔI_{vy} values from oedometer test data

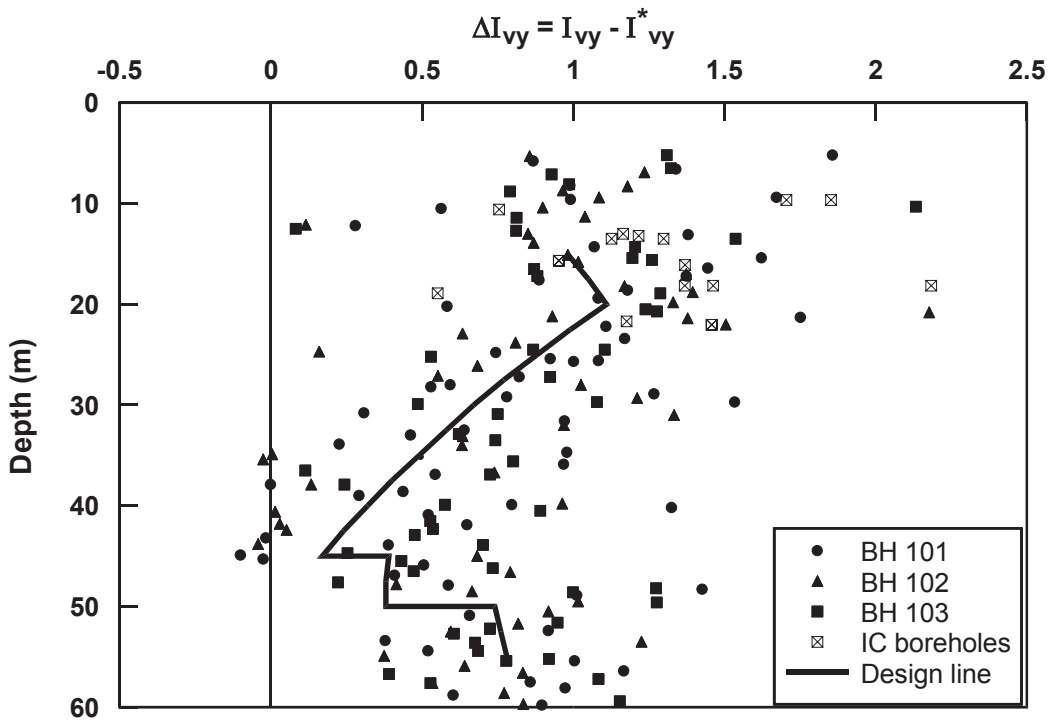

Figure B5(b) Pentre ΔI_{vy} values from Atterberg test data and correlations

B2.2 Test pile

The LDP pile was a 0.762 m diameter open-ended pipe pile driven to 55 m penetration from the base of a 15 m deep cased starter-hole. The nominal displacement ratio of the pile was 27% due to protective shoes over the internal instrument channels, but these obstructions did not extend to the pile tip. The internal soil column found at the end of driving had risen 1.73 m above the casing tip depth, contributing a soil volume similar to that of the instrument channels between 15 and 55 m. The cross-sectional areas of the channels were therefore neglected in calculating the equivalent radius R^* substituted into the shaft capacity calculations (through the h/R^* term). However, the instrument sections were accounted for when considering the plugging criteria applying to the end bearing calculation.

B2.3 Pile capacity prediction

Table B4 presents the spreadsheet ICP calculation that generally follows the 16 guidance notes given in Section 4.2.2 of this document as all sources of soil data are combined to make the assessment. This particular assessment was made by Shell UK Ltd, independently of the earlier analysis by Chow (1997).

Design profiles of unit weight, Atterberg limits, water content and strength were developed from the site boreholes and the plots given by Lambson et al. (1993). The unit weights and measured artesian pore pressure profile defined the undisturbed vertical effective stress profile. Plasticity and liquidity indices, and remoulded undrained shear strengths (using the correlation given by Wroth; 1979) were calculated from the water content and Atterberg limit profiles. The design triaxial strength profiles were checked by assessing the factor (N_k) needed to correlate these with the CPT q_c data (N_k =17 for UU test S_{u0} values and11.3 for CAU test S_u data). The remoulded strengths were checked by comparison with site tests.

The YSR profile shown was derived from S_{u0} using the equation in Note 7 of Section 4.2.2. Note 13 and Figure 12 were used to derive e^*, ΔI_{vy} and ΔI_{v0}. The latter two parameters were checked against the oedometer values of ΔI_{vy} (Figure B5(a)) and ΔI_{v0} obtained by Chow (1997). The effect of using either design profiles or individual test results of index tests to derive ΔI_{vy} is demonstrated in Figure B5(b). C_s was derived using the equation given by Chow (1997) when 1<YSR<20 as:

$$C_s = 0.126LL^{1.22} (0.3 + 0.7 \log YSR)$$

K_c was calculated using the three possible methods to check the robustness of the values obtained. In the example shown in detail, pile capacity is derived from ΔI_{vy}. Similar capacity assessments result from the other K_c approaches and also when using the CAU S_u profile coupled with the YSR assessment given in Figure 10.

Table B4. Pentre worked example

LDP pile

Pile Diameter, D (m)	0.762
Starter hole depth (m)	15
Toe depth, L (m)	55
Wall Thickness, t (mm)	15

Soil SG (G_s)	2.65
S_{ucu}/S_{u0}	1.5
N_k (S_{u0})	17
N_k (S_{ucu})	11.3

	Wall	Tip
Full cross sectional area, A_e [m^2]	0.46	
Pile displacement ratio	0.08	0.27
Annular area, A_{aw}, A_{as} [m^2]	0.04	0.12
R* [m]	0.11	

Depth, z [m]	dz [m]	Unit Wt (kN/m^3)	σ'_{v0} [kPa]	LL	mc	PL	PI	LI	S_{u0} [kPa]	S_{ucu} [kPa]	S_{ur} [kPa]	S_t	q_c [MPa]	h/R*	YSR	e^*_{100}	ΔI_{v0}	C_s	ΔI_{vy}	K_c (ΔI_{v0})	K_c (ΔI_{vy})	K_c (S_t)	σ'_{rc} [kPa]	δ_f [°]	τ_f [kPa]	τ_f.dz [kN/m]
15.0	1.25	9.25	136	0.35	0.300	0.20	0.15	0.67	38	56	8	4.8	0.64	378	1.83	0.67	0.74	0.017	0.98	0.61	0.54	0.65	73	16.0	17	21
17.5	2.5	9.25	156	0.35	0.300	0.20	0.15	0.67	44	66	8	5.5	0.74	354	1.86	0.67	0.80	0.017	1.05	0.60	0.53	0.64	83	16.0	19	47
20.0	2.5	9.25	177	0.35	0.300	0.20	0.15	0.67	50	75	8	6.3	0.85	331	1.88	0.67	0.86	0.017	1.11	0.60	0.52	0.63	92	16.0	21	53
22.5	2.5	9.35	198	0.36	0.295	0.20	0.16	0.59	56	84	11	5.1	0.96	307	1.85	0.69	0.75	0.018	0.99	0.63	0.56	0.66	111	15.5	25	62
25.0	2.5	9.45	219	0.37	0.290	0.20	0.17	0.53	63	94	15	4.2	1.06	283	1.81	0.70	0.64	0.018	0.88	0.66	0.61	0.70	133	15.0	28	71
27.5	2.5	9.55	240	0.38	0.285	0.20	0.18	0.47	69	103	19	3.6	1.17	260	1.77	0.72	0.55	0.018	0.77	0.69	0.65	0.73	156	14.5	32	81
30.0	2.5	9.65	262	0.39	0.280	0.20	0.19	0.42	75	113	24	3.1	1.28	236	1.73	0.73	0.46	0.019	0.67	0.72	0.69	0.76	181	14.0	36	90
32.5	2.5	9.75	284	0.40	0.275	0.20	0.2	0.38	81	122	30	2.7	1.38	213	1.69	0.75	0.37	0.019	0.58	0.75	0.73	0.79	208	13.5	40	100
35.0	2.5	9.85	306	0.41	0.270	0.20	0.21	0.33	88	131	37	2.4	1.49	189	1.64	0.76	0.29	0.019	0.49	0.79	0.78	0.82	238	13.0	44	110
37.5	2.5	9.95	328	0.42	0.265	0.20	0.22	0.30	94	141	44	2.1	1.59	165	1.60	0.78	0.21	0.019	0.40	0.82	0.82	0.85	270	12.5	48	120
40.0	2.5	10.05	351	0.43	0.260	0.20	0.23	0.26	100	150	51	2.0	1.70	142	1.56	0.79	0.14	0.020	0.32	0.86	0.87	0.88	306	12.0	52	130
42.5	2.5	10.15	374	0.44	0.255	0.20	0.24	0.23	106	159	59	1.8	1.81	118	1.53	0.81	0.07	0.020	0.24	0.90	0.93	0.92	346	11.5	56	141
45.0	1.25	10.25	397	0.45	0.250	0.20	0.25	0.20	113	169	68	1.7	1.91	94	1.49	0.82	0.01	0.020	0.17	0.95	0.99	0.97	392	11.0	61	76
45.0	1.25	9.00	397	0.50	0.300	0.25	0.25	0.20	100	150	68	1.5	1.70	94	1.29	0.89	0.28	0.020	0.39	0.82	0.85	0.93	336	11.0	52	65
47.5	2.5	9.00	417	0.50	0.300	0.25	0.25	0.20	100	150	68	1.5	1.70	71	1.22	0.89	0.30	0.020	0.38	0.84	0.87	0.96	364	11.0	57	142
50.0	1.25	9.00	437	0.50	0.300	0.25	0.25	0.20	100	150	68	1.5	1.70	47	1.16	0.89	0.32	0.019	0.38	0.88	0.93	1.02	405	11.0	63	79
50.0	1.25	9.50	437	0.40	0.270	0.23	0.17	0.24	125	188	58	2.2	2.13	47	1.81	0.75	0.50	0.020	0.74	1.00	0.94	1.15	412	15.0	88	110
52.5	2.5	9.50	459	0.40	0.270	0.23	0.17	0.24	131	197	58	2.3	2.23	24	1.81	0.75	0.52	0.020	0.76	1.14	1.07	1.31	491	15.0	105	263
55.0	1.25	9.50	482	0.40	0.270	0.23	0.17	0.24	138	206	58	2.4	2.34	8	1.80	0.75	0.54	0.020	0.78	1.40	1.31	1.61	633	15.0	136	170
Total	**40**																										

q_c at pile tip	2.34
Pile/CPT ratio	31

Pile plugs

Total shaft load [kN]	**4622**
Drained base load [kN]	**693**
Total compression load [kN]	**5314**

B2.4 Comparison of calculated and measured capacity

The Pentre pile test results are given in Table B5. High excess pore pressures were generated during driving and 90% dissipation took place remarkably quickly between 1.5 and 5.7 hours. A compression test was conducted after a 44 day equalisation period at a penetration rate of 0.5 mm/min for the first 27 minutes and 1 mm/min thereafter, developing a peak total load of 6.03 MN. Pile weight was taken into account in the derivation of the strain gauge data described by Gibbs et al. (1993). Failure of the strain gauges between 14 and 53 m meant that a constant shear stress with depth had to be assumed.

Table B5. Pentre pile test results

Test	**1**				
Starter hole depth (m)	15				
Toe depth (m)	55				
Test direction	Compression				
Approx. no. days after driving	44				
	Peak		Ultimate		
Total pile load (MN)	6.03		5.48		
Shaft load, Q_{sm} (MN)	5.17		4.26		
Base load, Q_{bm} (MN)	0.86		1.22		
Pile head displacement (mm)	36		97		
Chow (1997) Prediction	ICP	API	ICP	API	
Shaft capacity, Q_{sc}/Q_{sm}	0.86	1.53	1.15	1.85	
Base capacity, Q_{bc}/Q_{bm}	-	-	0.61	0.46	
Total comp capacity, Q_c/Q_m	-	-	1.03	1.54	
Worked Example (ICP only)			K_c (ΔI_{vy})	K_c (ΔI_{v0})	K_c (S_t)
Shaft capacity, Q_{sc}/Q_{sm}			1.09	1.12	1.21
Base capacity, Q_{bc}/Q_{bm}			0.57	0.57	0.57
Total comp capacity, Q_c/Q_m			0.97	1.00	1.07

The Shell analysis ties in well with Chow's earlier assessment. Chow predicted peak and ultimate shaft capacities that fell about 14% lower and higher than the respective measurements. Shell (UK) Ltd's three ultimate shaft capacity assessments bracket Chow's single value with a maximum deviation of about 5%. The test pile's overall capacity is well predicted.

APPENDIX C

LIST OF NOTATION

A, B, C	=	Constants employed (in different contexts) in Table 2, Table 4 and in cyclic loading sections
ALARP	=	As Low As Reasonably Practical
A_b	=	Effective base area for square and H piles
A_s	=	Area of steel for H piles
b	=	Breadth of rectangular pile section with dimensions $b.d$
B	=	Breadth of H section pile as shown on Figure 7
c_{vr}	=	Coefficient of consolidation for radially draining soil
C_c	=	Coefficient of compressibility = $\Delta e/\Delta \log \sigma'_v$
C_c^*	=	Intrinsic coefficient of compressibility; change in void ratio for normally consolidated reconstituted soil between = 100 kPa and 1000 kPa
C_s	=	Coefficient of compressibility applying to swelling or recompression = $\Delta e/\Delta \log \sigma'_v$
CAU	=	Consolidated Anisotropic Undrained style of triaxial test
CAU_C	=	Consolidated Anisotropic Undrained Compression style of triaxial test
CNS	=	Constant Normal Stiffness style of soil-soil or soil-interface shear box or simple shear test
COV	=	Coefficient of Variation: s/μ
COV_f	=	Foundation coefficient of variation
COV_i	=	Component of coefficient of variation in multivariable problem
CPT	=	Cone Penetration Test
CPTU	=	Piezocone CPT test
CRS	=	Constant Rate of Strain style of oedometer compression test
d	=	Width of rectangular pile section with dimensions $b.d$
d_{50}	=	Size of particle at 50% point on particle size distribution curve
D	=	Pile outer diameter, or dimension of H pile as shown on Figure 7
D_{CPT}	=	Diameter of CPT probe = 0.036 m
D_{inner}	=	Internal diameter of pipe pile
D_r	=	Relative density (%)
e	=	Void ratio (see Figure 13 for e_0, e_s., etc.)
e_L	=	Void ratio at liquid limit
e^*_{100}	=	Void ratio of reconstituted soil at 100 kPa vertical effective stress with *OCR* = 1
e_0	=	Void ratio of sample at in-situ stress state
EOID	=	End of Initial Driving
f	=	Function (generally)
f_L	=	Probability density function of load
f_R	=	Probability density function of resistance
f_x	=	Probability density function of any variable
F_L	=	Cumulative density function of load
F_R	=	Cumulative density function of resistance
FORM	=	First Order Reliability Method
FOS	=	Factor of Safety

G = Operational shear modulus
G_s = Specific gravity of soil
h = Height of point above pile tip
h/R = h (above) divided by radius of closed-ended cylindrical pile
h/R^* = h (above) divided by equivalent radius R^* of open or non-cylindrical pile
ICL = Intrinsic Compression Line of reconstituted soil in oedometer test at $OCR = 1$
ICP = Imperial College Pile
IFR = Incremental Filling Ratio for partially coring open pile
K = Coefficient of radial effective stress on shaft during equalisation process = σ'_r/σ'_{v0}
K_c = Coefficient of radial effective stress for shaft after full equalization = $\sigma'_{rc}/\sigma'_{v0}$
K_f = Coefficient of radial effective stress for shaft at failure = $\sigma'_{rf}/\sigma'_{v0}$
K_0 = Coefficient of earth pressure at rest = σ'_h/σ'_{v0}
ln = logarithm to base *e*
log = logarithm to base 10
L = Pile length
LDP = Large Diameter Pile
LI = Liquidity Index
LL = Atterberg Liquid Limit
LRFD = Load and Resistance Factor Design
m = No of rows of piles in a group of n by m piles
n = No of columns of piles in a group of n by m piles
N = Number of load cycles
N_c = End bearing capacity factor for clays
N_f = Number of cycles required to cause failure
N_k = Cone factor for clays
OCR = Overconsolidation ratio
OD = Outside Diameter
p'_0 = Initial mean effective stress
P = Cross-sectional perimeter of H or rectangular piles
P_a = Absolute atmospheric pressure = 100 kPa
Pf_a = Annual Probability of Failure
PI = Plasticity Index
PL = Atterberg Plastic Limit
q_b = Pile-end bearing stress (also expressed as q_b/q_c)
q_{ba} = End bearing stress under annulus of open pipe pile
q_c = CPT end resistance
Q = Pile axial capacity
Q_a = Resistance at a given confidence level
$Q_{average}$ = Average load experienced by a pile under cyclic loading
Q_b = Base capacity
Q_c = Calculated capacity
Q_{cyclic} = Amplitude of pile cyclic load
Q_i = Component of capacity
Q_m = Measured capacity
$Q_{max\ cyclic}$ = Maximum load that can be applied cyclically
$Q_{max\ static}$ = Maximum load that can be applied statically = Q
Q_s = Shaft capacity
Q_{total} = Total pile capacity = Q above

R	=	Pile radius
R_{cla}	=	Centre-line average roughness
R_{inner}	=	Internal pile radius
R_{outer}	=	External pile radius
R^*	=	Equivalent radius for open-ended piles
RI	=	Ranking Index
s	=	Standard deviation, also pile group spacing
SPT	=	Standard Penetration Test
SRD	=	Soil Resistance to Driving
S_t	=	Clay sensitivity
S_u	=	Undrained shear strength
S_{u0}	=	Initial undrained shear strength measured in unconsolidated undrained triaxial compression tests
S_{ur}	=	Undrained shear strength of remoulded soil measured in unconsolidated undrained triaxial tests
t	=	Time or pile wall thickness
T	=	H pile steel thickness defined in Figure 7, non-dimensional Time Factor in consolidation analysis or period of sinusoidal cyclic loading
T-Z	=	Soil/steel axial unit load (or stress)-deflection relationships
UU	=	Unconsolidated undrained
UK	=	United Kingdom
WSD	=	Working Stress Design
w_0	=	Initial in-situ water content
w	=	Water content in general
x	=	A variable
X_p	=	Geometrical parameter for H piles (see Table 4)
YSR	=	Yield Stress Ratio, or apparent *OCR*
α	=	Ratio between local shaft shear stress capacity and initial undrained shear strength
δ	=	Effective stress shaft friction angle
δ_{cv}	=	Constant volume or critical-state angle of interface friction
δ_f	=	Operational interface angle of friction at failure
δ_{peak}	=	Peak value of δ for clays
$\delta_{ultimate}$	=	Ultimate (minimum) value of δ for clays
Δr	=	Radial normal movement of soil close to pile-soil interface
ΔH_p	=	Increment in height of pile internal core during driving of open-ended piles
ΔI_{v0}	=	Relative void index (see Figure 12)
ΔI_{vy}	=	Relative void index at yield (see Figure 12)
ΔL	=	Increment in pile embedded length during driving
$\Delta\sigma'_r$	=	Change in σ'_r during loading (also $\Delta\sigma'_{rd}$ in sands)
γ'	=	Effective unit weight of soil
γ_{cyc}	=	Cyclic shear strain amplitude
η	=	Parameter employed when calculating shear modulus of sand (see Table 2)
ϕ'	=	Angle of effective shearing resistance
ξ	=	Pile group efficiency for axial capacity (see Section 7.2)
θ	=	Term in Converse Labarre group action equation (see Section 7.2)
σ'_a	=	Axial effective stress in laboratory triaxial tests
σ'_{h0}	=	Free-field horizontal effective stress

σ'_n = Normal effective stress during shear testing
σ'_r = Radial effective stress
σ'_{rc} = Equalised radial effective stress
σ'_{rf} = Radial effective stress at point of shaft failure
σ'_{v0} = Free-field vertical effective stress
σ'_v = Vertical effective stress
σ'_{vy} = Vertical effective yield stress
τ_f = Peak local shear stress
τ_{cyc} = Cyclic shear stress amplitude
$\tau_{max\ static}$ = Maximum shear stress that can be sustained under static loading
μ = Statistical mean value
μ_{vane} = Vane correction factor

General meaning of subscripts

c = at equilibrium (after consolidation)
f = failure
nc = normally consolidated
r = radial
t = at given time
u = ultimate
v = vertical
y = at yield
0 = free-field, before pile installation